N72-30951

NAS-9-12067

EXPLORATORY DEVELOPMENT OF A FLEXIBLE ABLATIVE COVERING FOR SPACE SHUTTLE APPLICATION

FINAL REPORT

BY

ARNOLD A. HILTZ

JUNE 1972

GENERAL ELECTRIC

Re-entry & Environmental Systems Division

3198 Chestnut St., Philadelphia, Pa. 19101

TABLE OF CONTENTS

Section		Page

LIST OF ILLUSTRATIONS

LIST OF ILLUSTRATIONS (Cont)

LIST OF TABLES

FOREWORD

This report was prepared by the Re-entry and Environmental Systems Division (RESD) of the General Electric Company, Philadelphia, Pennsylvania, under NASA Contract No. NAS 9-12067. The work was administered under the direction of the Manned Spacecraft Center's Structures and Mechanics Division with Dr. D. M. Curry of the Thermal Protection Section acting as Contract Monitor.

This report covers the work conducted from June 22, 1971 through April 22, 1972 at RESD's Materials and Structures Laboratory under the management of Mr. V. N. Saffire. Dr. A. A. Hiltz acted as Project Manager and compiled the Final Report.

The experimental and analytical investigations were undertaken by a team of people; the major contributors and their contributions are given below:

C. Adams -	Design
R. Brewer -	Thermal Analyses and Tests
Dr. J. Kibler/T. Hess -	Structural Analyses and Tests
J. Axelson/A. Hiltz -	Material Development

The manuscript of this report was released for publication on June 21, 1972.

NOMENCLATURE

Fiber and Weaving Terminology

cotton count (c.c.):	the number of 840-yard hanks per pound
denier:	the weight in grams of 9000 meters of a fiber
ends/inch:	the number of warp yarns/inch
5/32 gauge:	refers to a 5/32 inch-thick metal loop former, 7/8 inch high, with a knife edge for cutting the loops to form cut pile
picks/inch:	number of fill yarns/inch
256 pitch:	256 pile ends/27 inch width
roving:	the product which results when sliver is drawn down to from 1/4 to 1/8 its original size and is slightly twisted
sliver:	a soft, compact untwisted "rope" of fibers of circular cross-section and about one inch in diameter
tpi:	twists per inch
tpi-S:	twists/inch in the S-direction (left-hand)
tpi-Z:	twists/inch in the Z-direction (right-hand)

General

BAS:	barbed attachment concept
C_p:	specific heat
ESM:	elastomeric shield material
FSA:	flexible silicone ablator
H_o:	total enthalpy
H_r:	recovery enthalpy
orthosafe:	orthotropic structural analysis - finite element

SECTION 1

INTRODUCTION AND SUMMARY

1. INTRODUCTION AND SUMMARY

1.1 INTRODUCTION

This report documents a ten-month applied research program by the General Electric Company's Materials and Structures Laboratory. The program consisted of an exploratory development of a flexible ablative covering for space shuttle application. It was structured so as to concentrate resources on known key technical problem areas which existed at the beginning of the contract, and also on new problem areas which arose during the course of the research effort. During the initial phase of the study, major emphasis was placed upon the fabrication of a suitable woven carpet reinforcement and on a suitable flexible ablator composition that could be foamed directly in the woven construction. Later, the emphasis was placed on assessing the ablation performance of the flexible ablator system and on attachment and refurbishment concepts.

Also included in the report are recommended areas for additional effort to assess more thoroughly the potential of the flexible ablator concept for specific areas of the orbiter surface.

The report reviews the requirements, material development program, design, structural analysis, thermal analysis, and thermal testing.

1.2 SUMMARY

This report documents a 10-month applied research program which was undertaken by General Electric Company's Re-entry and Environmental System Division (RESD) to provide a preliminary design and development of a flexible ablative covering for the space shuttle vehicle that could be easily replaced and/or refurbished. The program was structured to concentrate resources on the major technical problem areas associated with the flexible ablator concept as defined in the RFP. These areas included:

1. Fabrication of a suitable woven carpet reinforcement
2. Modification of a flexible ablator formulation for filling the woven carpet construction
3. Testing of the flexible ablator concept

Several approaches were evaluated to obtain a flexible ablator. The final recommended solution was one in which the ablative filler was based on a low-density formulation of the Elastomeric Shield Material series (ESM). The preferred approach is one in which a light-weight fabric backing is bonded to preformed and fully cured ESM, and the composite tufted with Astroquartz® fiber to the desired tuft or pile density.

Ablation tests performed in the GE hyperthermal arc facility demonstrated the superior ablation performance of the concept and excellent overshoot capability of the system.

SECTION 2

DESIGN CONDITIONS AND CRITERIA

2. DESIGN CONDITIONS AND CRITERIA

2.1 DESIGN REQUIREMENTS

2.1.1 ENVIRONMENT DEFINITION

The work performed under this contract was based upon the point design conditions specified by NASA/Manned Spacecraft Center (MSC) and defined in detail in General Electric report, "Requirements", 26 August 1971. The main points of these requirements are presented here.

The thermal protection system shall be capable of meeting the performance requirements during and following exposure to environments of ground handling, storage, lift-off and orbital insertion, on-orbit, entry, post-entry, and landing. This will include conditions of pressure, humidity, rain, salt spray, thermal gradient, acoustics, and vibration (Figure 2-1).

Two areas of the orbiter underside were considered in this contract as defined in Figure 2-2.

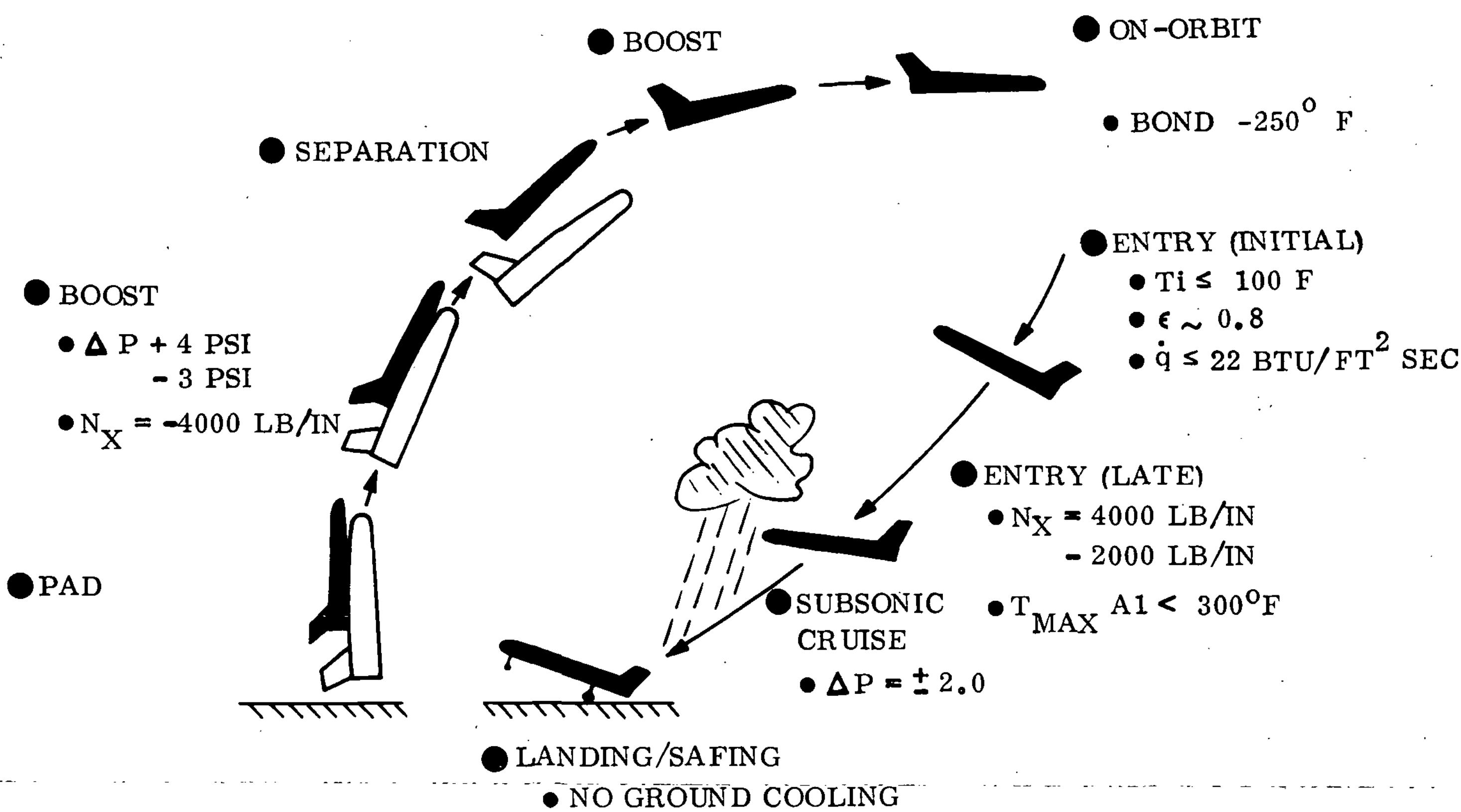

Figure 2-1. TPS Design Requirements

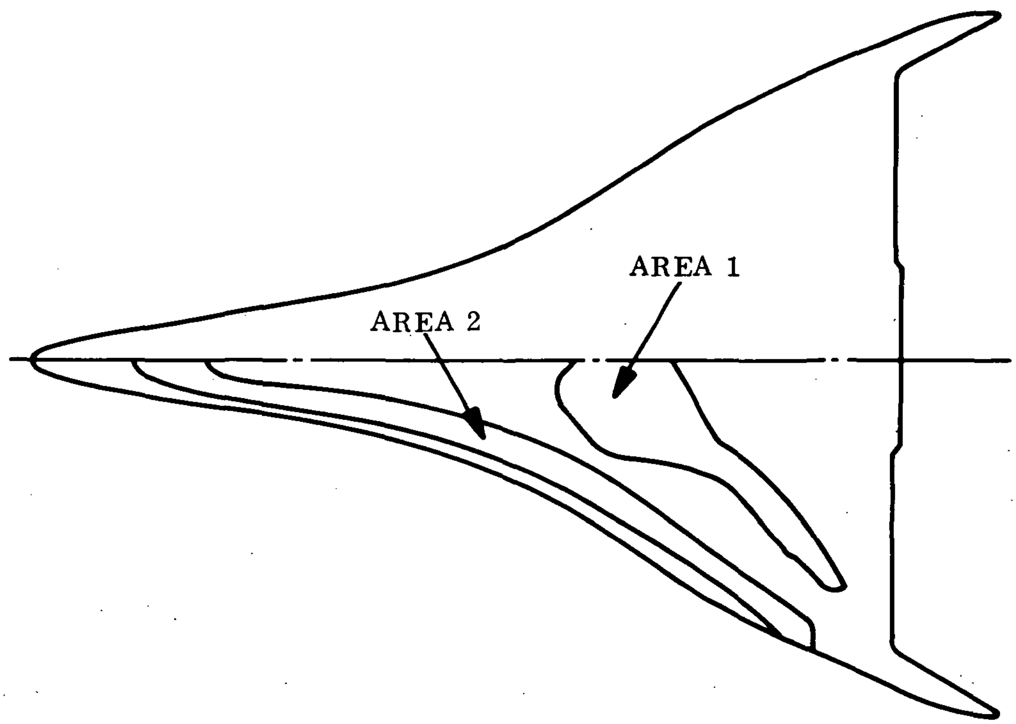

Figure 2-2. Orbiter Plan Form (Bottom) TPS Design Areas

2.1.2 THERMAL REQUIREMENTS

2.1.2.1 Thermal Environment

Cold wall convective heat flux during re-entry is shown in Figure 2-3. Heat flux histories for Areas 1 and 2, and an Area 2 heat flux history perturbed to higher heating levels and referred to herein as "Area 2 - Perturbed" are shown.

The stagnation point recovery enthalpy shown in Figure 2-4 was used to calculate heat transfer coefficients for both areas, and was calculated from representative altitude and velocity histories.

The surface temperature was maintained at or above 120°F during the subsonic cruise and after landing. This is a conservative assumption but is realistic for a landing in a hot climate, the 120°F representing a maximum air temperature that would be experienced at, for example, Edwards Air Force Base.

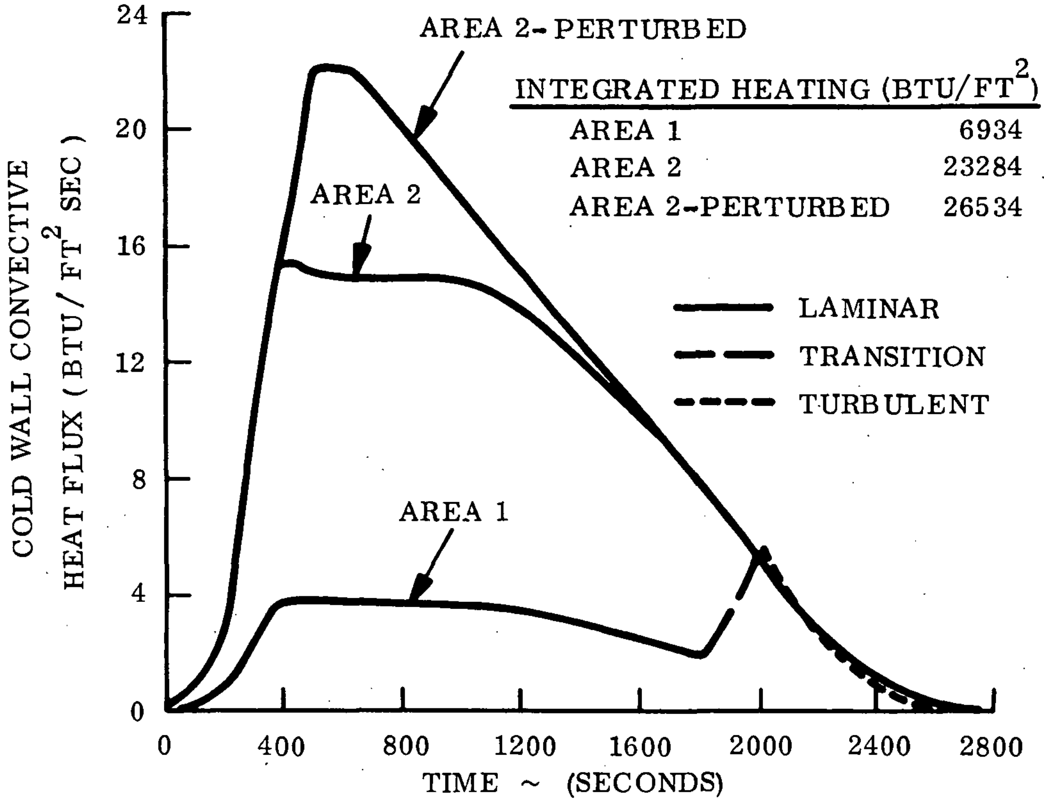

Figure 2-3. Cold Wall Convective Heat Flux

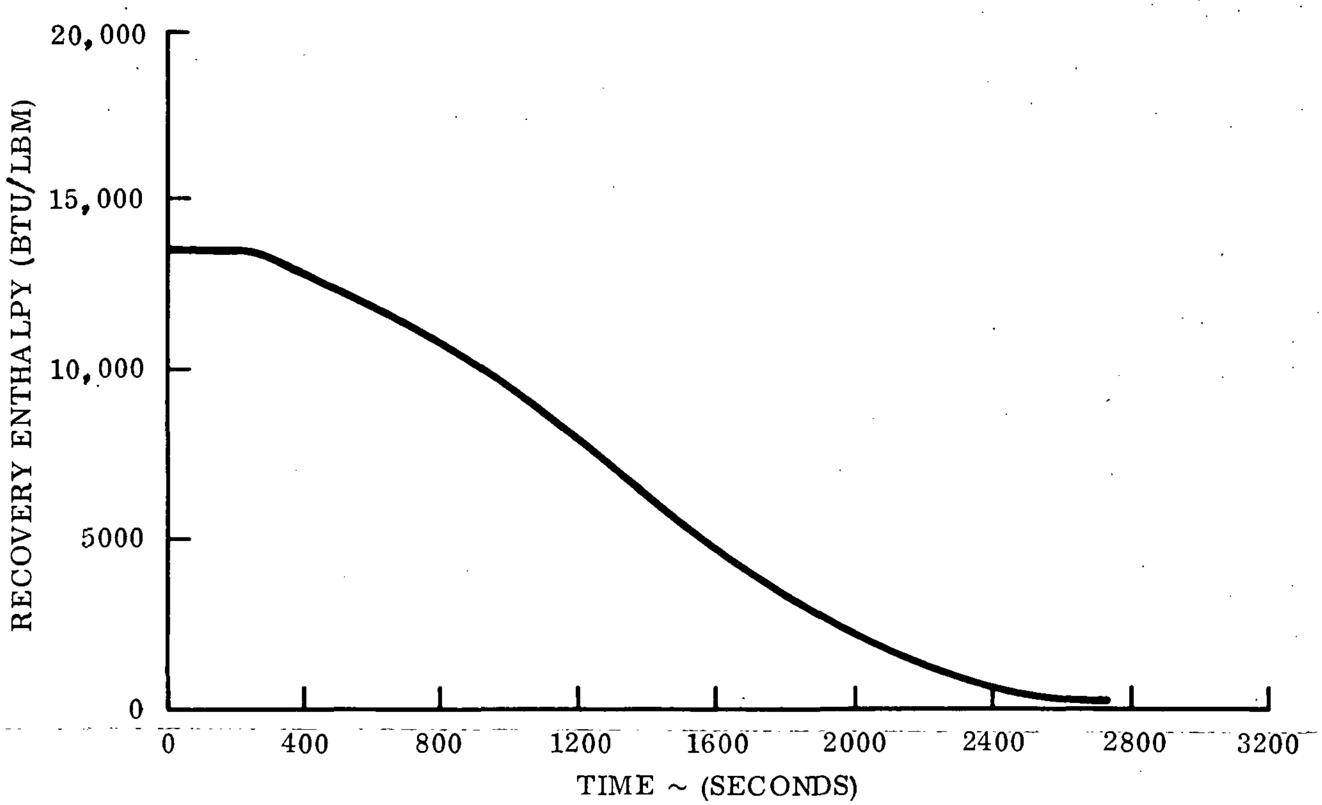

Figure 2-4. Recovery Enthalpy

Boundary layer edge pressure and free stream static pressure histories are reproduced in Figure 2-5. The basic analysis assumed the ablator was instantaneously vented to the boundary layer edge pressure. Since the external pressure environments are continuously increasing during re-entry, the assumption is conservative because it results in the highest possible pressure history within the ablator.

2.1.3 STRUCTURAL DESIGN REQUIREMENTS

Structural design is based upon the two locations on the bottom surface designated as Area 1 and Area 2. This represents the NASA/MSC point design requirements. The loading conditions are shown in Figures 2-6 and 2-7 in terms of pressure loading and line load for the two areas. Local heating rate is also shown for reference. Based upon these time histories of loading, a set of potentially critical conditions was selected for structure design as shown in Table 2-1.

The orbiter will be exposed to acoustic and aerodynamic pressure fluctuations which will cause structural vibrations throughout the Vehicle. The launch/exit acoustic spectrum is shown in Figure 2-8. This acoustic excitation lasts for about 45 seconds per flight and the overall sound pressure level is 162 dB. During entry, the spectrum shown in Figure 2-9 is encountered. This represents an overall sound pressure level of 141 dB. Duration of this excitation is 15 minutes per flight.

Vibration environments for launch/exit flight and for entry are given in Table 2-2.

Structural design of the TPS system shall be based on the following criteria:

a. No in-plane cracks in the ablator shall occur at 1.5 times limit load stress or strain.

b. No cracks shall occur through the entire ablator thickness at 1.5 times load stress or strain.

c. No catastrophic failures shall occur at ultimate load stress or strain.

Limit load stress/strain is defined as 1.0 times the stress/strain resulting from the highest expected mechanical load or thermal heating.

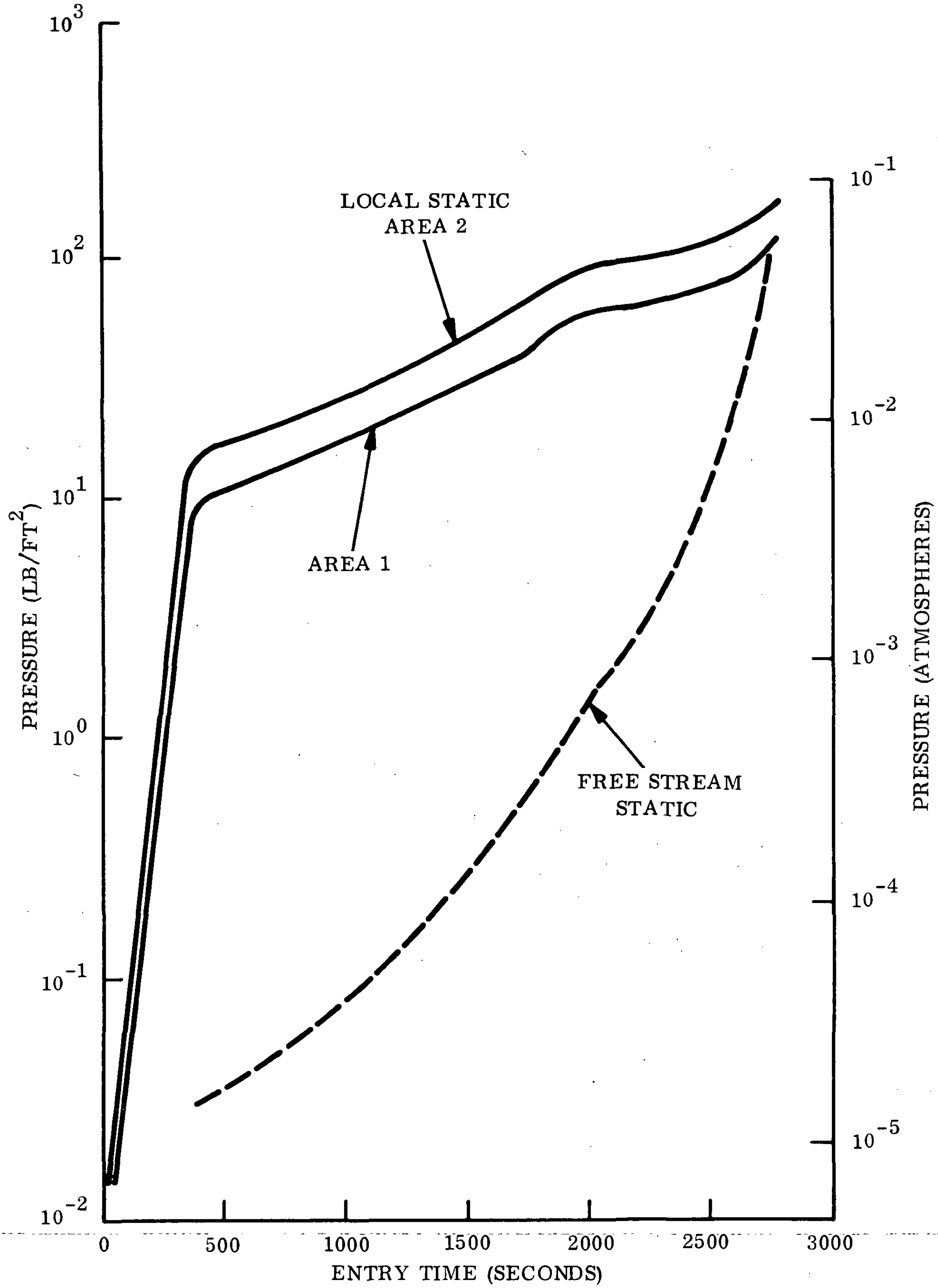

Figure 2-5. Free Stream And Local Pressure Histories On Orbiter Centerline During Entry

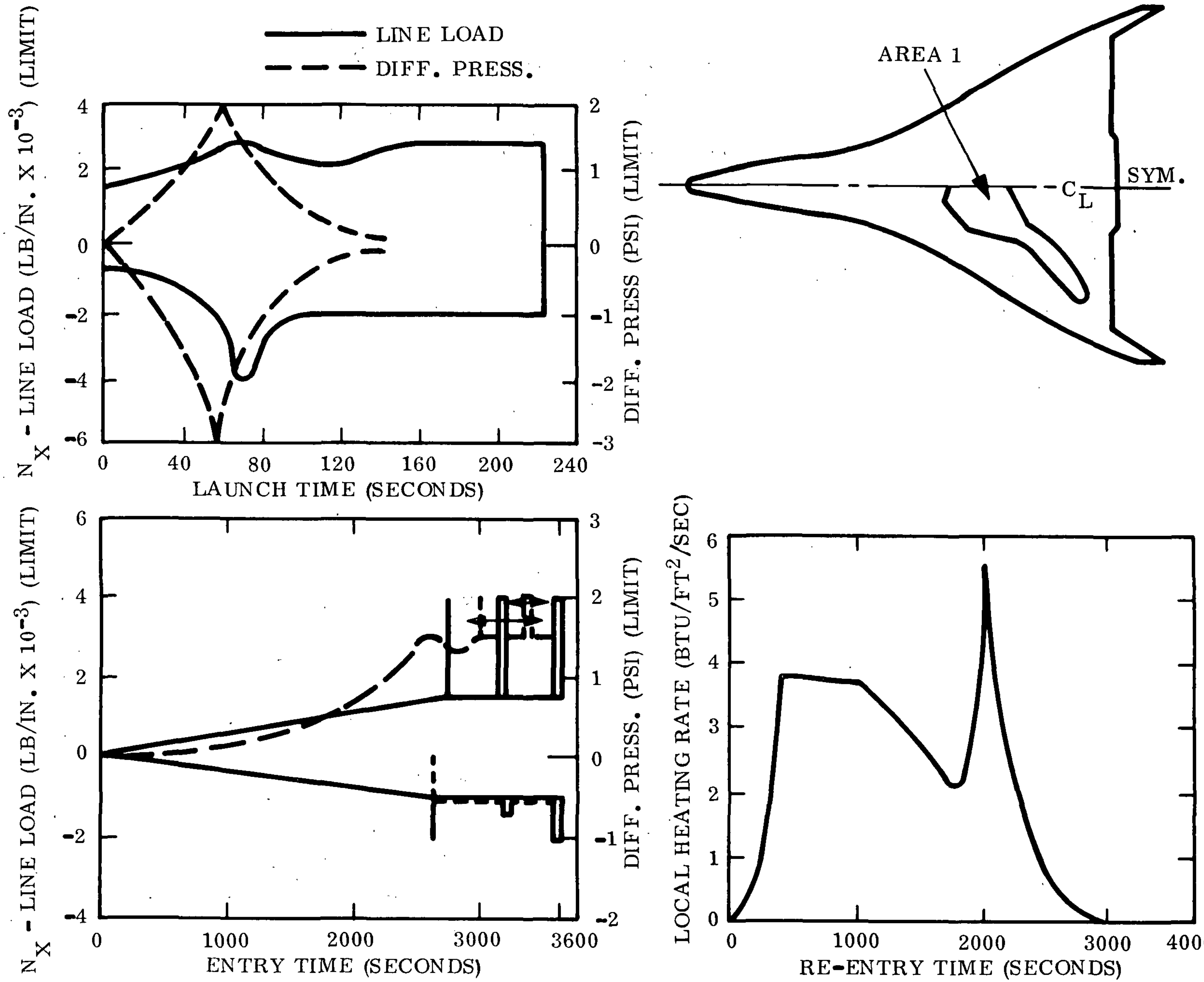

Figure 2-6. Area 1 Environments

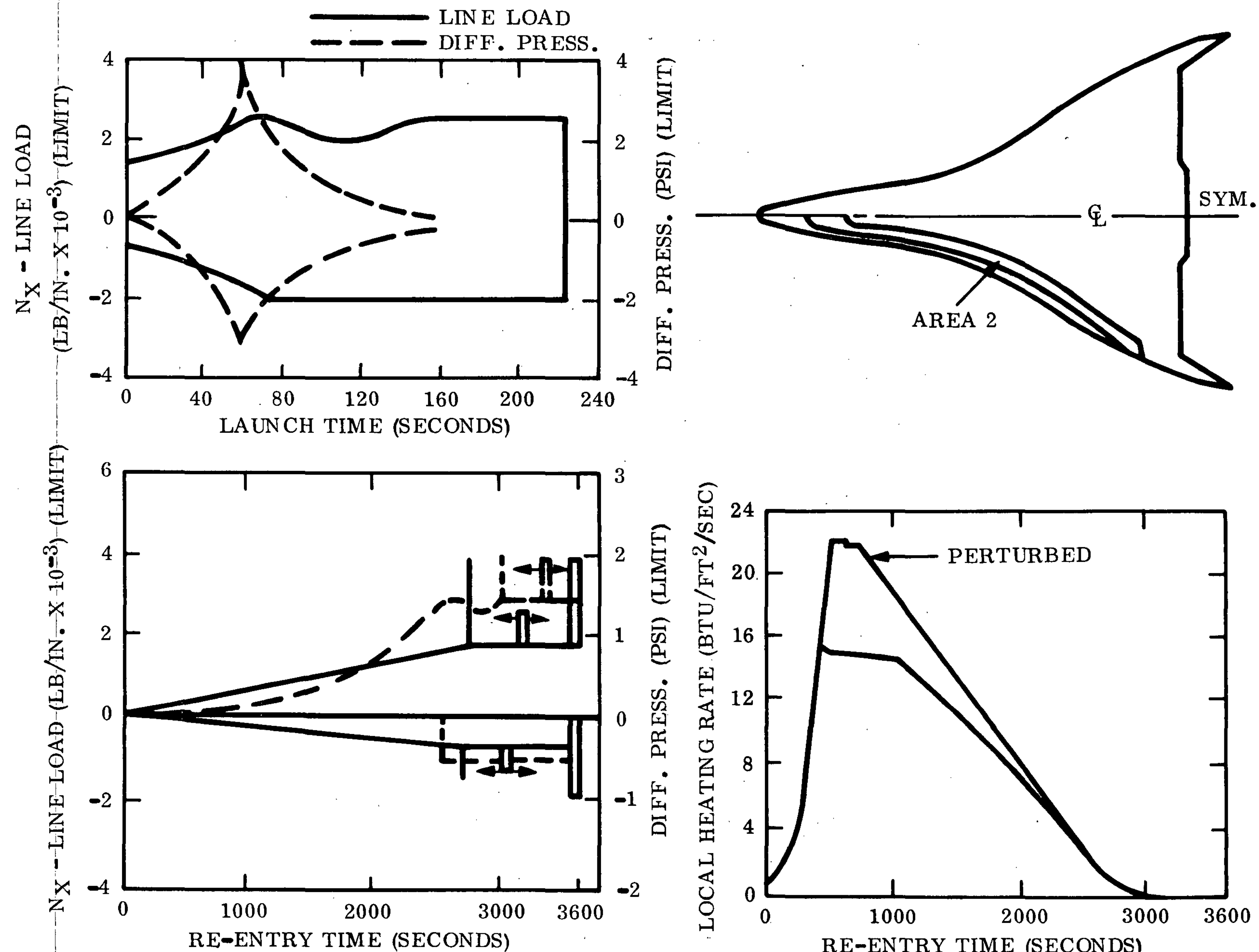

Figure 2-7. Area 2 Environments

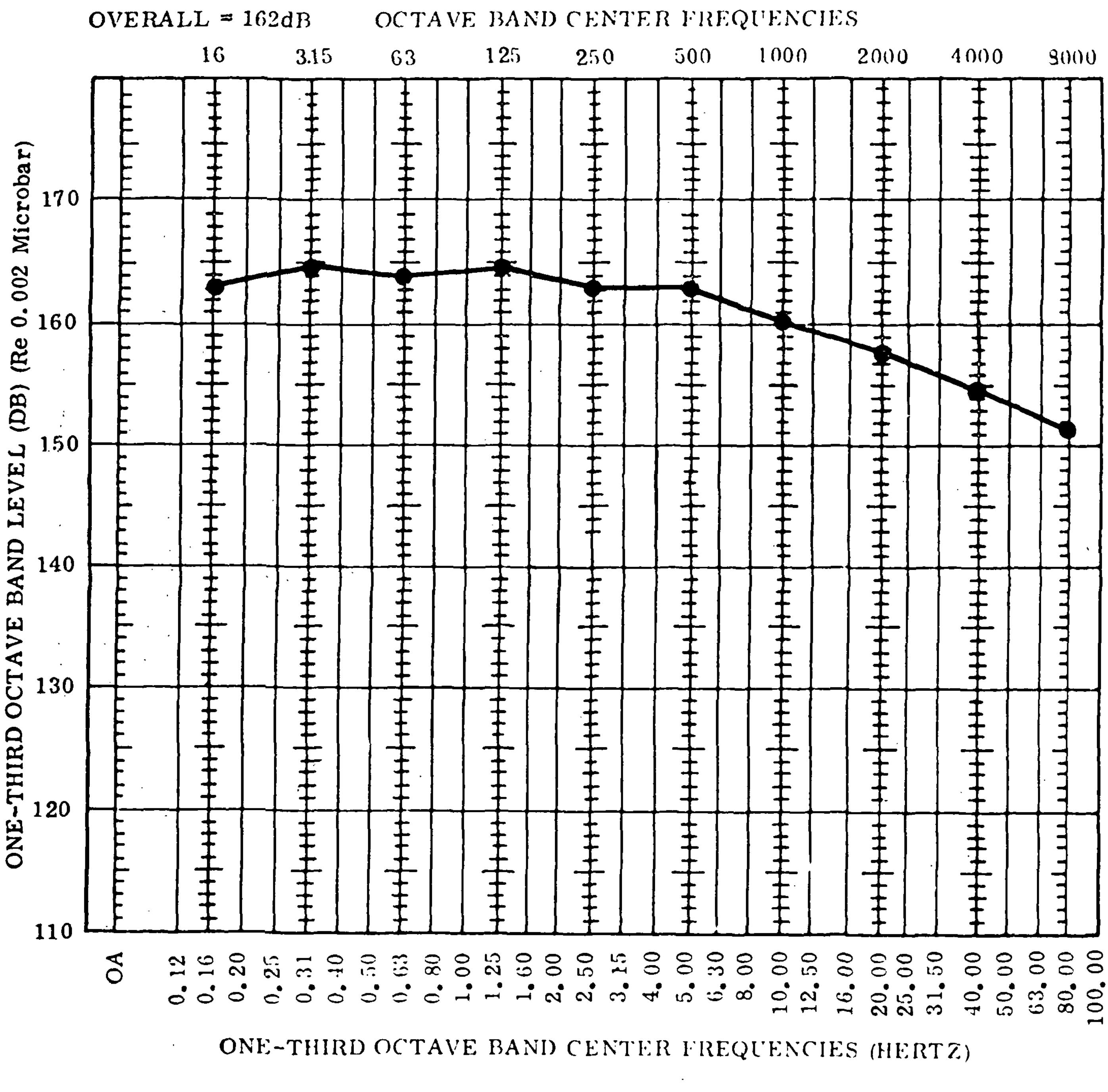

Figure 2-8. Octave Band Sound Pressure Levels, Lift-Off/Exit

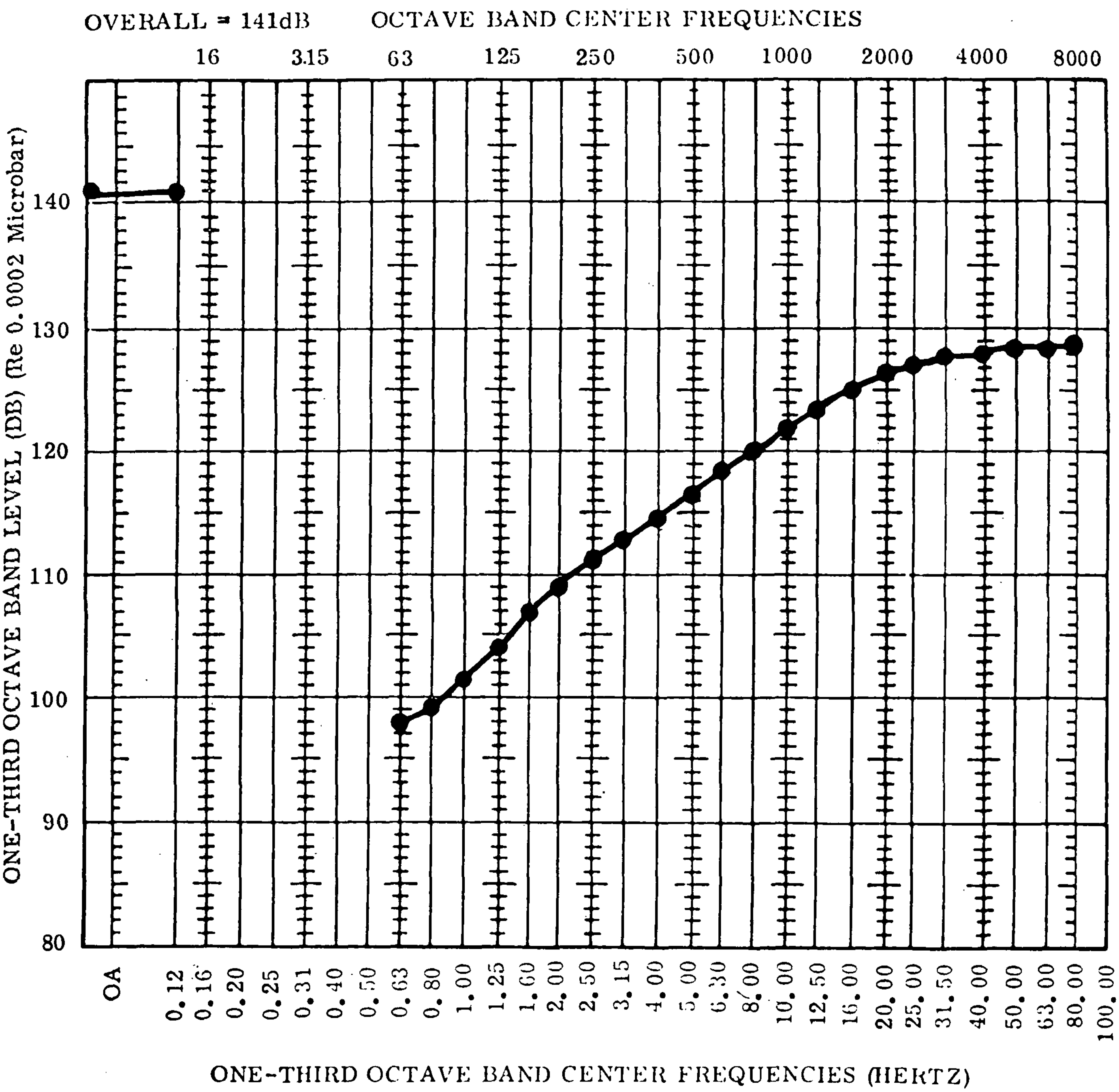

Figure 2-9. One-Third Octave Band Fluctuating Pressure Levels - Entry
(M = 4, Q = 100 psf)

TABLE 2-1. SUBSTRUCTURE DESIGN CONDITIONS

Area And Phase	Cond. No.	Nx (Lb/In.)	ΔP (PSI)
AREA 1 LAUNCH PHASE	1	2400	2.0
	2	-2000	2.0
	3	2700	0.9
	4	-4000	0.9
	5	2400	-3.0
	6	-2000	-3.0
	7	2700	-1.5
	8	-4000	-1.5
AREA 1 RE-ENTRY PHASE	9	4000	2.0
	10	-2000	2.0
	11	4000	-0.5
	12	-2000	-0.5
AREA 2 LAUNCH PHASE	1	2300	4.0
	2	-1500	4.0
	3	2700	1.8
	4	-2000	1.8
	5	2300	-3.0
	6	-1500	-3.0
	7	2700	-1.8
	8	-2000	-1.8
AREA 2 RE-ENTRY PHASE	9	4000	2.0
	10	-2000	2.0
	11	4000	-0.5
	12	-2000	-0.5

TABLE 2-2. VIBRATION LEVEL SUMMARY

Test Phase	Exit		Entry	
VIBRATION (RANDOM)	Freq (Hz)	Level	Freq (Hz)	Level
	20-155	0.015 g^2/Hz	20-100	+6dB/Oct
	155-700	+6dB/Oct	100-2000	0.1 g^2/Hz
	700-2000	0.3 g^2/Hz		
	(21.5 G RMS)		(13.8 G RMS)	
SINE SWEEP	2.0 g's ± 10%, 20-2000 Hz, 1 Oct/60 Sec.			

Ultimate load stress/strain is defined in the following ways:

a. 1.5 times limit mechanical load stress/strain when acting alone,

b. 1.5 times limit thermal stress/strain when acting alone, or

c. $K_1F_m + K_2F_t$, where $K_1 = K_2 = 1.5$ when additive; $K_1 = 1.0$, $K_2 = 1.5$, or $K_1 = 1.5$, $K_2 = 1.0$ when not additive; F_m = limit mechanical load stress, F_t = limit thermal stress.

In no case shall allowable ultimate stress/strain be less than 1.35 times $F_m + F_t$.

2.2 DEVELOPMENT REQUIREMENTS

In addition to meeting the requirements outlined in Section 2.1, the ablative covering must be sufficiently flexible to permit direct application to any area of the shuttle where thermal protection of this type is required. The ablative covering should remain dimensionally and shape stable under all conditions. To these ends the various factors that must be considered include:

The carpet reinforcement should preferably be constructed from a fiber that will withstand the temperatures encountered during the most severe heating. Candidate fibers include leached glass and quartz. The backing must also be able to withstand backface temperatures of at least 650°F. The construction and the viscosity of the uncured ablative material should be such that the carpet reinforcement can be filled with the ablator, and the pile fibers remain in the upright position. Also, the ablative material must adhere to the carpet pile and backing so as not to fall out under any conditions likely to be encountered by the Space Shuttle. There should be minimum dimensional change in the ablator during cure to eliminate any warping or buckling of the carpet construction. The mechanical properties of the composite must be adequate to withstand the loads encountered by the orbiter.

The composite system (i.e., ablator plus carpet) should permit cutouts and joints and seals which will be essentially impervious to the hot gases generated during ablation.

For attachment and easy removal of the ablative covering, ideally the backing should be such that it can be hooked into a hook-type construction which will be attached to the structure. For this purpose, the GE-BAS concept, the MSC spire concept, and the Velcro molded arrowhead concept were considered in addition to direct bonding. These approaches are described more fully in Paragraph 4.2.

The attachment system must have sufficient strength to withstand the loads that will be imposed on the system. It is especially necessary to have sufficient peel strength at the edges to prevent lifting of the edges of the ablative panels.

The total system must also be amenable to nondestructive inspection and testing techniques and normal handling procedures so that the reliability of the total system can be determined and assured.

The above factors were elaluated on small-scale laboratory specimens. From these studies, an assessment was made of the feasibility of the scale-up of the preferred system to flight size hardware.

SECTION 3

MATERIAL DEVELOPMENT STUDIES

3. MATERIAL DEVELOPMENT STUDIES

3.1 WOVEN CARPET CONSTRUCTION DEVELOPMENT

Two different approaches were used in the development of the pile support fabric for the flexible ablative heat shield since there are two major processes used in preparing commercial carpets, each requiring different manufacturing techniques.

The tufting process is essentially low in cost, even though it uses two consecutive processes, compared to the Wilton machine, which is a double warp card controlled (Jacquard loom) process. To make a tufted pile, the first step is to prepare a suitable ground fabric (Commercial carpeting uses a treated burlap). Three Nomex fabrics were prepared for this program, and they are listed in Table 3-1. When a tufted pile is made, a grooved needle pierces the backing fabric and carries the tufting yarn to the proper depth. It then retracts and is inserted at some predetermined increment which governs the pile density.

A loop of yarn is held in position by friction with the backing fabric; in commercial practice, this loop is stabilized in the backing by a layer of latex rubber or similar flexible material. The latex is characteristically thermally unstable. Note that the filling yarn in the Nomex backings is staple yarn. This selection was made to provide greater friction between the quartz loops and the Nomex by allowing short fiber ends to interlock with the quartz yarn. Figure 3-1 is a diagram illustrating the tufting process and showing how the loops are connected beneath the backing. Six tufted concepts were made — three cut pile, and three loop pile, as shown in Table 3-2. The cut pile was unstable and was unusable for any purpose. The loop pile, while more stable, tends to show some loop sliding with the result that pile height is erratic. Based on these trials, it was decided to abandon the tufting process and concentrate on the Wilton-Jacquard process (see Appendix B).

Seven Wilton-Jacquard weaves were made as shown in Table 3-3. The pile weaving pattern is shown in Figure 3-2. Sample 1 was made with a continuous filament yarn filling. When the tufts were observed to slip, sample 2 was made with a staple yarn filling. This solved the slipping problem and resulted in a stable configuration. Both samples were made with a cut wire, and preliminary observation caused the selection of two variables — lessened pile density and combination of loop and cut piles. Samples 6, 7, 8, and 9 were made to explore these variables, and all weaves were found to be stable. A combination of low and high loops resulted in samples 10 and 11, with sample 11 having the lowest pile density made thus far. Samples 12, 13, and 14 were similar to each other and consisted of a Fiberglas ground cloth and 8 Astroquartz tufts per inch^2.

From the filling trials (described in Paragraph 3.3), with the various constructions listed in the tables, it became apparent that weaves similar to those described as samples 15 and 16 in Table 3-3 should prove to be suitable for specimen fabrication. These constructions were used for fabrication of test specimens and also for fabrication of the deliverable items.

In addition to the woven carpets, samples of both the Fiberglas and Nomex backings, without the tufts, were obtained for additional experimentation.

TABLE 3-1. DESCRIPTION OF WOVEN CONCEPTS (Backing for Tufting)

SAMPLE #3: WILTON WEAVE	
256 pitch (1)	
Stuffer warp	- Nomex 1200 denier, 3.5 tpi Z (2)
Chain warp	- Nomex 1200 denier, 3.5 tpi Z
Filling	- (1 end of Nomex spun yarn 5/2 cotton count) (3) 20 picks/inch
SAMPLE #4: WILTON WEAVE	
256 pitch	
Stuffer warp	- Nomex 1200 denier, 3.5 tpi Z
Chain warp	- Nomex 1200 denier, 3.5 tpi Z
Filling	- (2 ends of Nomex spun yarn 5/2 cotton count) 16 picks/inch
SAMPLE #5: WILTON WEAVE	
256 pitch	
Stuffer warp	- Nomex 1200 denier, 3.5 tpi Z
Chain warp	- Nomex 1200 denier, 3.5 tpi Z
Filling	- (2 ends of Nomex spun yarn 5/2 cotton count) 20 picks/inch

(1) 256 pitch = 256 pile ends in 27 inches of width.
(2) 3.5 tpi Z = 3.5 turns per inch in the Z direction.
(3) 5/2 cotton count = 2 ends in a 5 cotton count fiber. (Cotton count = the number of 840-yard hanks per pound.)

TABLE 3-2. TUFTED CONCEPTS

TUFTING CUT PILE

Pile yarn - Astroquartz - 300 4/4, 4Z - 3.8 'S'*

SAMPLE #3A:

5/32 gauge tufter - 7/8" cut-pile - 5 stitches/inch
Backing from Sample #3
(30 tufts per square inch) 3-3/4" x 12" sample
Comments: 70% of pile yarn not cutting or pulling out of backing

SAMPLE #4A:

5/32 gauge tufter - 7/8" cut-pile - 5 stitches/inch
Backing from Sample #4
(30 tufts per square inch) 3-3/4" x 12" sample
Comments: 50% of pile yarn not cutting or pulling out of backing

SAMPLE #5A:

5/32 gauge tufter - 7/8" cut-pile - 5 stitches/inch
Backing from Sample #5
(30 tufts per square inch) 3-3/4" x 12" sample
Comments: 15% of pile yarn not cutting or pulling out of backing

TUFTING LOOP PILE

Pile yarn - Astroquartz - 300 4/4, 4Z - 3.8 'S'

SAMPLE #3B:

5/32 gauge tufter, 3/4" loop pile - 5 stitches/inch
Backing from Sample #3
(30 loops per square inch) 7-1/2" x 12" sample

SAMPLE #4B:

5/32 gauge tufter, 3/4" loop pile - 5 stitches/inch
Backing from Sample #4
(30 loops per square inch) 7-1/2" x 12" sample

SAMPLE #5B:

5/32 gauge tufter, 3/4" loop pile - 5 stitches/inch
Backing from Sample #5
(30 loops per square inch) 7-1/2" x 12" sample

* (See Appendix A)

TABLE 3-3. WILTON-JACQUARD WEAVES

PATTERN #45 - 1 Frame
256 pitch - pile 'W' weave
Stuffer warp - 2400 denier Nomex, 3-1/2 tpi Z
Chain warp - 2400 denier Nomex, 3-1/2 tpi Z
Pile yarn construction - Astroquartz 300 4/4, 4Z, 3.8 'S'

SAMPLE #1:
10 rows/inch or 20 picks/inch
Pile height - .875 cut
Filling - 2400 denier Nomex, 3-1/2 tpi Z
Pile - 50 tufts/in^2

SAMPLE #2:
10 rows/inch or 20 picks/inch
Pile height - .875 cut
Filling - Nomex spun yarn 5/2 cotton count
Pile - 50 tufts/in^2

PATTERN #45 - #56 - 1 Frame
256 pitch - pile woven thru back
Stuffer warp - Nomex 1200 denier, 3-1/2 tpi Z
Chain warp - Nomex 1200 denier, 3-1/2 tpi Z
Filling - 2 ends of Nomex spun yarn 5/2 cotton count

Pile yarn construction - Astroquartz yarn, 300 4/4, 4Z - 3.8 'S' 2400 denier

SAMPLE #6:
8 rows/inch - 16 picks/inch - .875 cut wire
(Pile 40 tufts per square inch) 8" x 12" sample

SAMPLE #7: Pattern #45
8 rows/inch - 16 picks/inch - .875 round wire
(Pile 40 tufts per square inch) 8" x 12" sample

SAMPLE #8: Pattern #56
8 rows/inch - 16 picks/inch - .875 cut wire
(32 tufts per square inch) 8" x 6" sample

SAMPLE #9: Pattern #56
8 rows/inch - 16 picks/inch - .875 round wire
(32 tufts per square inch) 8" x 10" sample

SAMPLES #10 & #11
256 pitch, pattern #56, pile through back
Stuffer warp - 1200 denier, 3.5 tpi Z Nomex
Chain warp - 1200 denier, 3.5 tpi Z Nomex
Pile yarn - 300, 4/4 - 4Z, 3.8 'S' Astroquartz
Filling yarn - 2 ends of spun Nomex 5/2 cotton count

TABLE 3-3. (CONTINUED)

SAMPLE #10

Pattern #56, 32 tufts/sq. inch
High and low loops
8 rows/inch or 16 picks/inch

SAMPLE #11

Pattern #57, 20 tufts/sq. inch
High and low loops
8 rows/inch or 16 picks/inch

High wire = .875"
Low wire = .375"

SAMPLES #12, 13, and 14

256 pitch, 1 Frame Pattern #58
Chain warp - 150 4/2 ECG Glass with 630 Binder
Stuffer warp - 150 4/2 ECG Glass with 630 Binder
Pile yarn - 300 4/4 Astroquartz

SAMPLE #12

16 picks/inch, .875" pile height
Filling yarn - ECG 150 4/2 Fiberglas with 630 Binder
8 tufts/in^2
Sample size - 13" x 36"

SAMPLE #13

16 picks/inch, .875" pile height
Filling yarn - ECG 150 4/2 Fiberglas with 630 Binder
8 tufts/in^2
Sample size - 13" x 36"

SAMPLE #14

16 picks/inch, .875" pile height
Filling yarn - ECG 150 4/2 Fiberglas with 630 Binder
8 tufts/in^2
Sample size - 13" x 36"

SAMPLE #15 - Astroquartz Pile with Fiberglas Backing

Backing - 150 4/2 ECG
Pile - 300 4/4 Astroquartz
Pile height - .875"
Pile density - 8 tufts/in^2

SAMPLE #16

Backing - 200/100 5-Ply Nomex
Pile - 300/4/4 Astroquartz
Pile height - .875"
Pile density - 8 tufts/in^2

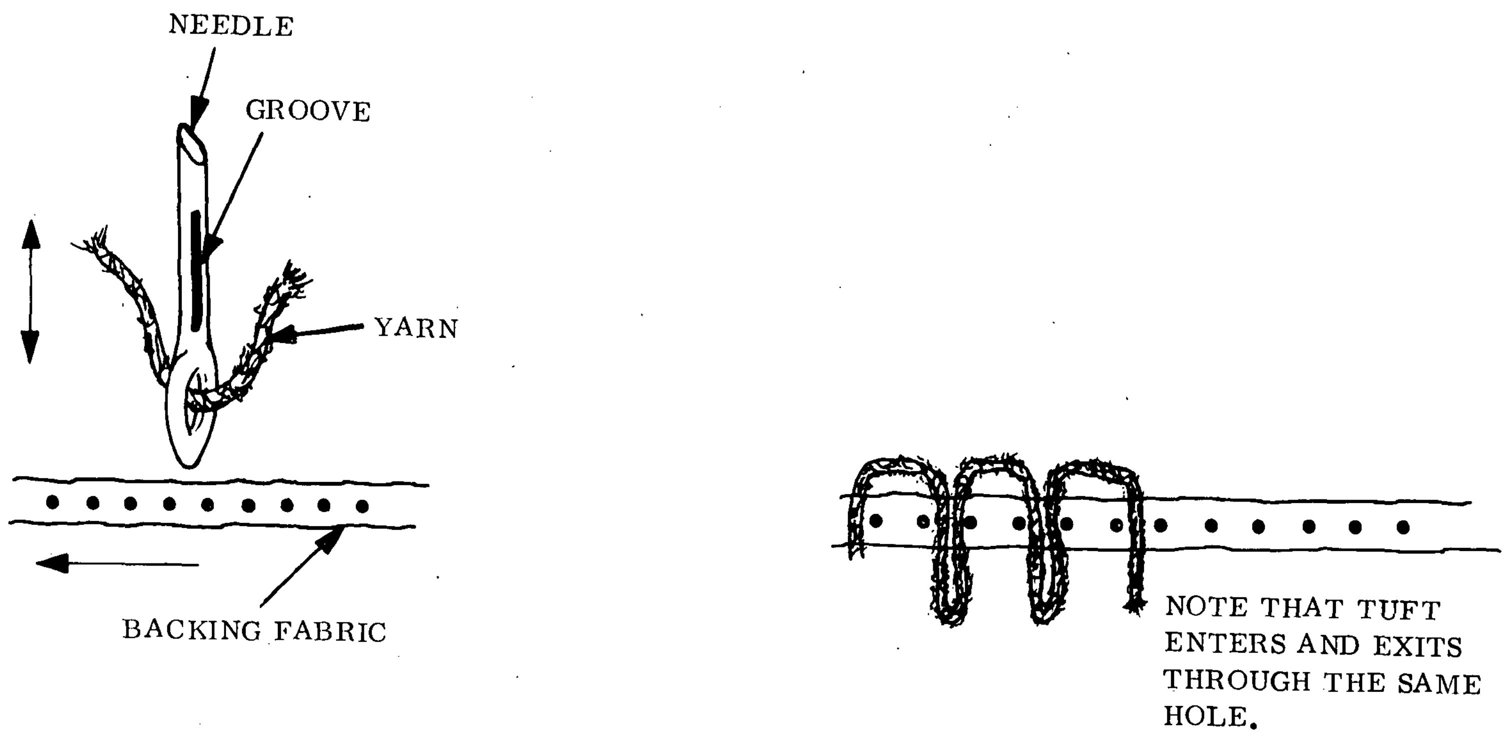

Figure 3-1. Tufting Process

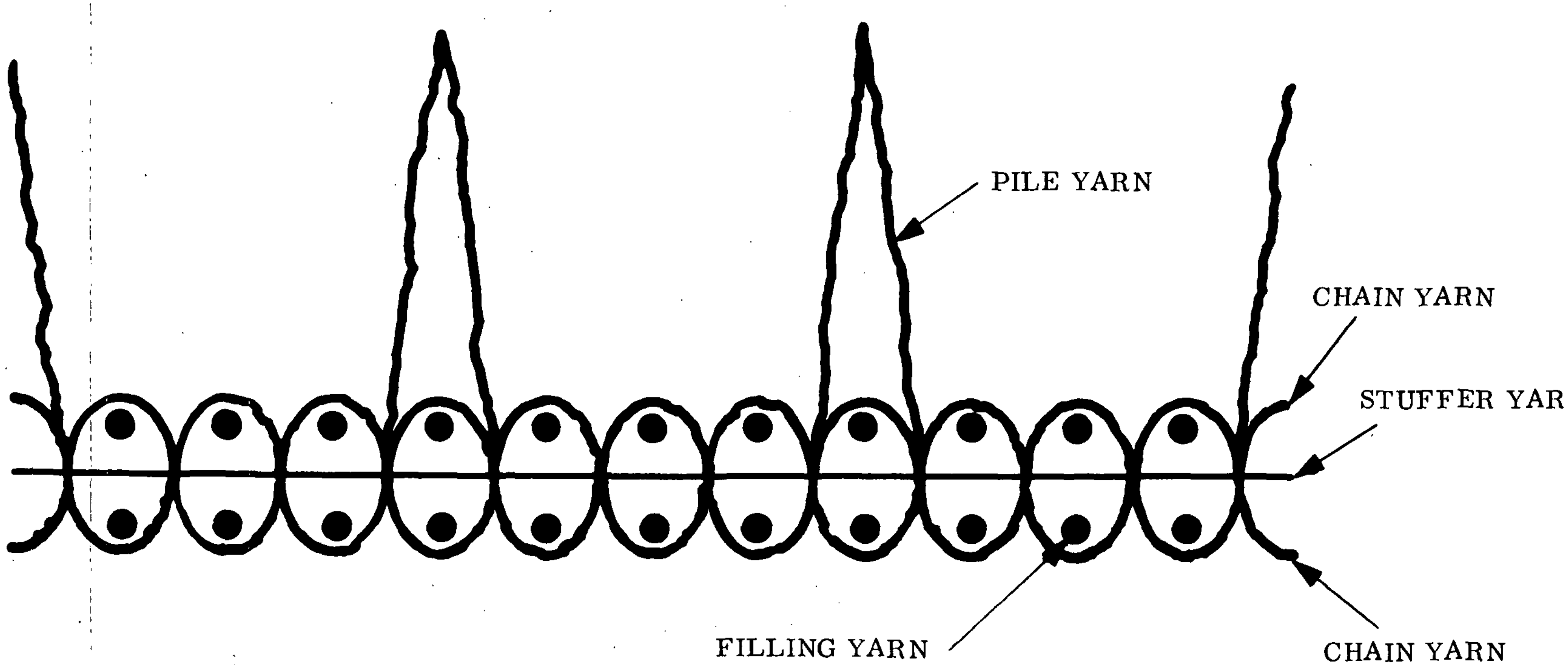

Figure 3-2. Wilton Pile Weaving Pattern

3.2 ABLATIVE FILLER DEVELOPMENT

Three main classes of flexible ablators were considered as potential candidates for the program. These are:

a. ESM 1004 Series - These materials are based on RTV 560 and can be fabricated at density levels from ~12 lb/ft^3 to ~90 lb/ft^3. Because they are prepared by a chemical foaming process and are reinforced with up to 13 weight percent of inorganic fibers, they are flexible in the virgin state and form strong, coherent chars as a result of ablation. These materials have been fabricated in honeycomb as well as in the unsupported state. The prime materials in this series are:

   1. ESM 1004AP - This material has a density of 35 ± 3 lb/ft^3. It has been well characterized and many of its properties have been made available (Reference 1). It has been extensively tested under a variety of conditions in the 5 M.W. arc facility, and has the potential as a shape stable ablator for leading edge application.

   2. ESM 1004X - This material has a density of $\sim 15 \pm 2$ lb/ft^3. The foaming process used in its fabrication results in an open cell structure. It has been well characterized but not as extensively as ESM 1004AP (Reference 1). It was developed as a candidate TPS during the pre-Voyager and pre-Viking work. Because of the open-cell structure of this material, it is coated with 10 mils of solid RTV 560 to prevent flow-through of hot gases during ablation.

b. ESM 1030 - This is a chemically foamed epoxy-modified silicone. It has a nominal density of ~18 lb/ft^3. It was also developed during the pre-Voyager/Viking work and has been characterized almost as extensively as ESM 1004X (Reference 1).

c. FSA 1040 - This material was developed near the end of the ENCAP program as a flexible heat shield material. However, the program was discontinued before characterization was initiated. It has been fabricated in densities ranging from ~10 to 60 lb/ft^3. An ablation test in the 5 M.W. arc at 10 BTU/ft^2-sec. showed it to be comparable to the ESM 1004 materials in performance. Because of its flexibility, toughness, and apparent efficient ablation performance, it was selected as the prime material for the flexible ablator study. At a density level of 30-35 lb/ft^3, it was considered to be a candidate leading edge material and at 15 lb/ft^3 as the prime material for Area 1 of the vehicle.

Subsequent work with samples of both unsupported and woven-carpet-supported FSA 1040 involved subjecting specimens to a vacuum exposure at room temperature. All samples experienced an immediate pronounced increase in dimensions. This increase, which in some cases amounted to a twofold increase in dimensions, persisted for about one hour. The samples then shrank to approximately one-half their original size. After several hours at atmospheric pressure, they returned to their original dimensions.

This phenomenon illustrates the closed-cell characteristics of the FSA-1040 foam as well as the imperviousness of the cell walls to gases. Although these characteristics could be overcome, a development study would have been required which is outside the scope of this program.

As a result of the foregoing, ESM 1004 was selected as the ablative filler for the carpet concept. Samples of both ESM 1004AP which is a closed cell foam, and ESM 1004X which is open cell, suffered no dimensional changes when subjected to vacuum exposure. In addition, both formulations are off-the-shelf items and have been extensively characterized. Typical data for both ESM 1004AP and ESM 1004X are summarized in Table 3-4.

3.3 STUDIES ON FILLING WOVEN CARPET CONSTRUCTIONS

Attempts were made at foaming the FSA 1040 formulation in all the carpet samples listed in Tables 3-1 through 3-3. In all cases, it was found that the foaming process of the ablative material was affected by the pile yarns. The yarn surfaces appeared to act as nucleation centers, causing the gas bubbles within the liquid silicone rubber to cling to the fiber and distort the foam structure. From these studies, it was apparent that a cut pile distorted the foam structure less than a loop pile fabric, and a cut pile was then selected for additional studies.

It was also noted that the pile fibers produced an over-all retardation effect on the foaming process so that the ablator was 2-5 lb/ft^3 more dense than the foam from a similar formulation free-foamed.

It has been noted that when the tufting fibers were cut at the end of the weaving process, there was a tendency for untwisting to occur which resulted in considerable fraying of the fibers. As a means for overcoming this, and also in an attempt to reduce the effect of the yarn surface on the foaming process, a decision was made to rigidize the pile yarn, prior to use, with a coating of GE silicone primer SS4004. This treatment was also selected to improve adhesion between the silicone elastomeric ablative filler and the pile fibers.

With the observation of the dimensional instability of FSA 1040 in vacuum (Paragraph 3.2), ESM 1004 formulations were used for subsequent filling trials. Figure 3-3 is a photograph of a cross-section of a typical ESM 1004X unsupported foam. The open-cell structure and uniformity of the foam are well illustrated.

TABLE 3-4. PROPERTIES OF LOW-DENSITY ELASTOMERIC SHIELD MATERIALS (ESM 1004)

PROPERTIES	ESM 1004-X		ESM 1004AP	
THERMAL				
A. SPECIFIC HEAT (BTU/LB-°F)	VIRGIN	CHAR	VIRGIN	CHAR
0°F	0.28	—	—	—
100°F	0.31	—	0.30	—
300°F	0.35	—	0.39	—
500°F	0.38	—	0.43	—
600°F	—	0.25	—	0.26
B. DYNAMIC ENTHALPY	STRONG ENDOTHERM - 0.01 ATM, AIR; SLIGHT EXOTHERM - 1 ATM, AIR		------ EXOTHERM (AIR, 1 ATM, 725°F)	
C. THERMAL CONDUCTIVITY X 10^5 (BTU/FT-SEC-°F) 1 ATM, AIR	VIRGIN	CHAR	VIRGIN	CHAR
0°F	1.00	—	—	—
100°F	1.14	—	2.25	—
300°F	1.46	—	2.14	—
1200°F	—	5.2	—	9.9
D. TGA - 5% WT. LOSS	*650°F		800°F	
50% WT. LOSS	1150°F		1120°F	
RESIDUAL WT.	35%		43%	
ONSET OF RAPID WT. LOSS:	~750°F		~750°F	
E. WEIGHT LOSS IN VACUUM 10^{-5} MM HG. - R.T. 5 DAYS	0.17%		-------	

* ESM 1004AP POST CURE = 500°F, ESM 1004X POST CURE = 300°F. INITIAL WEIGHT LOSS DUE TO UNREACTED RESIDUAL VOLATILES AND NOT THERMAL DECOMPOSITION.

PROPERTIES		ESM 1004-X	ESM 1004AP
THERMOPHYSICAL			
VIRGIN DENSITY, ρ_V LB/FT^3		15	35
CHAR DENSITY, ρ_C, LB/FT^3		6	14.4
SURFACE EMISSIVITY,		0.85	0.85
PYROLYSIS GAS SPECIFIC HEAT, Cp_G BTU/LB°R		0.384	0.384
MOLECULAR WEIGHT OF INJECTED SPECIES, M_G		24.5	24.5
ORDER OF REACTION,		2	2
PRE-EXPONENTIAL FACTOR, Z SEC^{-1}		30,000	30,000
ACTIVATION ENERGY, E BTU/LB MOLE		47,500	47,500
HEAT OF DECOMPOSITION H_{GF} BTU/LB GAS GENERATED	1135°R	50	50
	1460	450	450
	1710	1,000	1,000
	2610	1,960	1,960
MECHANICAL/PHYSICAL			
A. DENSITY (LB/FT^3)		15 ± 2	35 ± 3

B. TENSILE PROPERTIES	ESM 1004-X STRESS (PSI)	ESM 1004-X ELONG. (%)	ESM 1004-X ELASTIC MODULUS (PSI)	ESM 1004AP STRESS (PSI)	ESM 1004AP ELONG. (%)	ESM 1004AP ELASTIC MODULUS (PSI)
-150°F	32	40	95	150	50	300
-100°F	14	--	--	90	46	210
-50°F	9	22	60	70	34	200
75°F	7	22	45	60	25	200
300°F	6	17	45	50 (EST)	22	200

PROPERTIES	ESM 1004-X	ESM 1004AP
C. BOND SHEAR STRENGTH SHIELD/BOND SYSTEM	SHEAR STRENGTH (PSF) (RTV 560 TO Ti)	SHEAR STRENGTH (PSF) (RTV 560 TO BE)
-150°F	5820 (COHESIVE FAILURE IN ESM 1004-X)	-----------------
75°F	1320 (COHESIVE FAILURE IN ESM 1004-X)	10800 (COHESIVE FAILURE IN ESM 1004AP)
300°F	1180 (COHESIVE FAILURE IN ESM 1004-X)	6750 (COHESIVE FAILURE IN ESM 1004AP)
500°F	1120 (COHESIVE FAILURE IN ESM 1004-X)	4500 (COHESIVE FAILURE IN ESM 1004AP)
800°F	518 (ADHESIVE TO Ti)	-----------------
D. BOND SHEAR STRENGTH - BOND ALUMINUM TO ALUMINUM RTV 560 ADHESIVE	SHEAR STRENGTH (PSI)	SHEAR STRENGTH (PSI)
75°F	600 (AVERAGE)	600 (AVERAGE)
400°F	250 (AVERAGE)	250 (AVERAGE)
E. THERMO STRUCTURAL - LOW TEMPERATURE COMPATIBILITY	NO FAILURE DOWN TO -300°F AS SUBSTANTIATED BY TEST.	NO FAILURE DOWN TO -300°F AS SUBSTANTIATED BY TEST.
OPTICAL		
A. TOTAL SOLAR ABSORPTANCE	0.755	---
TOTAL HEMISPHERICAL EMITTANCE	0.85 ± 0.1	0.85
RF TRANSMISSIVITY		
R.T. DIELECTRIC CONSTANT	1.70-J0.016	1.70-J0.016
LOSS TANGENT	0.009	0.009
ATTEN. COEFF. CM^{-1}	0.01229	0.01229
MAX. CHANGE IN SIGNAL TRANSMISSION HEATING	-0.4 DB	-0.4 DB
COOLING	0.2 DB	0.2 DB

	BASE ELASTOMER	REINFORCEMENT	TYPE FOAM	DENSITY (LB/FT^3)	NORMAL CURE	BOND
ESM 1004-X	RTV 560	12% INORGANIC FIBERS	CHEMICAL	15 ± 2	RT + 300°F	RTV 560
ESM 1004AP	RTV 560	12% INORGANIC FIBERS	CHEMICAL	35 ± 3	160°F + 300°F	RTV 560

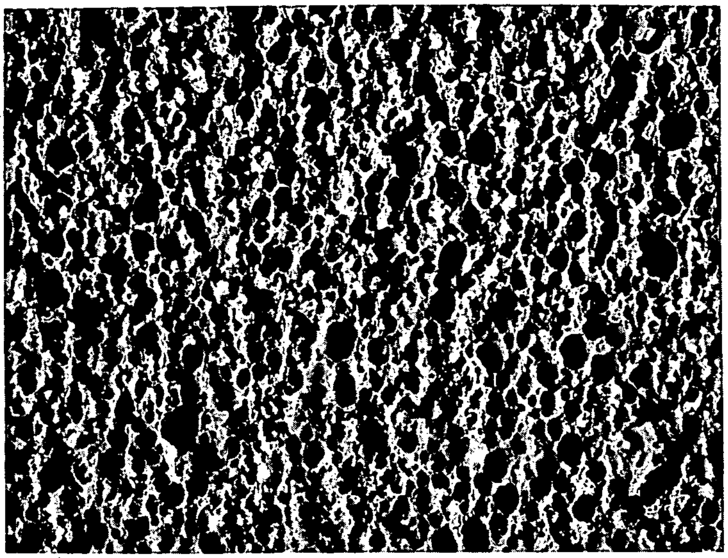

Figure 3-3. Cross-Sectional Photograph of ESM 1004X - Unsupported (Magnification 10X)

An ESM 1004X formulation at a density of 15 lb/ft^3 was foamed in place in a woven carpet reinforcement (Sample #15, Table 3-3) which had a Fiberglas backing and rigidized, cut, Astroquartz pile fibers. The pile fibers were primed with GE SS4004 primer and were inserted through the backing at 8 tufts/inch^2. The overall density of the resulting composite was 20 lb/ft^3. Unfortunately, the sample warped so that the upper surface of the ablator was concave (Figure 3-4). A change to a carpet with Nomex backing (Sample #16, Table 3-3) produced even more warpage. It is felt that the excessive warpage observed with the Nomex carpet was due to the dimensional instability of the Nomex fabric at the cure temperature (350^o) required for ESM. The warpage is attributed to the fact that RTV 560, which is the base silicone for the ESM 1004 formulation, cures by a condensation mechanism, and the shrinkage of the ablator is due to the loss of volatiles formed in the curing process.

Various attempts were made to eliminate or minimize the warpage. For instance, the carpet was bonded to a curved surface (curved in the opposite direction to that obtained normally) and filled and cured in this configuration. Difficulty was experienced in filling

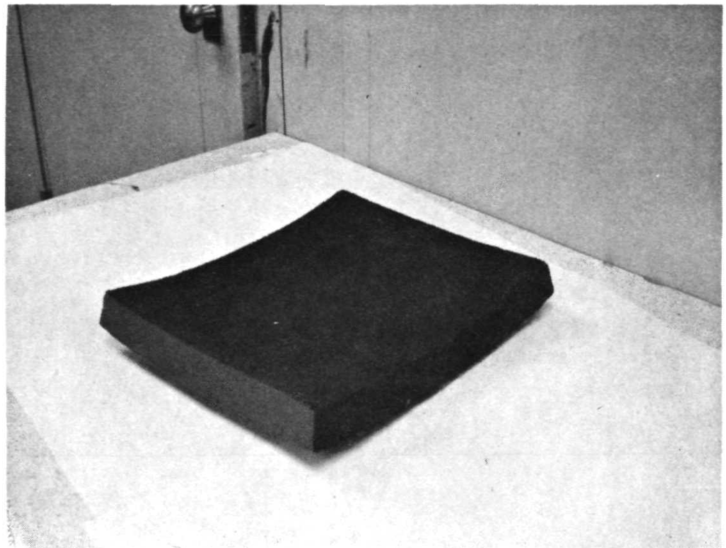

Figure 3-4. Sample of Woven Carpet Filled with ESM 1004X (Note Warpage)

the structure with the ablator, and in obtaining uniform foaming. Another approach involved fabricating the composite in the normal way and slitting the backing. This method was discontinued, after two early attempts, because of weakening of the integrity of the backing.

It was demonstrated that one method which reduced the warpage consisted of foaming the ESM to a thickness of 1-1/2 - 2 inches above the pile fibers in a carpet which was bonded with RTV 560 to an aluminum plate at least 1/8" thick. The ESM was cured and post-cured in this configuration, trimmed to thickness, and removed from the aluminum structure. This approach was used to fabricate the deliverable specimens.

Another approach which was demonstrated to eliminate warpage was one in which a loosely woven Fiberglas fabric was bonded to a piece of preformed, fully cured ESM. This was then mechanically tufted with Astroquartz fiber at a density of 9 tufts/inch^2. This method is suggested as the prime approach for additional work in this area and is illustrated in Figure 3-5. The approach is economically attractive, and in addition, the tufts are vertical and should provide optimum char reinforcement. Although this method has been demonstrated, additional effort would be required to arrive at an optimized solution. For instance, studies could be made to arrive at the optimum pile density, and also to determine the proper material composition of the pile fibers. Ideally, if the pile fibers fused with the char of the ablator, additional adhesion between the file fibers and the ablative filler would not be required.

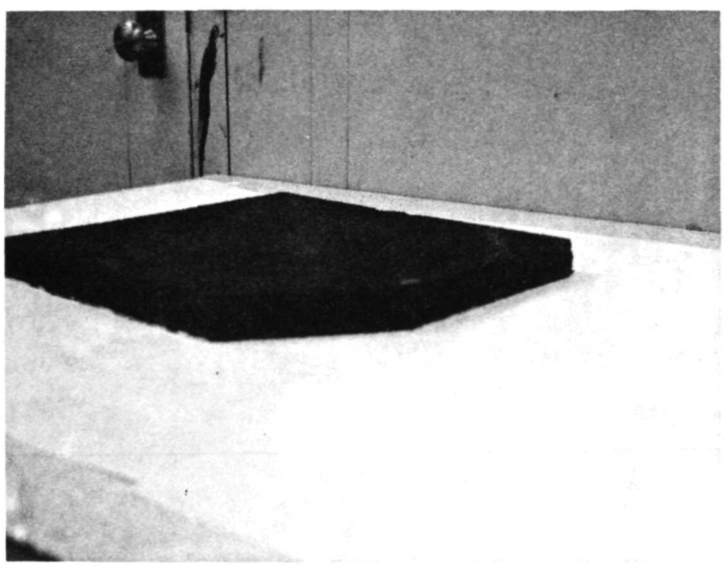

Figure 3-5. 12" x 12" Specimen of ESM 1004X with Backing Bonded On. (Note Lack of Warpage)

SECTION 4

DESIGN AND ANALYSIS

4. DESIGN AND ANALYSIS

4.1 DESIGN ANALYSIS

The thermal environment used in the design analysis and as defined by NASA-MSC is shown in Figures 2-3 through 2-5. Figure 2-3 shows the heat flux history for two typical orbiter locations, Area 1 representing typical lower fuselage heating and Area 2 and 2P representing typical wing leading edge heating. The recovery enthalpy time history is shown in Figure 2-4, and the local static and free stream static pressure histories are shown in Figure 2-5. These environments were used to generate ESM 1004X thickness requirements for Area 1 and Area 2P, and are compared with REI Mullite requirements. The flexible ablator thickness requirements were calculated, using the well-calibrated Reaction Kinetics Ablation Program (REKAP) (see Appendix C). Table 4-1 shows the REKAP model used for the ESM 1004X ablative filter. While the thermal conductivity of REI Mullite is very pressure-dependent as well as temperature-dependent, ESM 1004X does not have the same pressure dependency. Thermal conductivity measurements are presented in Reference 1 and show little dependency upon pressure down to 10^{-2} atm - 10^{-3} atm. Since most of the heating occurs when the local pressure is about 10^{-2} atm, the thermal conductivity assumed in this analysis for ESM 1004X was that measured at 1 atmosphere pressure. Surface coating and carpet and piles were ignored in the mathematical modeling which consisted of a layer of ESM 1004X and heat capacitances representing the bond and the structure.

Maximum structure temperature as a function of ESM 1004X thickness is shown in Figure 4-1 for the Area 1 and Area 2P environments. The effect of varying the structure thickness can also be seen in this figure.

Using thicknesses from Figure 4-1, weights for the ESM shield were calculated and are shown in Table 4-2 and Figure 4-2. Weights of the REI system were taken from Table 4.1.2-1 of Reference 2.

It is interesting to note that the ablator system is lighter than the REI TPS for heat loads greater than about 20,000 Btu/ft^2; i.e., for the hotter areas of the orbiter such as near the vehicle nose and the wing and tail leading edges. For the cooler areas (Area 1), the REI system is approximately 32% lighter. These weights are for a maximum structure temperature of 300^{o}F and include no margins of safety.

TABLE 4-1. ESM 1004X REKAP MODEL

T °R	Hgf BTU/LBM	Cp BTU/LBM °R	K BTU/FT SEC °R
1	50	.001	$.55 \times 10^{-5}$ ↓
250	↓	.18	.75
500	↓	.29	1.05
600	↓	.31	1.18
700	↓	.332	1.35
800	↓	.355	1.55
900	↓	.378	1.8
1000	↓	.398	2.0
1250	↓	.4	2.24
1500	45	↓	2.43
1750	1250	↓	2.65
2000	2730	↓	2.87
2250	2960	.46	3.12
2500	3050	.55	3.39
2750	3120	.643	3.68
3000	3165	.725	3.99
3250	3200	.805	4.32 ↓
20000	↓	↓	↓

ρ Density = 15 LBM/ft^3

ϵ Surface Emissivity = .8

ρ_c Char Density = 6 LBM/ft^3

kc/kv = 3.25

$c_{p_c}/C_{p_v} = 1$

η Order of Reaction = 2

Z Pre-exponential Factor = 15000 Sec^{-1}

E Activation Energy = 44700 BTU/LBM

M_{BL}/Mg = 1.18

Cpg = .4 BTU/LBM °R

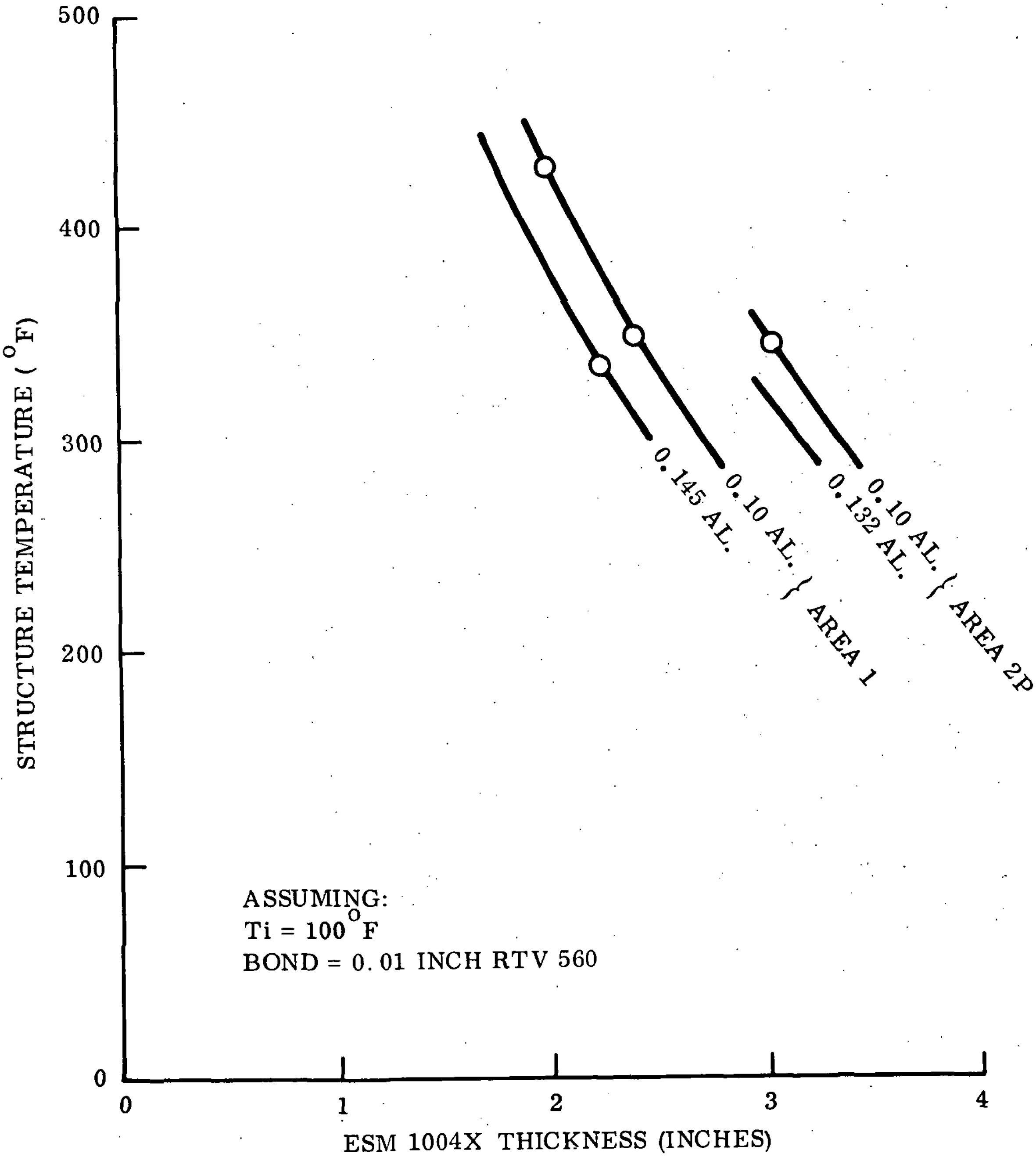

Figure 4-1. Maximum Structure Temperature as a Function of Shield Thickness

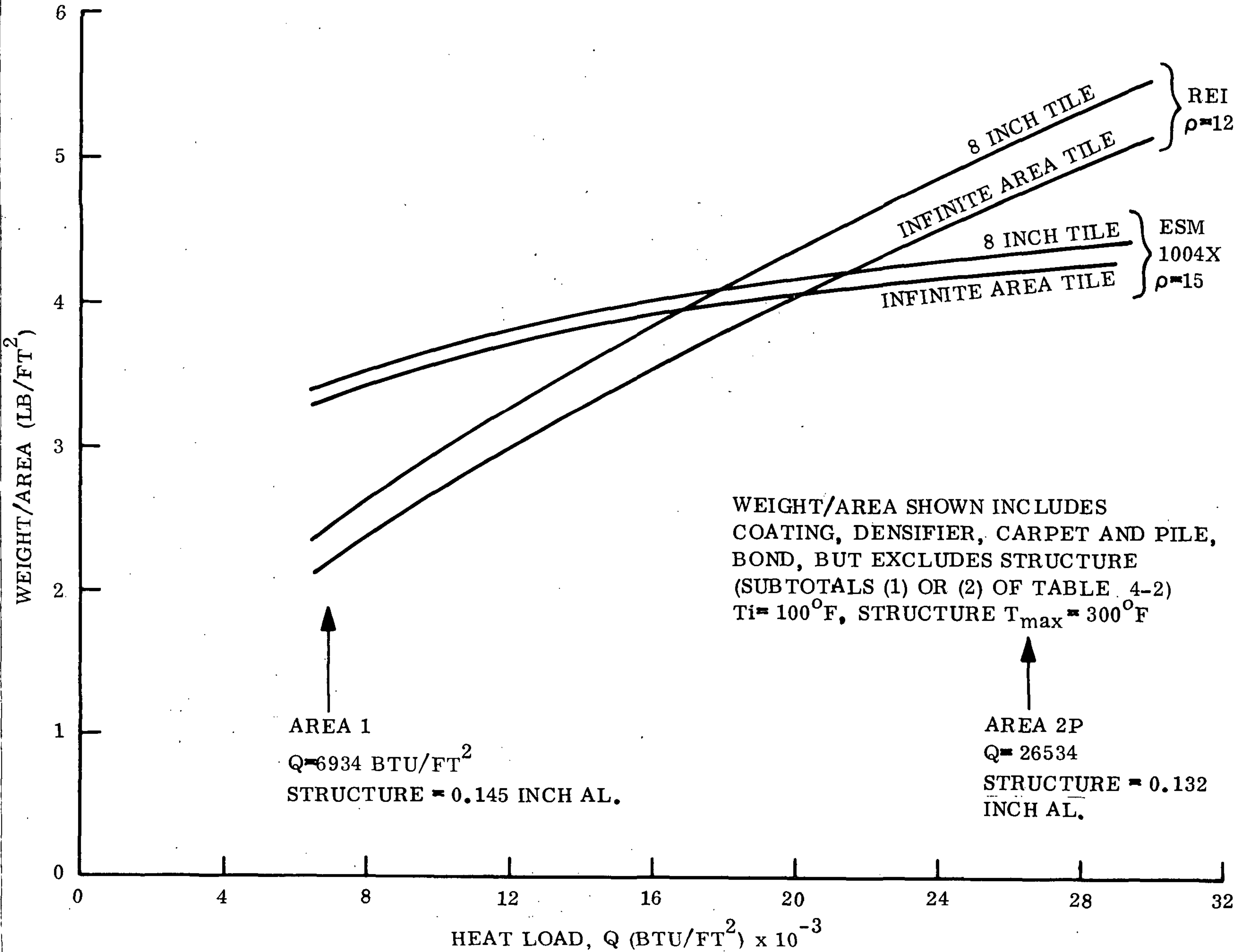

Figure 4-2. Comparison of Flexible Ablator To REI Mullite TPS Weight Requirements (15 lb/ft^3 Ablator)

TABLE 4-2. TPS WEIGHT REQUIREMENTS

	ESM 1004X						REI Mullite				
		Area 1		Area 2P				Area 1		Area 2P	
	ρ	Thick-ness	W/A	Thick-ness	W/A		ρ	Thick-ness	W/A	Thick-ness	W/A
RTV 560 Surface Coating	89	.01	.074	.01	.074	SR2 Surface Coating Surface Densifier	135	.017	.191 .10	.017	.191 .10
ESM 1004X	15	2.45	3.06	3.15	3.94	REI	12	1.7	1.7	2.0	2.0
Carpet and Piles			.14		.14						
RTV 560 Bond	89	.01	.074	.01	.074	PD 200-F28 Bond	28	.08	.187	1.1	2.57
Subtotal (1): Excluding structure and excluding coating on sides of tiles			3.35		4.23				2.18		4.86
Aluminum Structure	173	.145	2.09	.132	1.90		173	.145	2.09	.132	1.90
Total			5.44		6.13				4.27		6.76
Subtotal (1)			3.35		4.23				2.18		4.86
Additional W/A Due to Coating on Sides of Tiles			.090		.116	Additional W/A Due to: SR2 Coating on Sides Densifier on Sides			.163 .085		.191 .100
Subtotal (2): Excluding structure			3.44		4.35				2.43		5.15
Aluminum Structure			2.09		1.90		173	.145	2.09	.132	1.90
Total			5.53		6.25				4.52		7.05

Density ~ lb/ft^3, Thickness ~ Inches, Weight/Area ~ lb/ft^2

It was noted that in test samples which have been made, the density of ESM 1004X is greater than the nominal 15 lb/ft^3 used in this analysis. The increased weight is thought to be due to the foaming action being inhibited by the presence of the carpet and piles. The weight of the carpet and pile fibers is measured at 0.14 lb/ft^2, and a fabricated one-inch-thick model had an overall density of 20 lb/ft^3; thus the ESM density is approximately 18 lb/ft^3. Table 4-3 and Figure 4-3 are similar to Table 4-2 and Figure 4-2, except that 18 lb/ft^3 density was assumed in determining weights. It is noted that this is only an approximation since the thicknesses used to develop Table 4-3 were the thickness requirements for 15 lb/ft^3 material. This results in increased ESM 1004X weights. The ablator weight for Area 1, for example, is now about a factor 2 higher than the REI requirement.

4.2 CONCEPTUAL SYSTEM DESIGN

Conceptual design studies have been concentrated on a flexible ablative covering and associated attachment concepts for potential Space Shuttle application. Primary emphasis was placed on attachment techniques which provide general utility and ease of refurbishment. This section describes the baseline configurations resulting from the study and discusses relative feasibility of each design concept.

4.2.1 ABLATOR BASELINE SIZING

A design study baseline configuration was established to assist in relative evaluation of various attachment techniques and integral combinations. The basic ablator material is ESM 1004X (15 PCF density), reinforced with Astroquartz® pile, backed with an E-glass carpet weave, and exterior-surface-coated with solid RTV 560 (88.6 PCF). Design thicknesses were derived from the REKAP calculations, plotted in Figure 4-1 for NASA/MSC Area 1 and Area 2P environments. If the maximum structure (0.10 aluminum) temperature is limited to 300°F, the respective ablator thicknesses are 2.70 and 3.36 inches. These dimensions are representative of total thickness required for direct bonding attachment and were used as the base dimensions for trade studies involving other types of attachments.

4.2.2 ATTACHMENT CONCEPTS

From the standpoint of light weight and general utility, four basic techniques were selected for comparative design studies. These candidate techniques are identified as (A) Direct Bonding, (B) Velcro, (C) NASA/MSC Spire, and (D) GE-RESD BAS. The concepts are

TABLE 4-3. TPS WEIGHT REQUIREMENTS

	ESM 1004X						REI Mullite				
		Area 1		Area 2P				Area 1		Area 2P	
	ρ	Thickness	W/A	Thickness	W/A		ρ	Thickness	W/A	Thickness	W/A
RTV 560 Surface Coating	89	.01	.074	.01	.074	SR2 Surface Coating Surface Densifier	135	.017	.191 .10	.017	.191 .10
ESM 1004X	18	2.45	3.68	3.15	4.73	REI	12	1.7	1.7	2.0	2.0
Carpet and Piles			.14		.14						
RTV 560 Bond	89	.01	.074	.01	.074	PD 200-F28 Bond	28	.08	.187	1.1	2.57
Subtotal (1): Excluding structure and excluding coating on sides of tiles			3.97		5.02				2.18		4.86
Aluminum Structure	173	.145	2.09	.132	1.90		173	.145	2.09	.132	1.90
Total			6.06		6.92				4.27		6.76
Subtotal (1)			3.97		5.02				2.18		4.86
Additional W/A Due to Coating on Sides of Tiles			.090		.116	Additional W/A Due to: SR2 Coating on Sides Densifier on Sides			.163 .085		.191 .100
Subtotal (2): Excluding structure			4.06		5.14				2.43		5.15
Aluminum Structure	173	.145	2.09		1.90		173	.145	2.09	.132	1.90
Total			6.15		7.04				4.52		7.05

Density ~ lb/ft^3, Thickness ~ Inches, Weight/Area ~ lb/ft^3

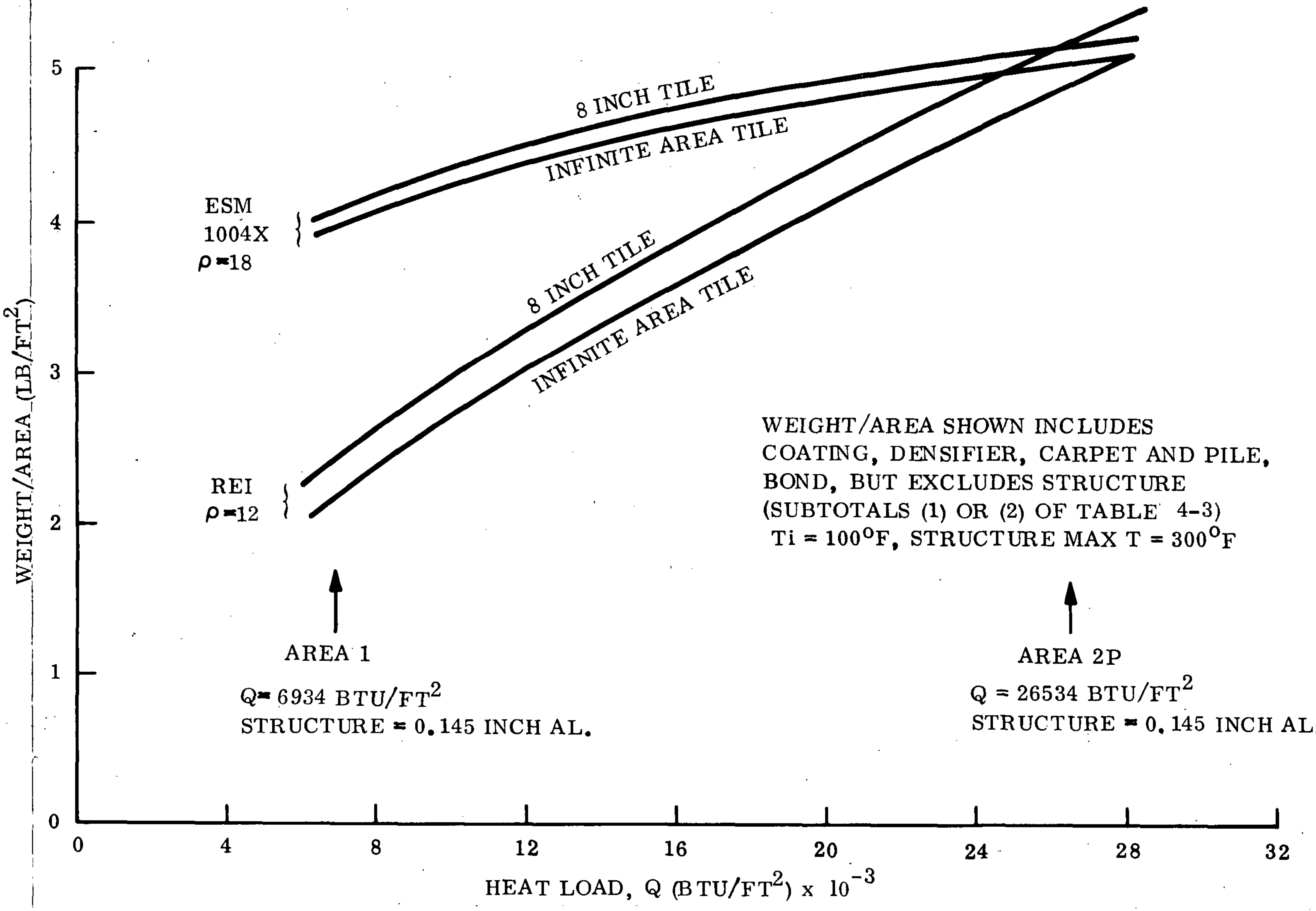

Figure 4-3. Comparison of Flexible Ablator to REI Mullite TPS Weight Requirements (18 lb/ft^3 Ablator)

attractive because several design variations can be derived to provide continuous type of attachments and offer the most favorable interface with the airframe structure. The various concepts are shown in the photographs of Figures 4-4 through 4-7.

Table 4-4 shows the four techniques and illustrates two variations for the GE-RESD Barbed Attachment System (BAS). The in-depth temperatures and their maximum distance from the outer surface were obtained from REKAP calculations plotted in Figures 4-8 and 4-9.

In the direct bonding concepts (A), the principal ablator system is attached directly to the structure using a 10 mil layer of RTV 560 adhesive. The Velcro technique (B) is standard polyester #85 arrowhead hook and pile closure. The hooks are bonded to the ablator backing with a 10 mil layer of RTV 560. The pile is bonded to the structure by means of a 10 mil layer of RTV 560. In both of these concepts the Astroquartz reinforcing pile ran the full depth of the ablator. Other variations are possible, but require the addition of another adhesive line, thereby increasing the weight.

The principal ablator for the NASA/MSC Spire (C1) and GE-RESD BAS (C2) concepts was sized for a backface temperature of 350°F. A separate layer of non-reinforced insulation protects the structure from soak-out temperatures in excess of 300°F, and provides a pre-load to ensure proper hooking into the ablator carpet. For convenience of study, the separate pad was considered to be ESM 1004X material; however, other low-density flexible insulators may offer potential weight-saving advantages.

Basic dimension of the MSC Spire fastener was derived from NASA/MSC drawing SK712110, dated 10/21/71. The fastener is made of aluminum alloy and is stud-welded to the aircraft skin. The GE-RESD BAS fastener is essentially a 0.030 stainless steel spear brazed or welded to 0.010 stainless shim stock. The base of the fastener is bonded to the structure using 10 mils of RTV 560. (An alternative of spot welding to the structure has been considered, but was not utilized in weight comparisons.)

The GE-RESD BAS design shown as concept (D) is essentially the same as (C2) except the principal ablator is sized for a backface temperature of 600°F. This requires a longer BAS spear and a thicker inner insulating pad. This concept is quite attractive since it offers several design alternatives for maximum reuse of materials and various weight-saving potentials. As in concept (C), only the base of the BAS is bonded to the structure; the inner pad is sandwiched between the principle ablator and structure.

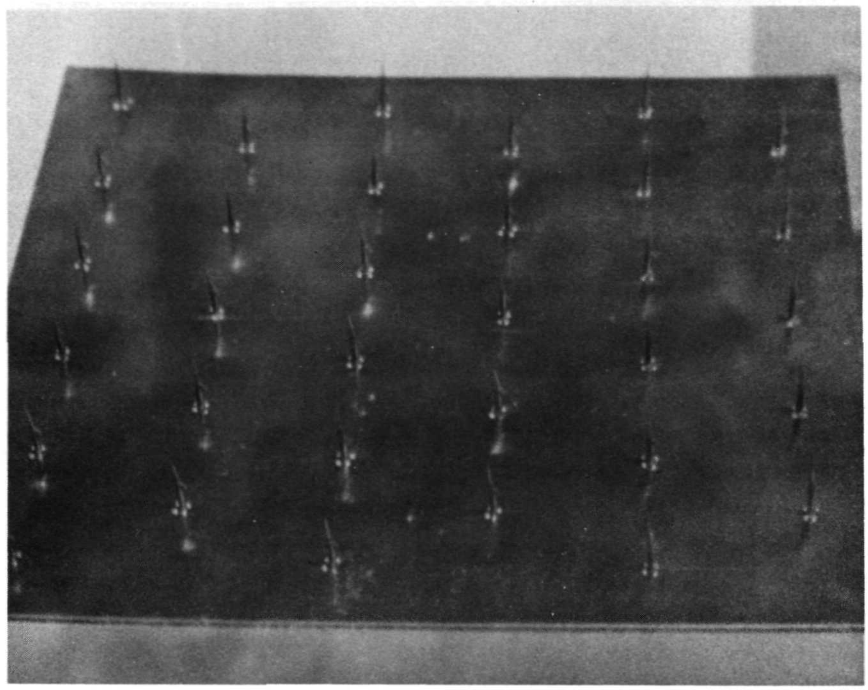

Figure 4-4. GE BAS Attachment Concept

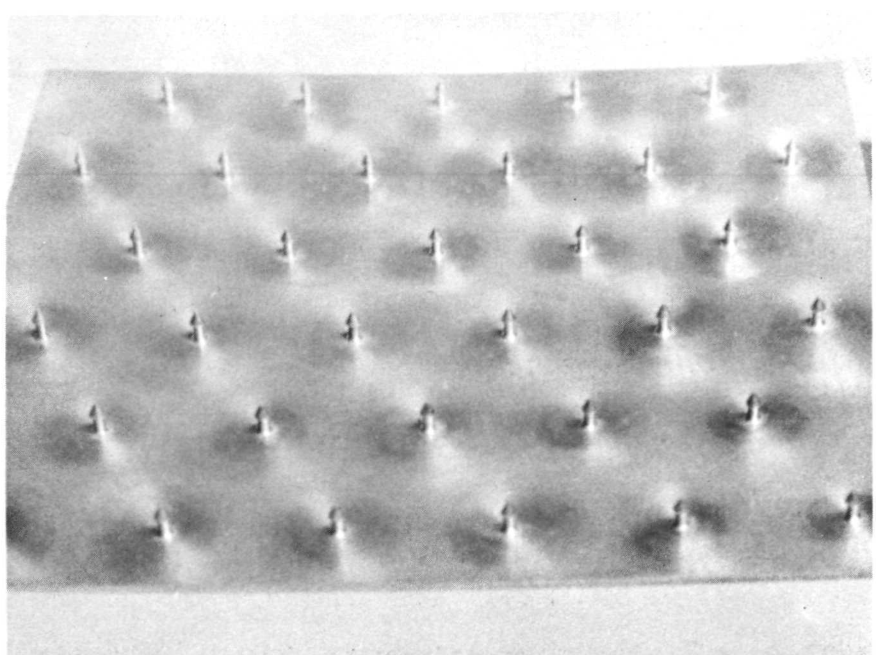

Figure 4-5. NASA MSC - Spire Attachment Concept

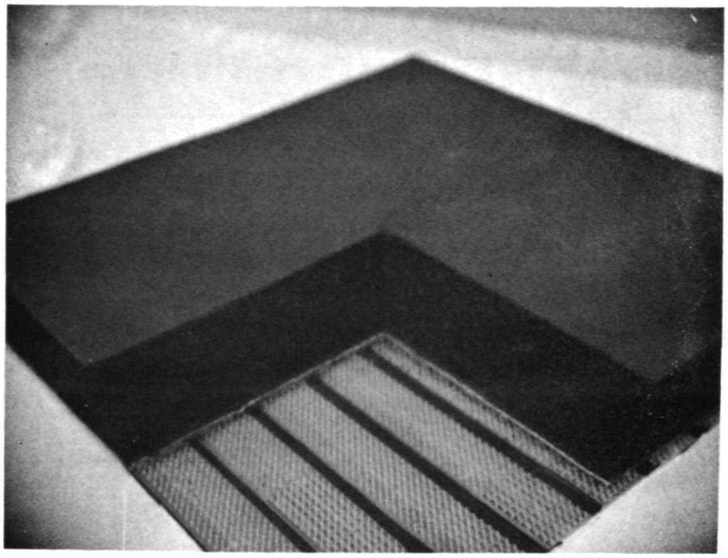

Figure 4-6. 12" x 12" Specimen of ESM 1004X with Carpet Backing Attached by Velcro Molded Arrowhead Concept

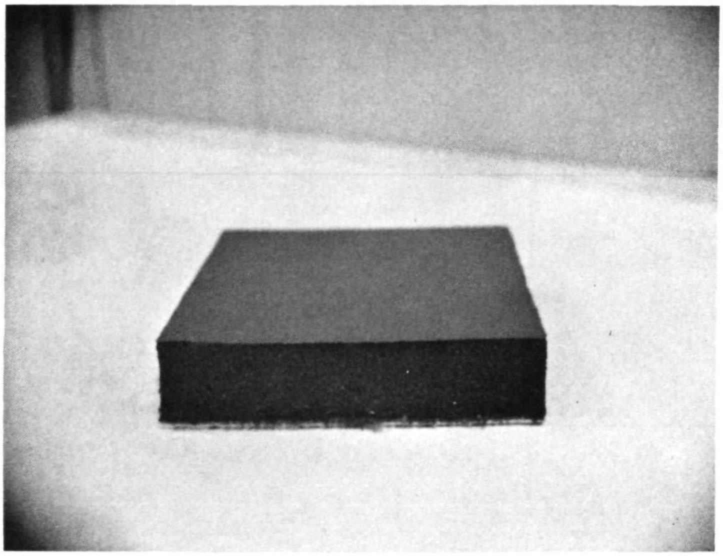

Figure 4-7. 12" x 12" Specimen of ESM 1004X in Woven Carpet Bonded to Aluminum with RTV 560

TABLE 4-4. CONCEPTUAL DESIGNS

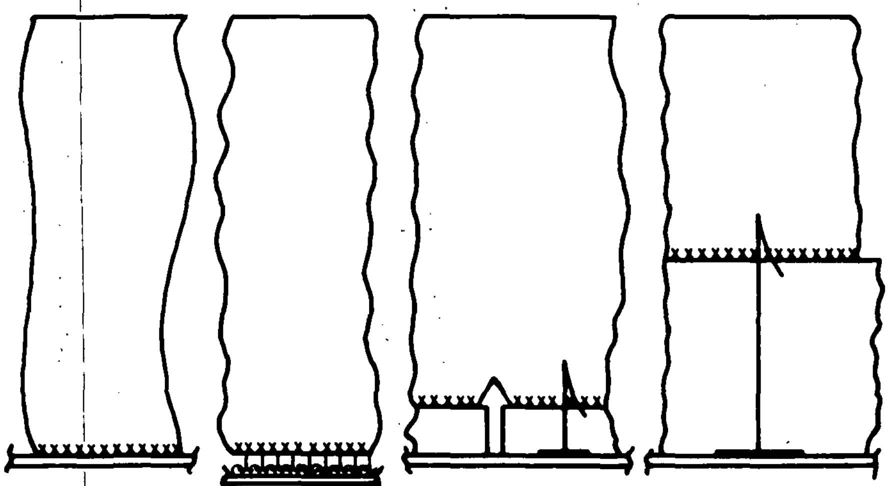

(A) Direct-Bonding

(B) Velcro

(C1) NASA/MSC Spire & (C2) GE-RESD BAS

(D) GE-RESD BAS

	Area 1 Design		Area 2P Design	
Start Ablation	1045°F @ 790 Sec.		1082°F @ 250 Sec.	
Max. Surface Temperature	1270°F @ 1987 Sec.		1764°F @ 510 Sec.	
Design Temperature	Depth (In.)	Entry Time (Sec.)	Depth (In.)	Entry Time (Sec.)
Surface	0	1987	0	510
1000°F	0.57	2047	1.05	2001
600°F	1.40	2487	1.87	2501
350°F	2.40	4289	2.81	4208
300°F	2.70	>4300	3.36	>4909

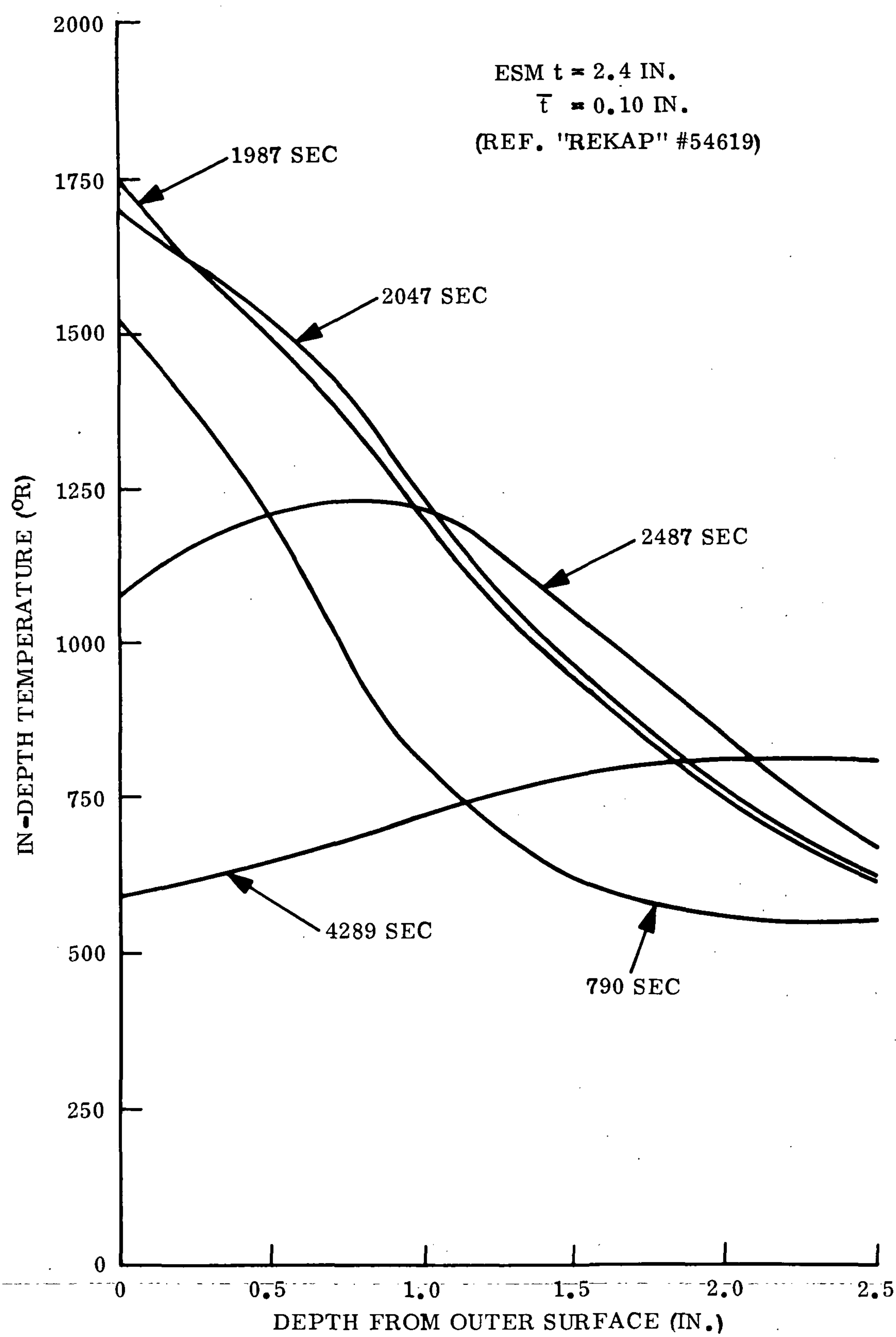

Figure 4-8. Area 1 Thermal Profile

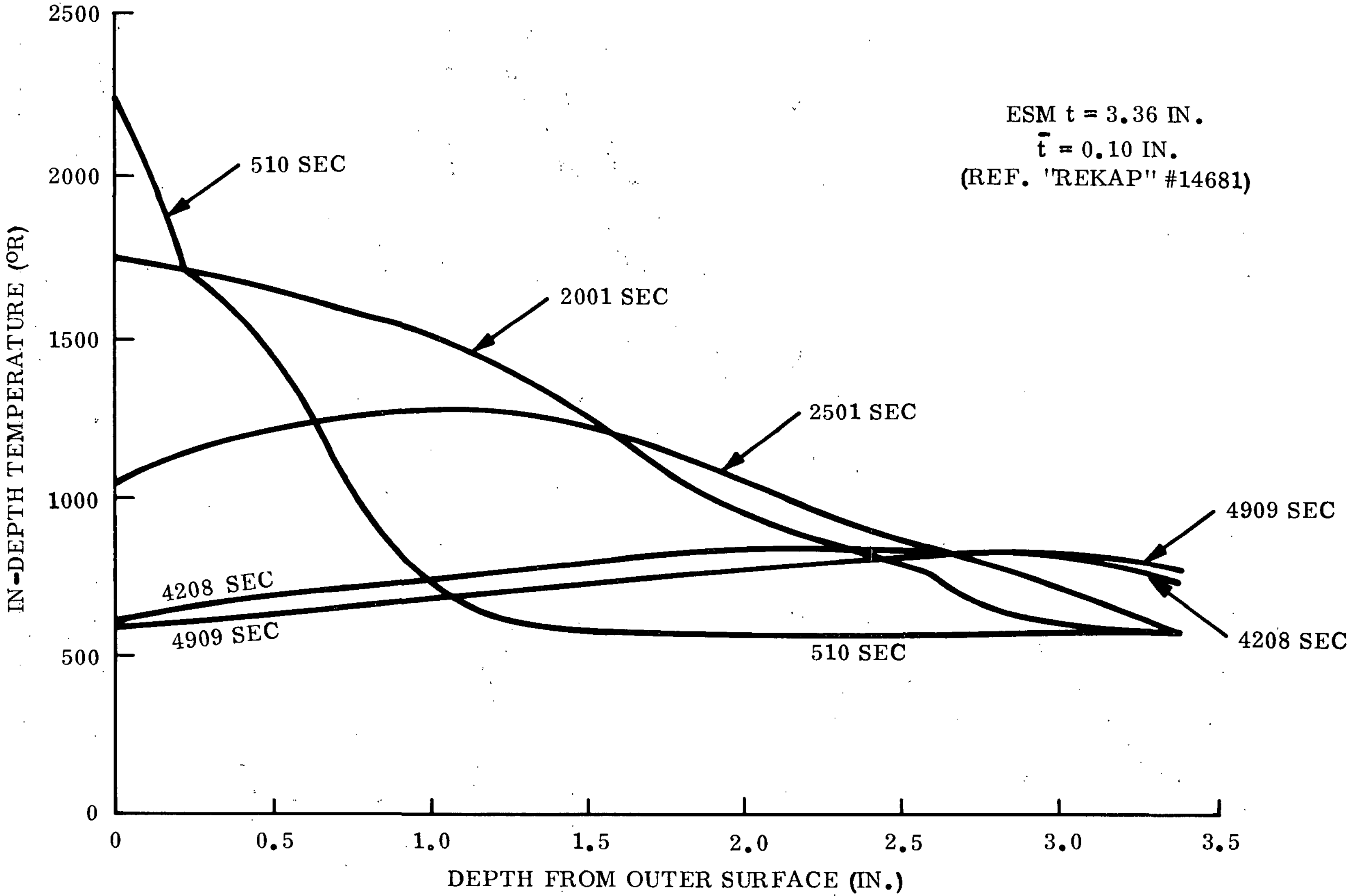

Figure 4-9. Depth from Outer Surface (In.)

In both the BAS and Spire concepts, the flexible ablator can be readily removed without disturbing the underlying system. Both systems have sufficient mechanical integrity to permit the woven fabric backing to be removed (by breaking individual fibers) without damage to the barbs or spires.

4.2.3 CONCEPT EVALUATION

The five attachment designs were evaluated relative to system weight; ease of installation, replacement or refurbishment; operational costs; and potential growth for optimizing the designs. Results of the weight analysis indicate that the total system weight (ablator plus attachment) is relatively the same for four of the concepts. The Velcro (B) design was approximately 7 to 11 percent heavier, depending on environmental area. Unit weights (lb/ft^2) of each concept and associated elements are summarized in Tables 4-5 and 4-6 for Area 1 and Area 2P, respectively.

The direct bonding method was established as the basic index for comparing physical, functional, and economical characteristics of the candidate fasteners because it represents a currently reliable state-of-the-art technique. The RTV 560 adhesive is commercially available and is compatible with the fabric-reinforced ablator.

The principle objection to direct bonding is the amount of care and time required for removal and replacement. Field refurbishment is considered complex since the structure must be cleaned and primed to ensure proper bonding of the new panel. Clamping fixtures are required to install the replacement ablator and maintain position during curing. In order to obtain maximum bond line strengths, the adhesive should be cured at $200^{o}F$ for a period of time. For the ablator thicknesses under consideration, the recommended curing temperature can be achieved only by heating the structure from the backside. This is considered to be most difficult; therefore, the adhesive must be cured at room temperature for periods of several days to guarantee adequate structural properties at operational temperatures.

The Velcro type of attachment (B) is most attractive from the standpoint of initial installation, replacement, and system cost. The arrowhead type of closure (polyester hooks) is currently available in widths of one inch. Preliminary test results obtained from NASA /MSC indicate

TABLE 4-5. SYSTEM WEIGHT FOR AREA 1

	A	B	C1	C2	D
	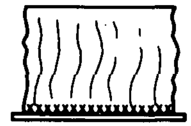	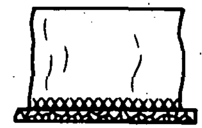	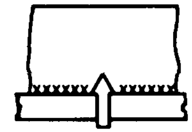	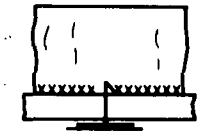	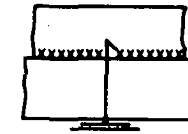
Ablator	(#/Ft^2)	(#/Ft^2)	(#/Ft^2)	(#/Ft^2)	(#/Ft^2)
ESM Coating	0.070	0.070	0.070	0.070	0.070
ESM 1004X	3.375	3.375	3.375	3.375	3.375
Carpet & Fiber	0.242	0.242	0.232	0.232	0.198
Total Insulation Wgt.	3.687	3.687	3.677	3.677	3.643
Attachments	(#/Ft^2)	(#/Ft^2)	(#/Ft^2)	(#/Ft^2)	(#/Ft^2)
Adhesive	0.07	0.14	N.R.	0.006	0.006
Velcro	-	0.25	-	-	-
NASA/MSC Spire	-	-	0.017	-	-
GE-RESD BAS	-	-	-	0.050	0.075
Total Attachment Wgt.	0.07	0.39	0.017	0.056	0.081
Total Ablator System Wgt.	3.757	4.077	3.694	3.733	3.724

TABLE 4-6. *SYSTEM WEIGHT FOR AREA 2P*

	A	B	C1	C2	D
	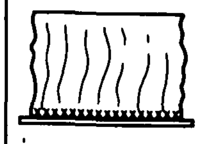	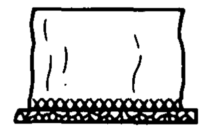	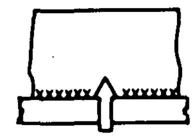	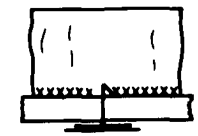	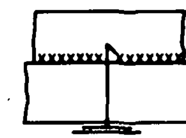
<u>Ablator</u>	(#/Ft^2)	(#/Ft^2)	(#/Ft^2)	(#/Ft^2)	(#/Ft^2)
ESM Coating	0.070	0.070	0.070	0.070	0.070
ESM 1004X	4.20	4.20	4.20	4.20	4.20
Carpet & Fiber	0.284	0.284	0.262	0.262	0.225
Total Insulation Wgt.	4.554	4.554	4.532	4.532	4.495
<u>Attachments</u>	(#/Ft^2)	(#/Ft^2)	(#/Ft^2)	(#/Ft^2)	(#/Ft^2)
Adhesive	0.07	0.14	N.R.	0.006	0.006
Velcro	-	0.25	-	-	-
NASA/MSC Spire	-	-	0.027	-	-
GE-RESD BAS	-	-	-	0.057	0.079
Total Attachment Wgt.	0.07	0.39	0.027	0.063	0.085
Total Ablator System Wgt.	4.624	4.944	4.559	4.595	4.580

the flat-wise tension strength to be about 7 psi (ultimate) at room temperature. This tensile capability is believed to be adequate for the ablator loadings; however, very little data is available relative to the load/deformation characteristics at $300^{o}F$.

Primary objection to the Velcro fastener is weight of the total system. The hook-and-pile combination weighs approximately 0.25 lb/ft^2, and the weight of two layers of adhesive must be added to assemble the elements on the ablator and structure. Assuming the adhesive to be RTV 560, the calculated attachment system weight is approximately 0.40 lb/ft^2. This is at least 7 per cent heavier than the other fastener concepts.

The NASA/MSC Spire concept (C1) offers the potential of a very light-weight attachment system. The spire, defined by MSC drawing SK712110, is machined from aluminum and then stud-welded to the substructure. Like the GE-RESD BAS, there is no requirement to bond the inner pad to the substructure when the fastener head is properly hooked into the ablator carpet.

The major objection to the spire assembly is that it perturbates the airframe skin assembly and requires closely controlled alignment and interfaces. Other methods of assembly are envisioned as less complex but would increase the unit weight. The initial installation cost of the spire is considered high because of the machining and welding requirements, but after proper fabrication the ablator may be easily removed and replaced.

The Barbed Attachment System (BAS), concepts (C2) and (D), under development at GE-RESD offers considerable design versatility and growth to overcome the disadvantages associated with the other attachment concepts. With this concept, the reinforced ablator is pushed onto the barbed studs which hook into the carpet strands. The resilient insulation pad between the structure and the reinforced ablator provides preload to retain the strands under the barbs and to dampen vibration loads. The most significant advantage of this concept over the others is that the system can be designed for maximum reuse of non-ablated materials. In concept (D) the reinforced ablator is about 50% of the total required thickness, and the replacement panel is installed without disturbing the previously installed inner pad and barbed fastener. For consistency of comparing with other attachment techniques, the inner pad in this study was defined as ESM 1004X. Other design innovations have shown lighter weight designs by optimizing the inner pad material.

The major objection identified with the BAS concept is the caution required because of the very sharp points and barbs. This characteristic exists only in the currently economical prototype development hardware. Detail design for large volume production would radius these points and eliminate potential safety hazards.

4.2.4 EVALUATION SUMMARY

The five concepts previously discussed were evaluated relative to physical, functional, and economical characteristics. Results are tabulated in Table 4-7. The unit weight and structural integrity are essentially the same for each system concept. There is a slight variation in system cost based on multi-mission utilization.

The GE-RESD BAS concept offers greater design flexibility and larger growth potential to provide a general utility type of attachment for several different categories of TPS materials such as ablators, RSI, gaskets, and internal insulation. Significant features of the system, in addition to economical/lightweight construction, are as follows:

a. All bonded surfaces may be fabricated under factory-controlled processes and NDT'd with precision factory equipment. Only minor field repairs will require field process type of bonding and inspection.

b. Offers the options of reusing a large portion of the ablator system without disturbing factory-installed elements.

c. Provides the option of eliminating large area of adhesive by attaching the studs directly to the airframe

4.3 PLASMA ARC TEST PROGRAM

A plasma arc test program has been conducted to evaluate the thermal performance of a number of test models of the flexible ablator concept. The tests were performed in the GE 5 MW plasma arc facility at conditions designed to simulate the space shuttle orbiter entry environment. A total of six models were tested. A description of the flexible ablator concepts tested, the test conditions and facilities, and a discussion of the test results and analysis follow. In all cases, the basic ablator used in formulating the test samples was GE ESM 1004X, with the exception of one model which was a modified version of ESM 1004X.

TABLE 4-7. CONCEPT EVALUATION

		System Wgts.		Initial Installation	Refurbish	System Cost (Multi-Mission)	Major Feature	Major Objection
		Area 1 (#/Ft^2)	Area 2P (#/Ft^2)					
A	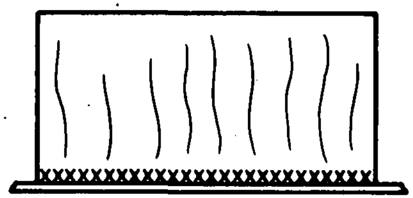	3.76	4.62	Simple	Complex	Moderate	Currently Reliable	Replacement Time
B	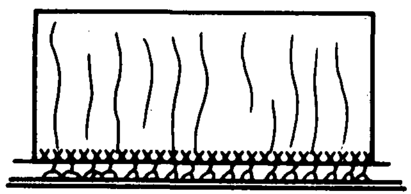	4.08	4.94	Simple	Simple	Low	Availability	Strength to Weight Limitations
C1	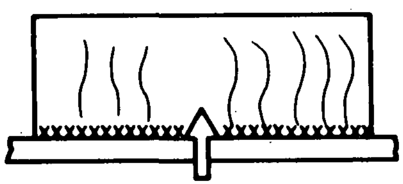	3.69	4.56	Difficult	Simple	Moderate	Light Weight	Structure Interface
C2	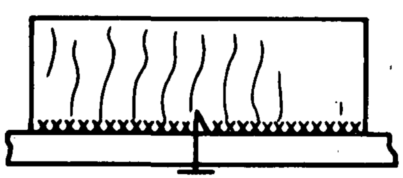	3.73	4.60	Complex	Simple	Moderate	Design Versatility	Installation Hazard
D	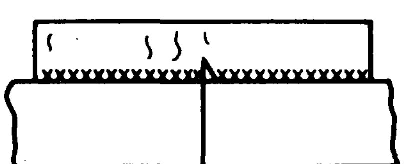	3.72	4.58	Complex	Simple	Low	Material Re-use	Installation Hazard

4.3.1 MODEL DESCRIPTION

A brief description of the models tested in this program is presented in Table 4-8. Also included in Table 4-8 are the model dimensions and actual conditions.

A total of 6 flexible ablator models have been tested in the GE 5 MW arc facility. One of the models was attached to the backplate with the Velcro molded arrowhead concept. For this model, the ESM was not foamed in the carpet and pile construction. Instead, a backing was bonded to the precured ablator. Four models included the Astroquartz® pile reinforcement. The sixth model was a modified version of ESM 1004X and was unsupported; i.e., no carpet and pile, but was bonded directly to an aluminum substrate.

A standard, water-cooled wedge-shaped holder was used for all testing. The model holder has a sharp leading edge and will accept models up to 5.5" long by 6.0" wide by 3.0" thick. The models tested in this program were nominally 6" by 5 1/2" by 1" ~ 1 1/4" thick.

Thermocouples were located in the models to determine surface and in-depth temperature response. All surface measurements were made with platinum/platinum 10% rhodium thermocouples, which were beaded isothermally at the surface. Chromel-alumel thermocouples were located in depth in the ESM and on the aluminum substrate. These thermocouples were installed normal to the model (non-isothermal), with the thermocouple leads leaving the model through the backplate.

4.3.2 TEST FACILITY

These tests were conducted in the GE Hyperthermal Arc Facility in the tunnel mode of operation. Air is heated to high enthalpy in a tandem Gerdien arc heater. Part of the heated air passes over the copper electrodes, carrying off any contaminants, and exits from the back of the arc unit. The remainder of the heated air is expanded through a nozzle whose throat is 3/8"D and exit is 13.5"D. From the nozzle, the test gas enters a large (~5' diameter) test tank, in which the model is held. After passing over the test model, the gas then exits through a diffuser section downstream of the test section. A steam ejector system is used to pump the gas from the tank and control tank ambient pressure.

TABLE 4-8. MATRIX OF TEST MODELS

Model Number	Description	Dimensions (Inches)	Run Time (Minutes)	Test Conditions
ESM-1	Backing Bonded On, Tufted with Astroquartz	6 x 5-1/2 x 1.05	5.5	-
ESM-2	Woven Carpet	6 x 5-1/2 x 0.714	5.5	-
ESM-3	No Tufts. Backing Bonded on Velcro Attachment	6 x 5-1/2 x 0.9	7.5	-
72-1	Woven Carpet	6 x 5-1/2 x 1.25	10	$q = 10$ Btu/Ft^2 sec; $H_R = 8500$ Btu/lb
72-2	Woven Carpet	6 x 5-1/2 x 1.25	10	" "
72-3	Modified ESM 1004X, Unsupported	6 x 5-1/2 x 1.25	10	" "

NOTE: MODEL PRESSURE ~ 10^{-2} ATMOSPHERES

The arc operating point was selected from the calibration program (Reference 3). The test sample orientation was selected to be 10^{o} angle of attack and at the 6" station (6 inches downstream of the nozzle exit).

The arc heater was started and adjusted to the desired operating condition with the test model in a retracted position. When the conditions were correct, the test model was injected for the specified time period. From time to time during the test, minor adjustments in power were made to ensure a constant test environment. At the end of the run, the model was retracted prior to shutting the arc down, and soakout data was taken.

4.3.3 TEST RESULTS AND ANALYSIS

The first three models listed in Table 4-8 were tested in an extremely severe environment due to an abnormal test condition in the plasma arc facility. The planned test conditions were:

Heat Flux = 10 BTU/ft^2 -sec

Enthalpy = 8500 BTU/lb

The actual surface temperatures measured on all three models ranged from $3400^{o}F$ to $3500^{o}F$, which is much higher than the surface temperature anticipated from the planned test conditions ($\sim 1700^{o}F$). The extremely high surface temperatures resulted because the flow possessed an extremely high energy content. The in-depth and backface temperature response of the samples is consistent with the measured surface temperatures. Despite the severe thermal environment [$\dot{q}$ (equilibrium radiation) $\simeq$ 100 BTU/ft^2-sec for $T_{surface}$ = $3500^{o}F$], the ESM 1004X ablative material performed quite well. The chars are very hard, and in general, the surface cracks are superficial. There is also no evidence of a weak zone between the charred portion and the virgin material. In model ESM-3 the Velcro was heated to temperatures in excess of $1500^{o}F$ and consequently melted and flowed. However, the sample did not come off the backplate. The thermocouple response data for these three models are shown in Figures 4-10 through 4-12.

Models 72-1, 72-2 and 72-3 were tested at a heat flux of 10 BTU/ft^2-sec, a recovery enthalpy of 8500 btu/lb, and at a pressure of 10^{-2} atmospheres. The surface and in-depth temperature response of Model 72-1 is shown in Figure 4-13 and is compared with the analytical predictions made with the Reaction Kinetic Ablation Program (REKAP). It is seen that the

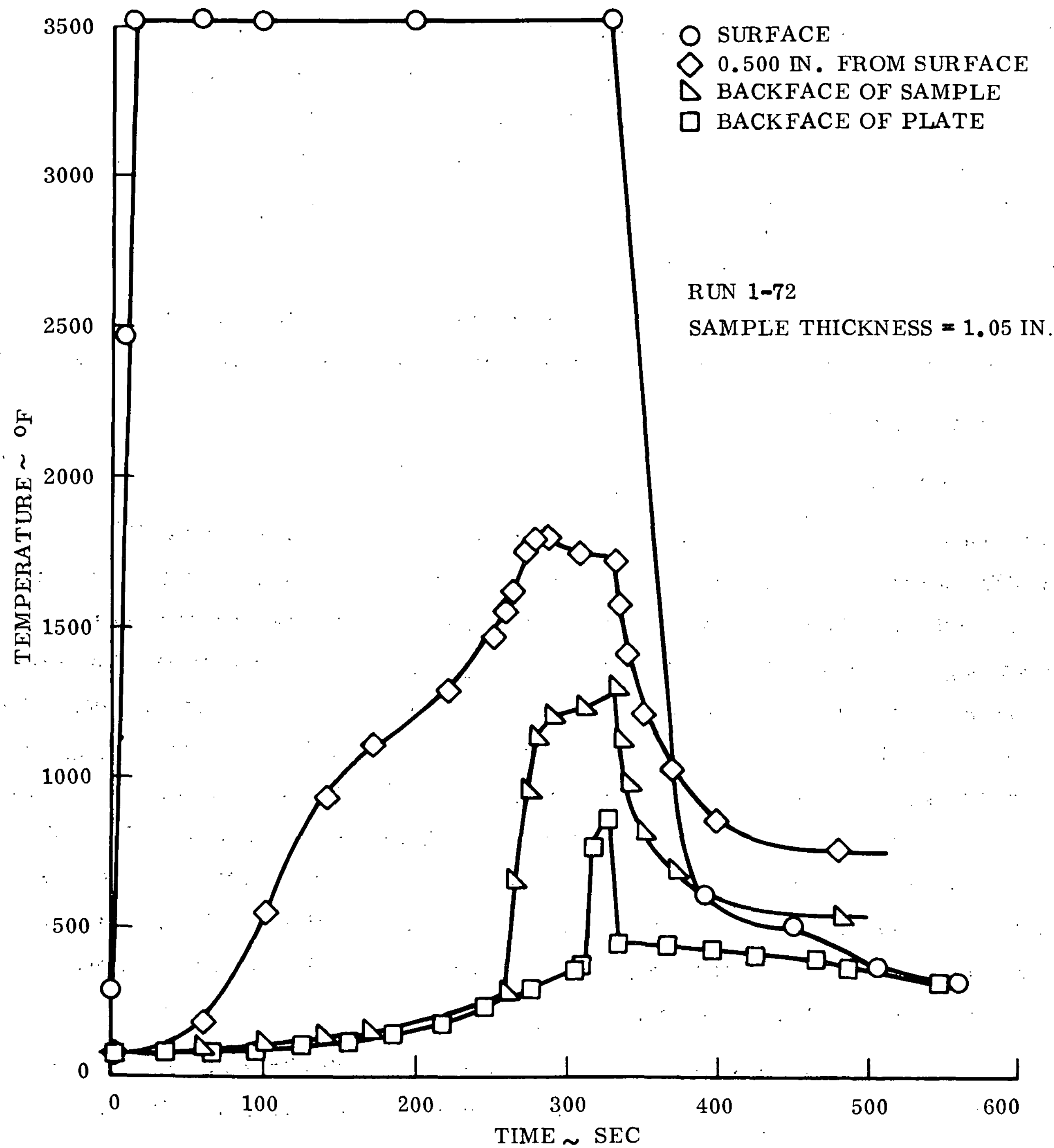

Figure 4-10. GE Hyperthermal Arc Test Results - ESM 1

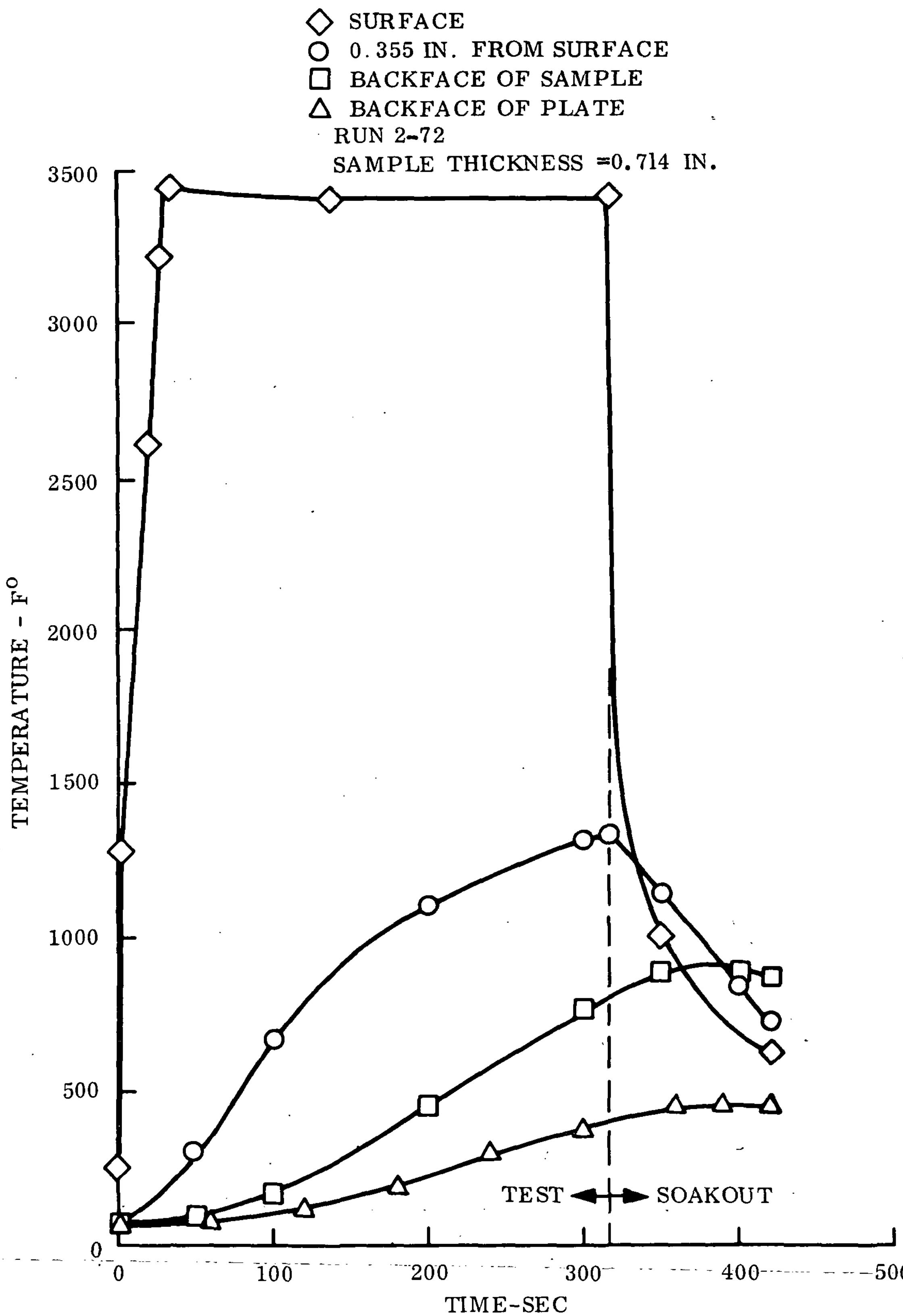

Figure 4-11. GE Hyperthermal Arc Test Results - ESM 2

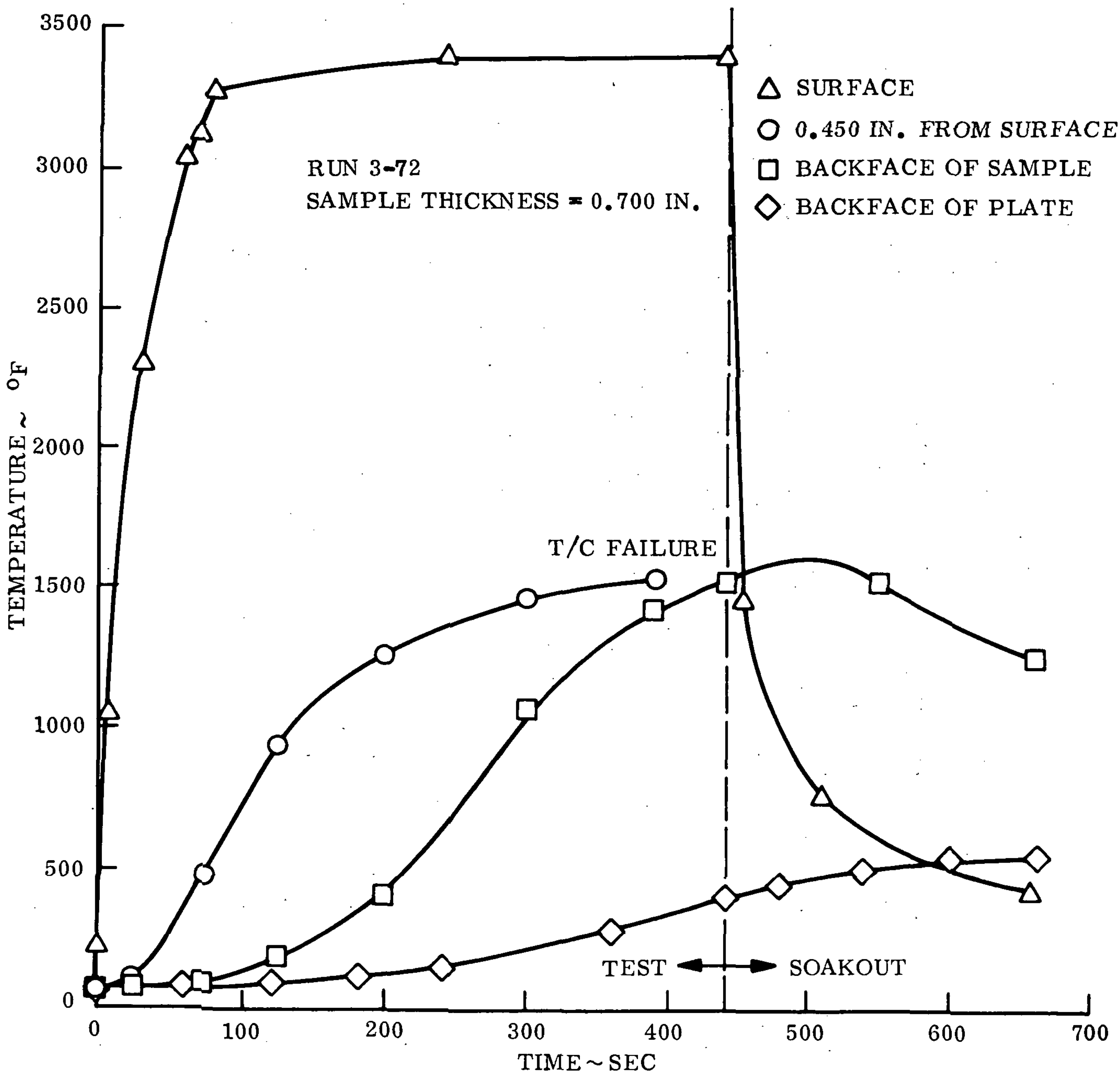

Figure 4-12. GE Hyperthermal Arc Test Results - ESM 3

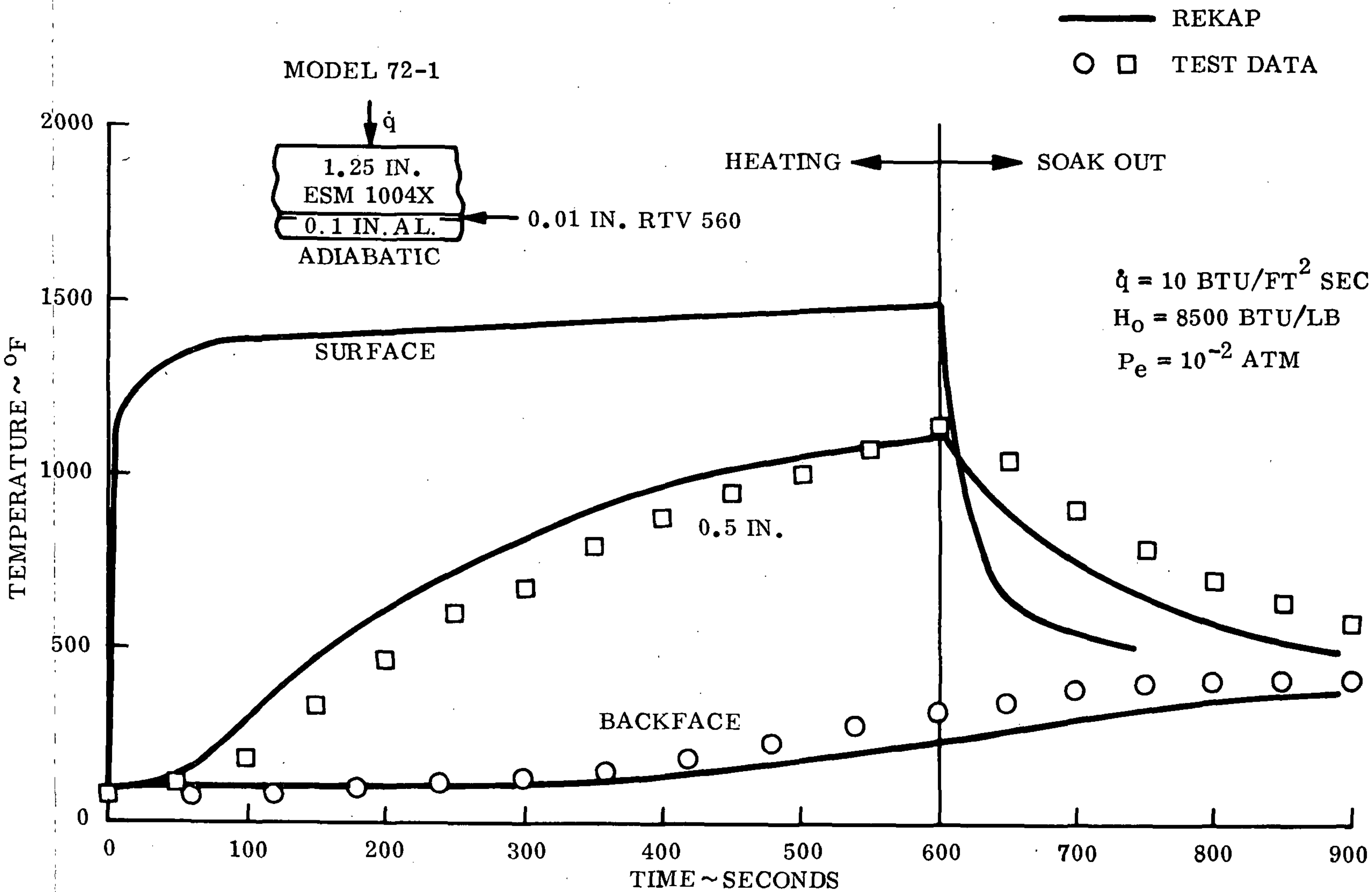

Figure 4-13. Plasma Arc Test - ESM 1004X Flexible Ablator

performance is predictable. Figure 4-14 shows the in-depth temperature profile at the end of the test. Since it is known that a black char forms on ESM at temperatures of 1100°F or higher, the analytical prediction shows a char depth of about 0.5". The actual char depth measured on the model is about 0.6". Figure 4-15 shows the accommodation of thermal energy for the flexible ablator. There are only a few minor superficial surface cracks. The char is very hard and is tenaciously held to the virgin material. It appears that the tufts are assisting in anchoring the char to the virgin elastomer. Pre- and post-test photographs of Model 72-1 are shown in Figures 4-16 through 4-18. Model 72-2 was a repeat test and the thermal performance measured and predicted is shown in Figure 4-19. For this model, the predicted response matches the data more closely. The model configuration and test environment were the same as for Model 72-1.

Figure 4-20 shows the thermal response measured for Model 72-3 compared with the previously described analytical predictions. The model geometry and test conditions were the same as for Models 72-1 and 72-2. However, this model was a modified version of the ESM 1004X ablator and had a much smaller pore size. It can be seen from Figure 4-20 that improved thermal performance was obtained from the model, the backface temperature having increased to only 130°F after 10 minutes of heating compared to 230°F for Model 72-2 and 320°F for Model 72-1. This material has not been characterized thermally at this time, but since the measured surface temperature history is predicted reasonably well with the existing ESM 1004X thermal model, it would appear that this material has a considerably lower thermal conductivity than ESM 1004X. It may be conjectured, using available data for fibrous insulation materials (Reference 4), that the finer pore size of the modified ESM 1004X is reducing the convective component of the total thermal conductivity, particularly at the test pressure $\sim 10^{-2}$ atmospheres.

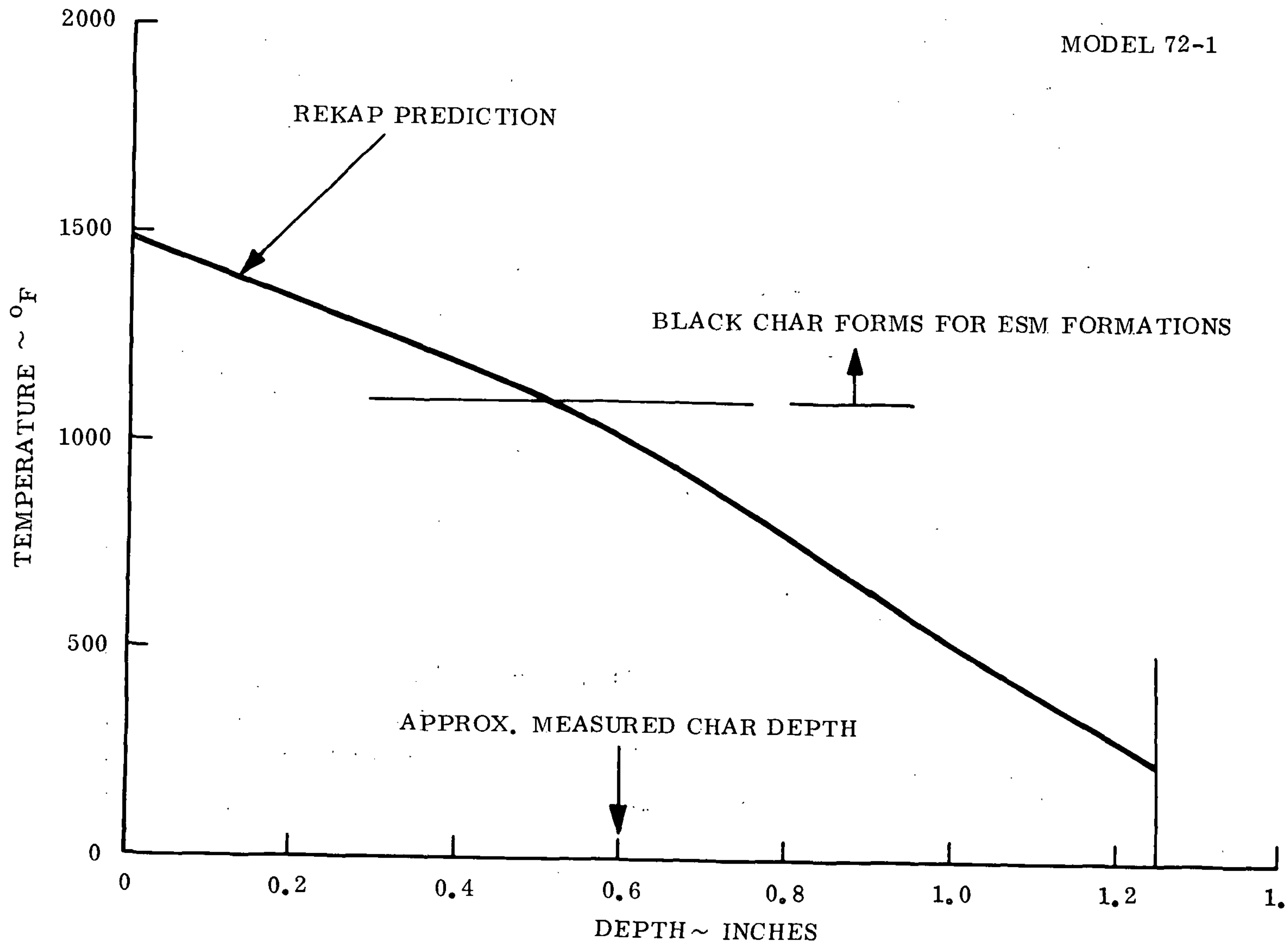

Figure 4-14. In-Depth Temperature Gradient at t = 600 Seconds

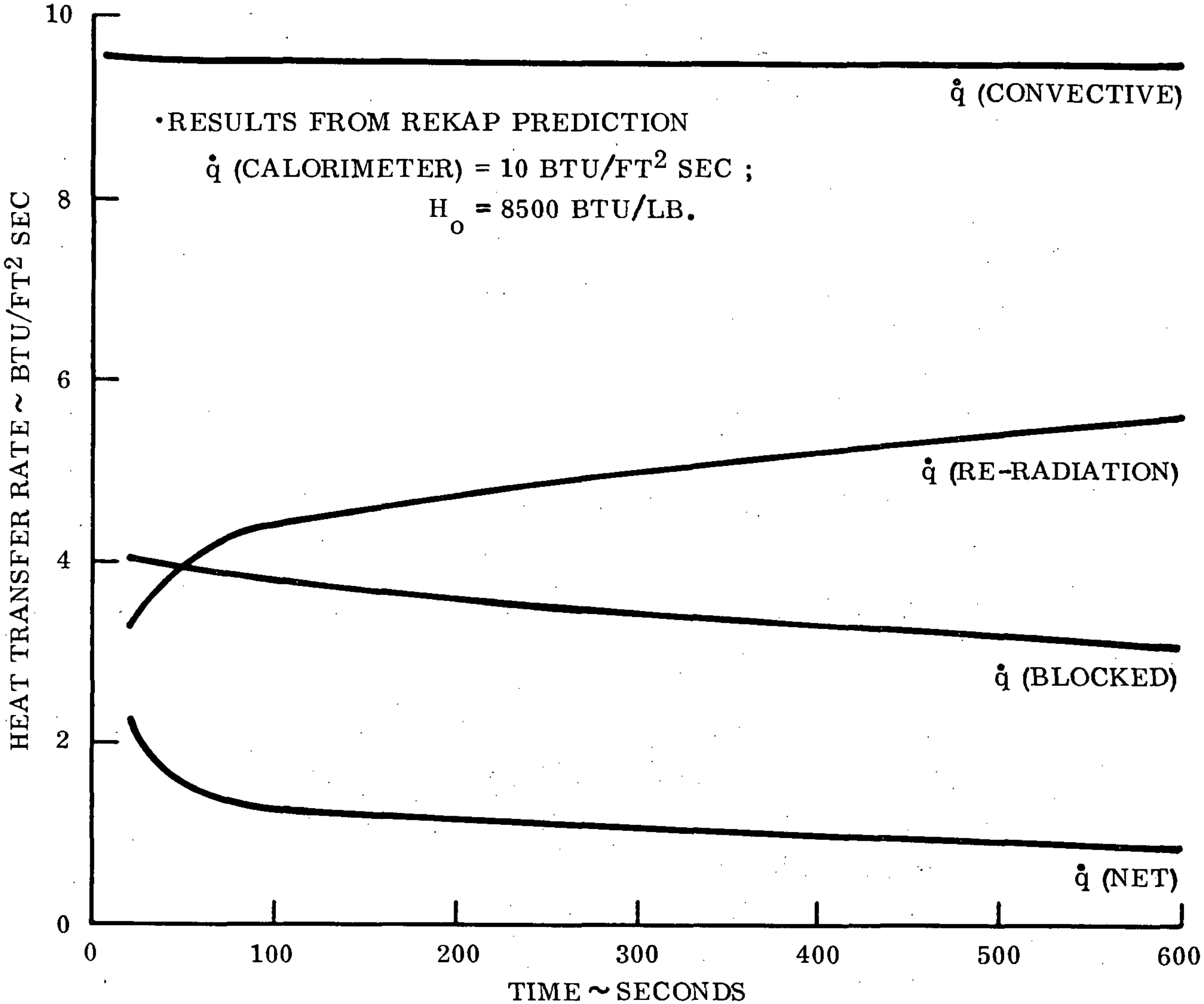

Figure 4-15. Accommodation of Thermal Energy - ESM 1004X

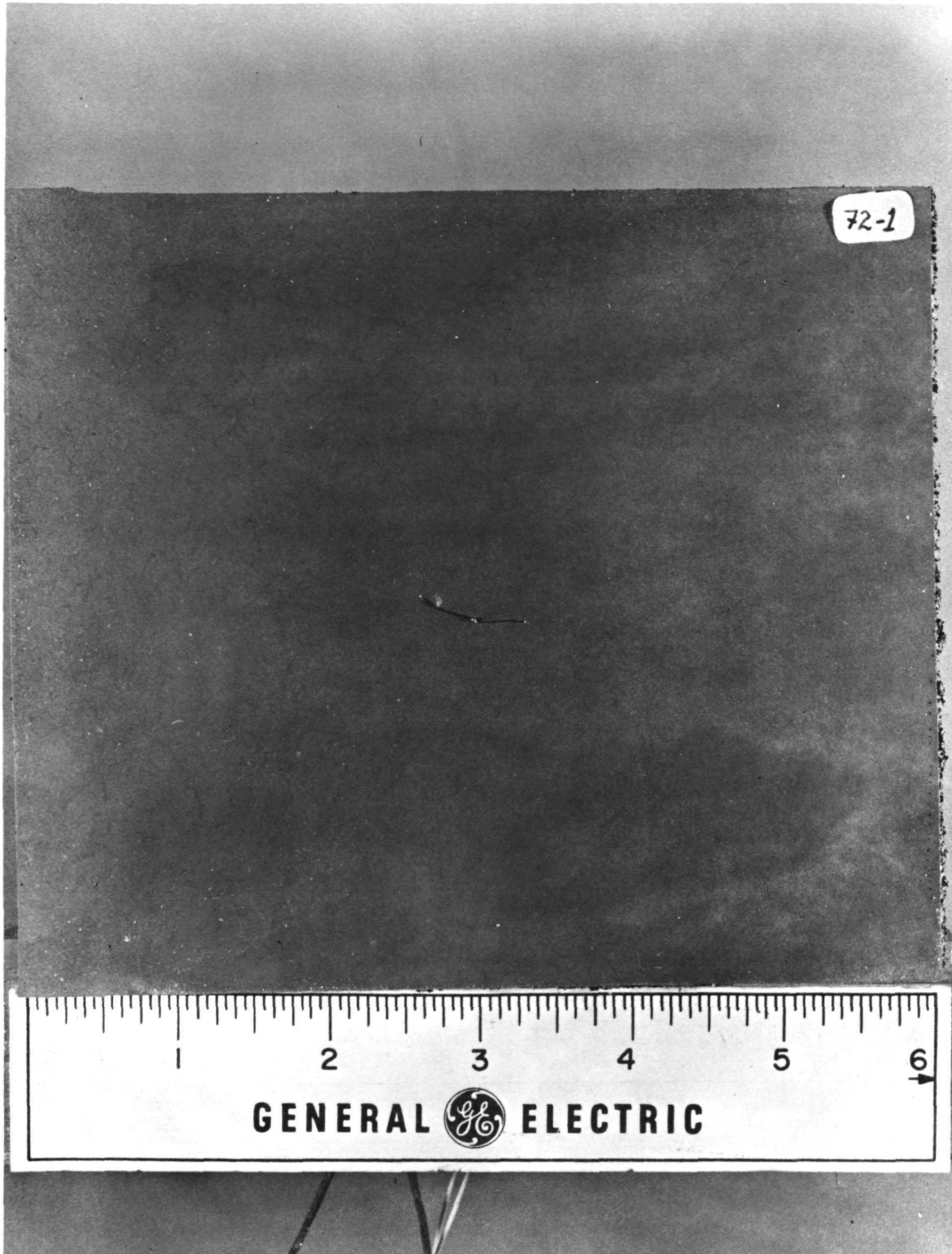

Figure 4-16. ESM 72-1 Before Test

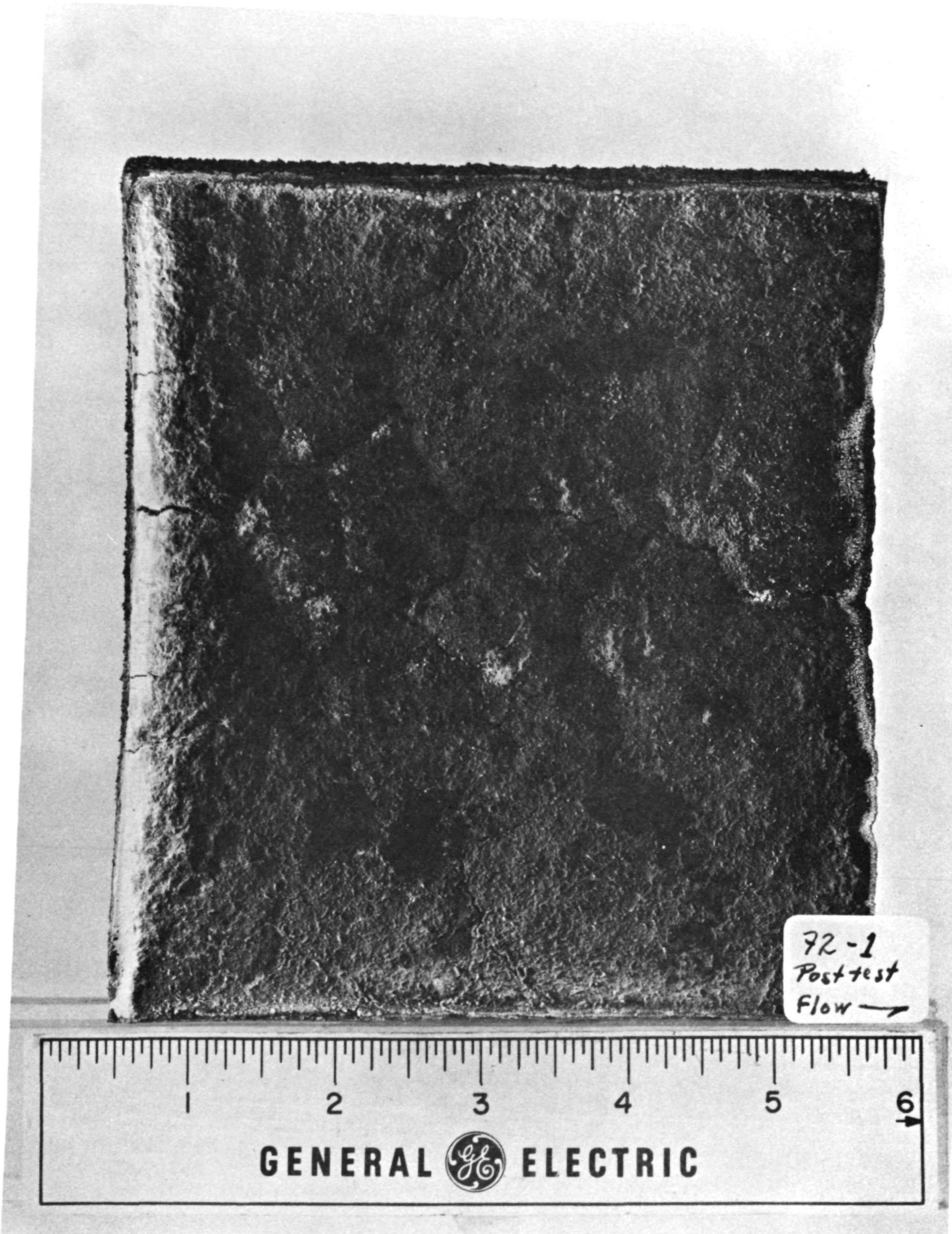

Figure 4-17. ESM 72-1 After Test

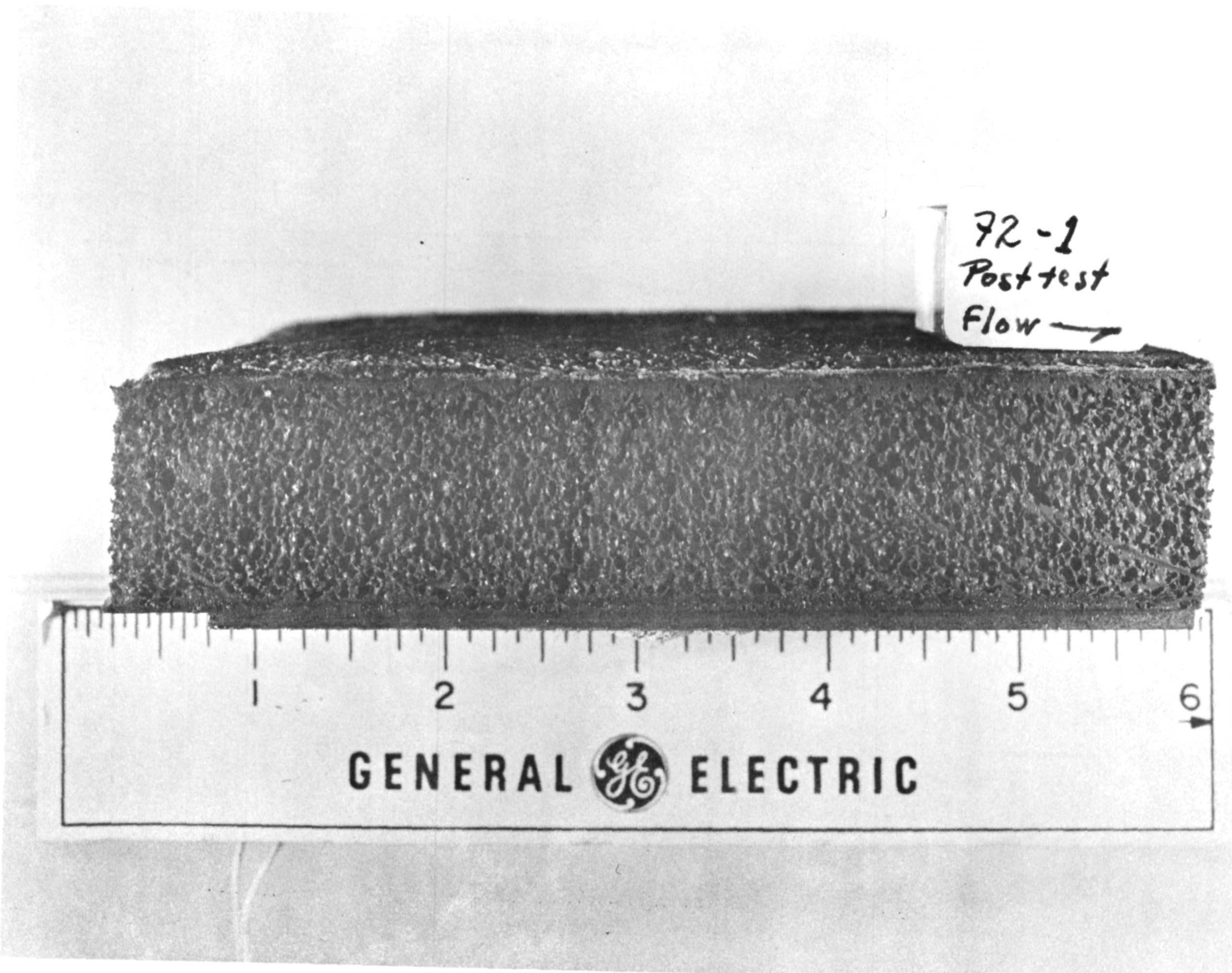

Figure 4-18. ESM 72-1 After Test - Side View

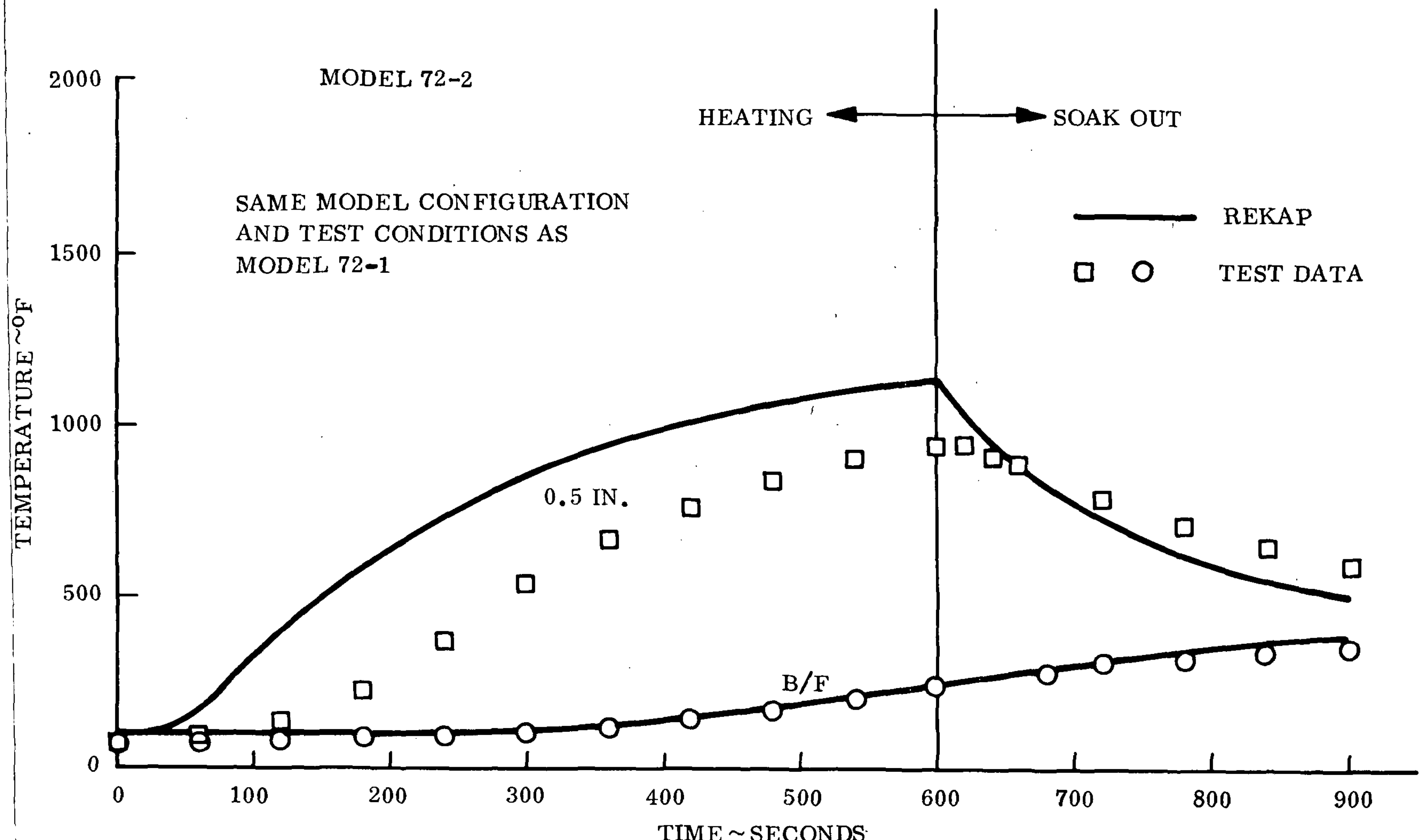

Figure 4-19. Plasma Arc Test ESM 1004X

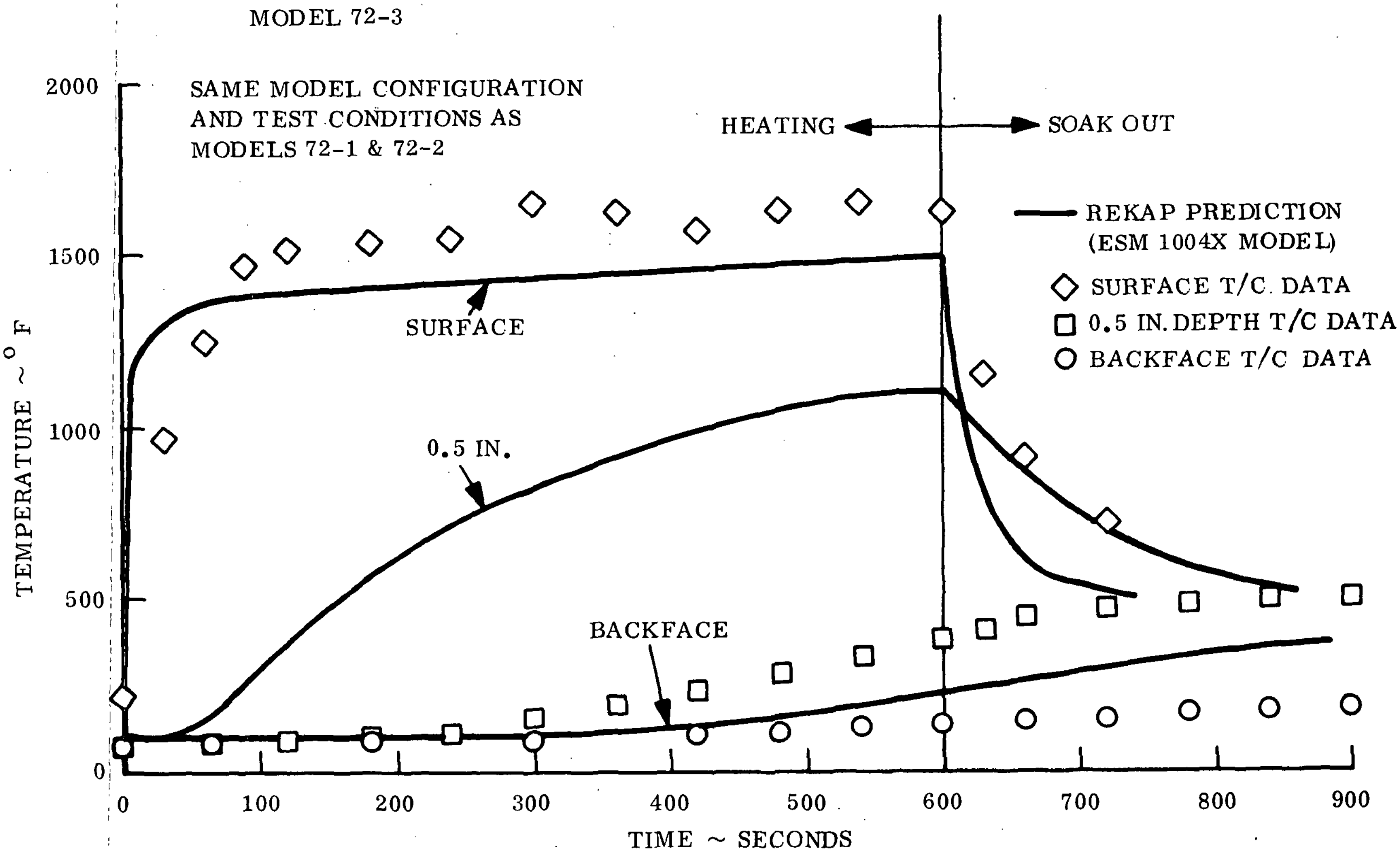

Figure 4-20. Plasma Arc Test - ESM 1004X (Modified)

4.4 EVALUATION OF ESM JOINT PERFORMANCE

For such a large vehicle as the space shuttle orbiter, any ablative system to be used as the thermal protection system will have to be applied to the airframe in the form of panels or strips. This will result in numerous seams between adjacent panels. A plasma arc test program was conducted for a prior study in the GE 5 MW Arc Facility to evaluate the thermal performance of the seams, including the following variables:

a. Seam configuration (butt or scarfed)

b. Seam filler (RTV 560 or the base elastomer)

c. Presence or absence of post-cure of the seam filler

This program was conducted on GE ESM 1004 AP ($\rho = 35$ lb/ft^3), but the results are expected to be perfectly valid for the flexible ablator concept of this program. The results of that seam test program are presented in Reference 5, and a review of main results follows.

To evaluate insulative performance, seam performance, and performance of repaired areas, 6 x 6 inch models were tested in order to provide a large enough model to properly assess the effects of char shrinkage. On small models, shrinkage effects are relieved by inward contraction of the char away from the edges of the model. The 6 x 6 inch models provided sufficient size to prevent this relief and to permit shrinkage to affect the seams, repairs, and model surface.

The seam performance test models were ESM sheet stock bonded with RTV 560 to 0.1 inch thick, 6 x 6 inch phenolic glass segments taken from rejected vehicle liners. ESM sheet stock thickness was a nominal 0.65 inches. These models were subjected to a charring environment ($\dot{q}_{cal} = 50$ BTU/ft^2 sec) in the 5 MW Arc Facility until the bondline temperature reached 250°F. Nominally, this took about 250 seconds and subjected the samples to a time-integrated cold wall heat load of about 12,500 BTU/ft^2, which is a hot wall value of about 10,000 BTU/ft^2.

Data obtained from the test runs included bondline temperature response and total char depths. Post-test photographs of some of the models are included in Figures 4-21 through 4-24. The elapsed time to reach a temperature rise of 250°F is summarized in Figure 4-25.

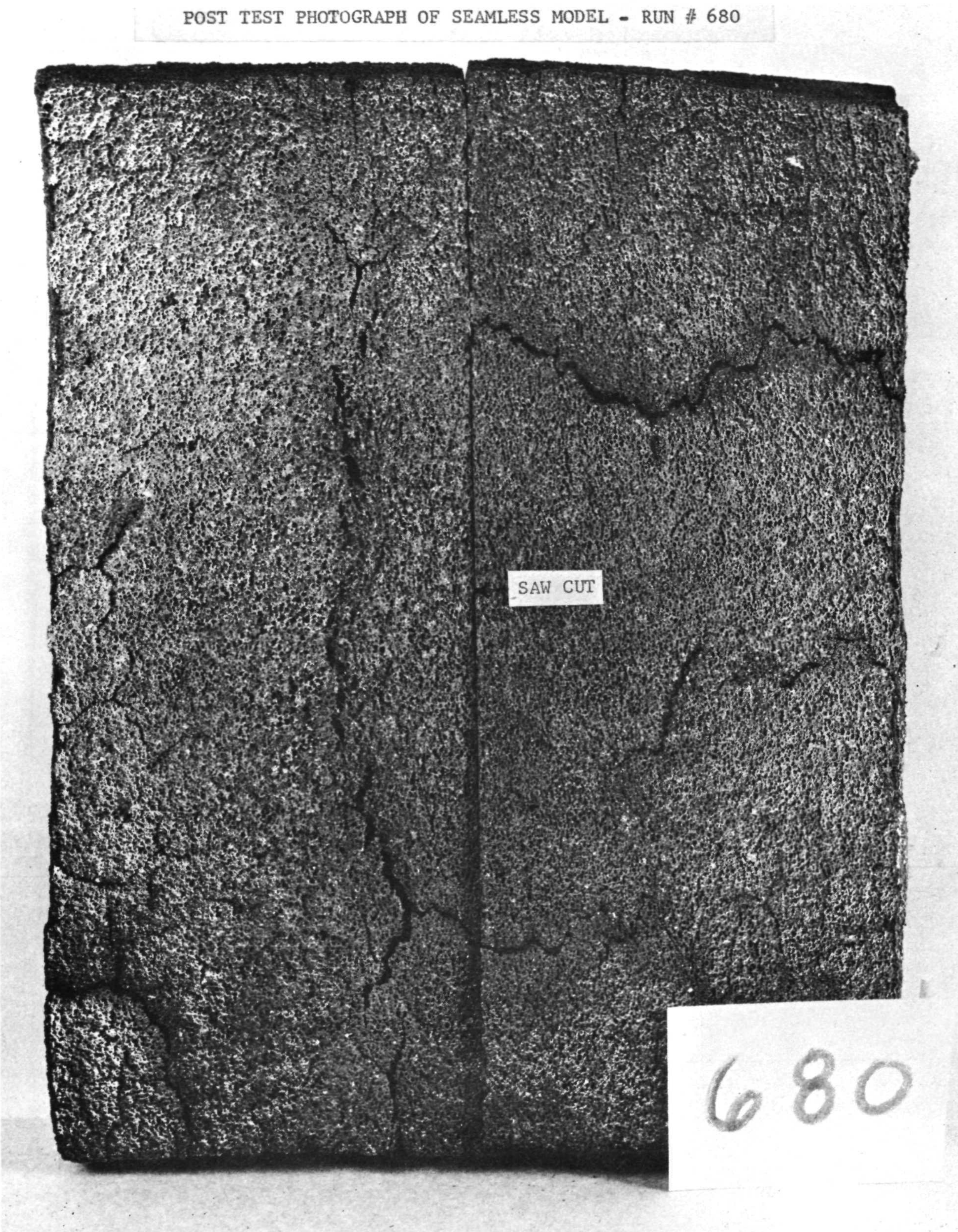

Figure 4-21. Post-Test Photograph of Seamless Model

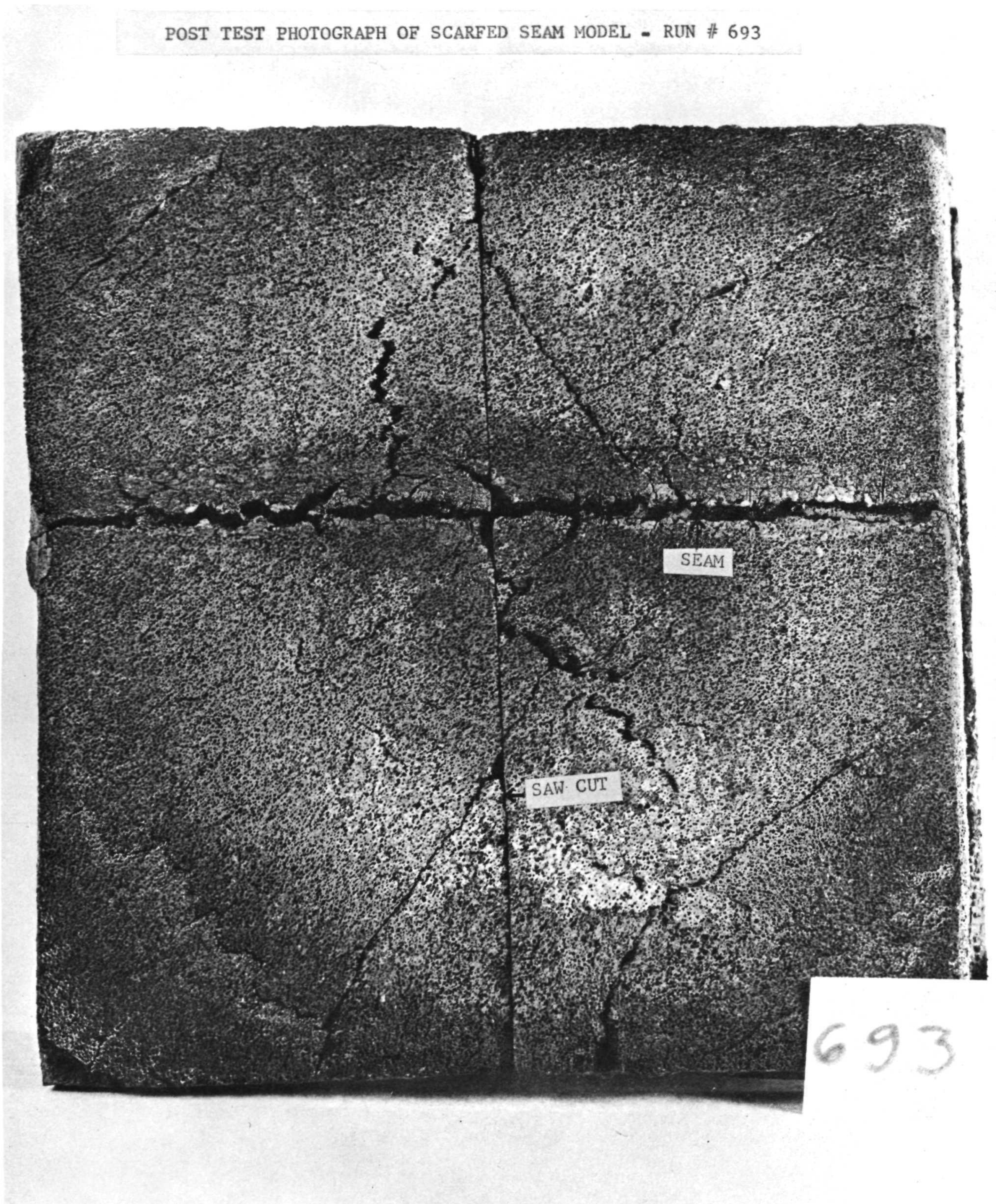

Figure 4-22. Post-Test Photograph of Scarfed Seam Model

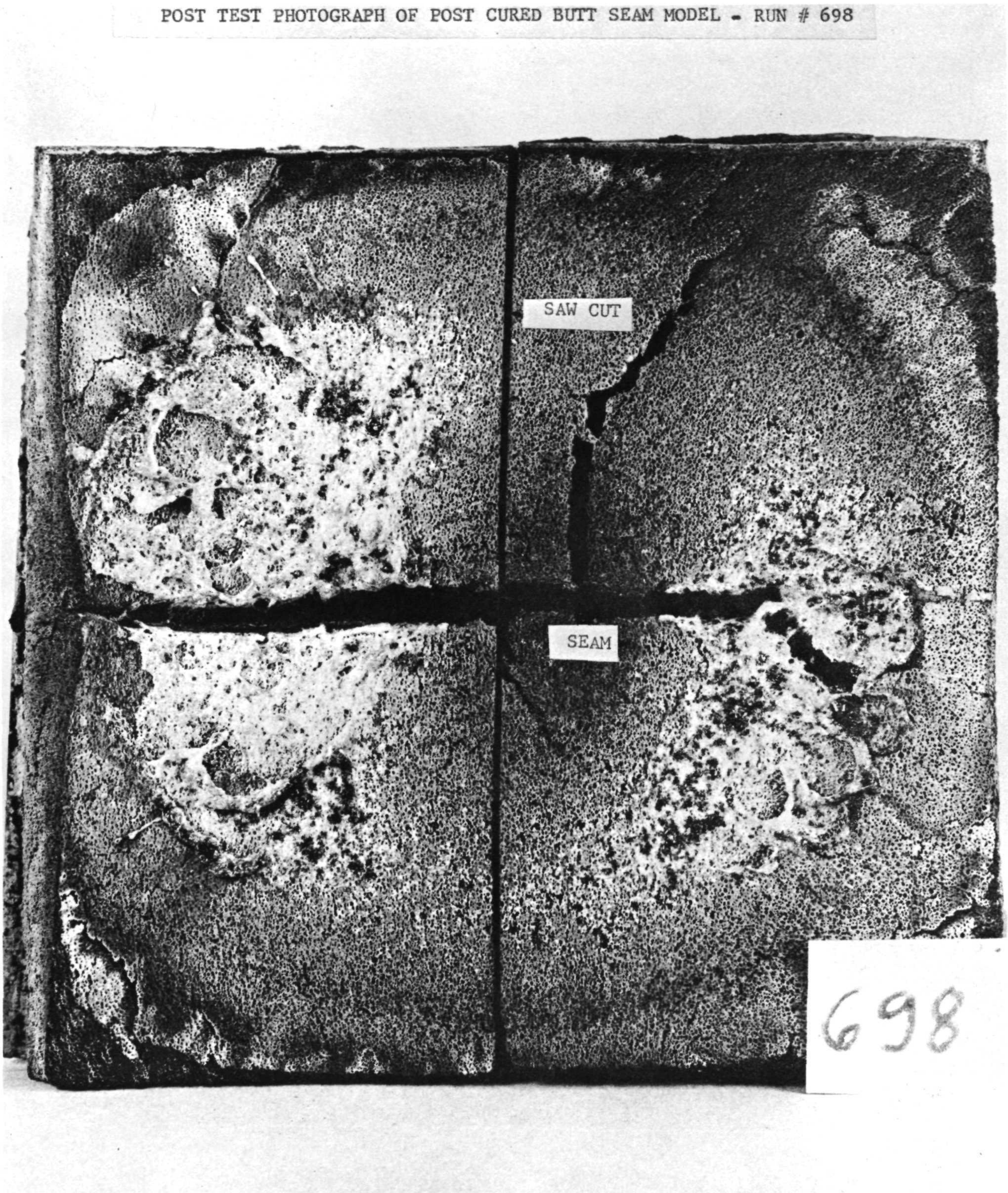

Figure 4-24. Post-Test Photograph of Post-Cured Butt Seam Model

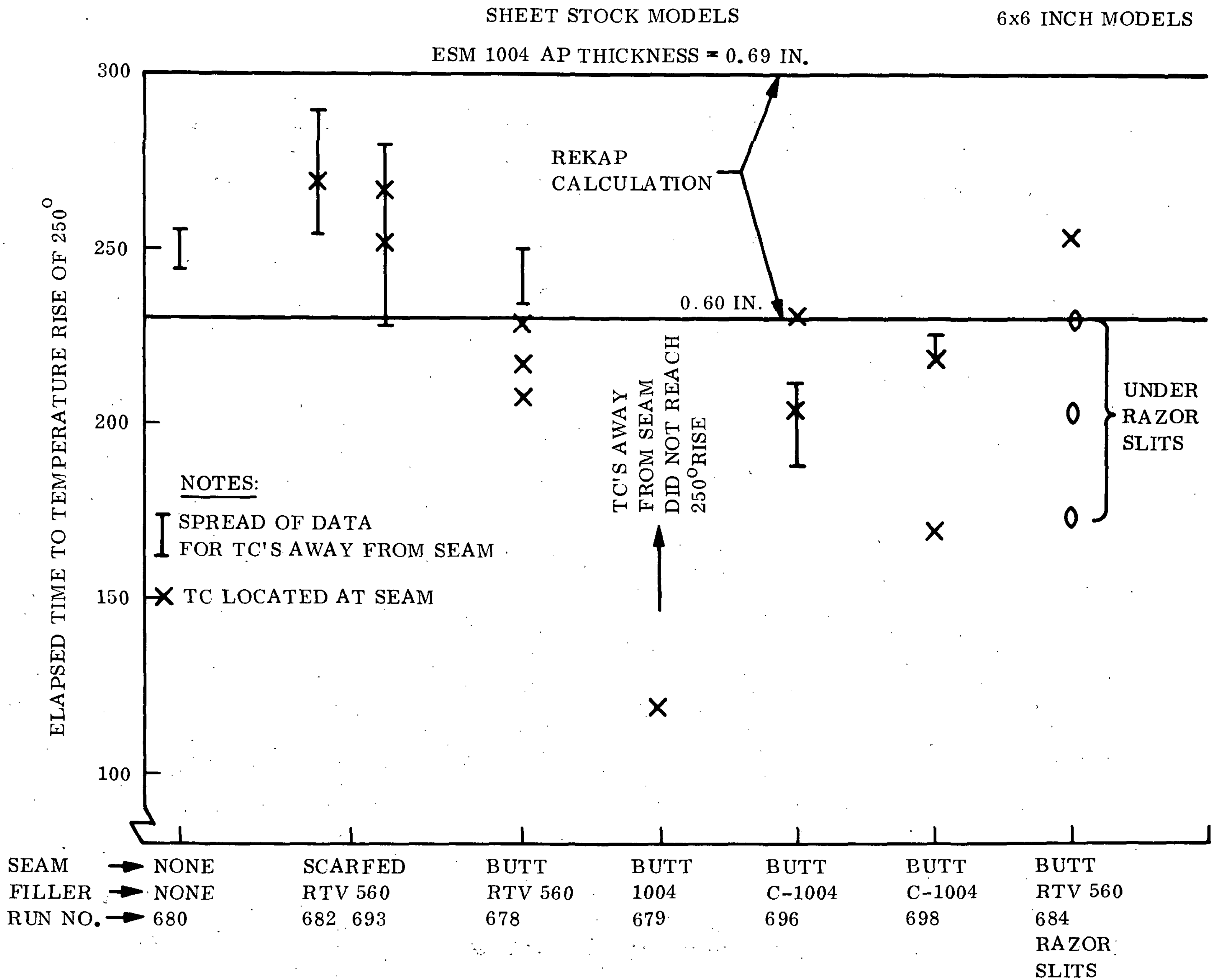

Figure 4-25. Summary of ESM Seam Model Temperature Response

Visual observation of the tested sample with no seam (see Figure 4-21) shows that char shrinkage occurs, forming randomly oriented and randomly spaced cracks. Where a seam is present, the shrinkage tends (except as noted below) to open the seam, forming one large crack which opens to the bottom of the bond char layer and permits local increased in-depth heating at the seam location. The extent of char shrinkage can be seen in Figures 4-23 and 4-24.

In models with butt seams, characteristically the seam opened to the bottom of the hard char layer. The hard char layer was deeper at the opening than elsewhere on the model, and temperature response of thermocouples behind the seam were higher than elsewhere on the model.

In models with scarfed seams, a shrinkage crack formed at the seam but opened perpendicular to the surface rather than following the scarfed seam in depth. The opening did not extend to the bottom of the hard char layer. Thermocouples behind the seam responded no more severely than elsewhere on the model, and the depth of the hard char layer was no deeper behind the seam than elsewhere on the model.

The superior performance of the scarfed seams (post-test photograph, Figure 4-22) is illustrated in Figure 4-25. The model thicknesses varied between 0.6 and 0.69 inches of ESM 1004AP. Temperature response calculations were made with REKAP and are superimposed for this range of model thicknesses on Figure 4-25. Note that the models with no seam and scarfed seams performed essentially the same and agree well with the REKAP calculations.

Test runs were made to demonstrate the effect of post-curing a butt seam filled with the base elastomer ESM 1004. It is seen from Figure 4-25 that no apparent benefit was derived.

The general conclusions obtained from examination of the data are:

a. Scarfed seams appear to offer the best resistance to seam separation and perform as efficient thermally as no seam.

b. Butt seams opened to the bottom of the char layer apparently due to char shrinkage. This results in local in-depth heating and hence a thicker char layer and higher in-depth temperatures locally.

c. No apparent benefit was derived by using ESM base elastomer post-cured or not post-cured as seam filler instead of RTV 560.

4.5 STRUCTURAL ANALYSIS OF FLEXIBLE ABLATOR PANELS

The flexible ablator panels have been analyzed to determine the lineload and thermostructural response of the Arrowhead Velcro and RTV 560 attachment systems. Both 6" and 12" panels of 1.20 inch ablator containing nine Astroquartz yarns per square inch were modeled as shown in Figure 4-26 for the finite element thermostructural analysis. The GE ORTHOSAFE finite element program was employed for the analysis.

One finite element model was used for both the 6" and 12" panels, since centerline symmetry could be employed. The model consisted of 11 elements through the thickness (8 of which were ablator material) and twenty elements along the length. Through-the-thickness deflection of the aluminum substrate was restrained, assuming an infinitely rigid substructure, which resulted in conservative predictions of the attachment stresses. The line load results represent attachment stresses in a 20" wide panel.

The material properties assumed for the analysis are given in Figures 4-27 through 4-30 and in Table 4-9. The effect of Astroquartz yarn was neglected in the in-plane behavior of the ESM 1004X, while the through-the-thickness tensile behavior of the ablator was assumed to be that of nine Astroquartz fibers per square inch. Char properties were not assumed for the ablator since char behavior is not well characterized.

Mechanical properties of the Velcro were obtained from data supplied by NASA-MSC, resulting in a design tensile strength of roughly 7 psi. In-house mechanical properties of standard hook and pile Velcro were determined from several samples of material tested in tension and shear to determine an effective elastic modulus and shear modulus, and an estimate of the material capability. The tension test was a simple butt specimen with one inch squares of Velcro bonded to aluminum fixtures. The specimen was reassembled and tested several times to get a rough indication of the repeatibility of the data. The results given in Table 4-10 indicate reasonably uniform results; however, the tensile strength at failure was considerably less than expected. The shear test configuration provided a straight-load path for the loading. The results (Table 4-10) were uniform, and indicate a rather low capability of the hook and pile. Consequently, the standard hook and pile Velcro was dropped from consideration.

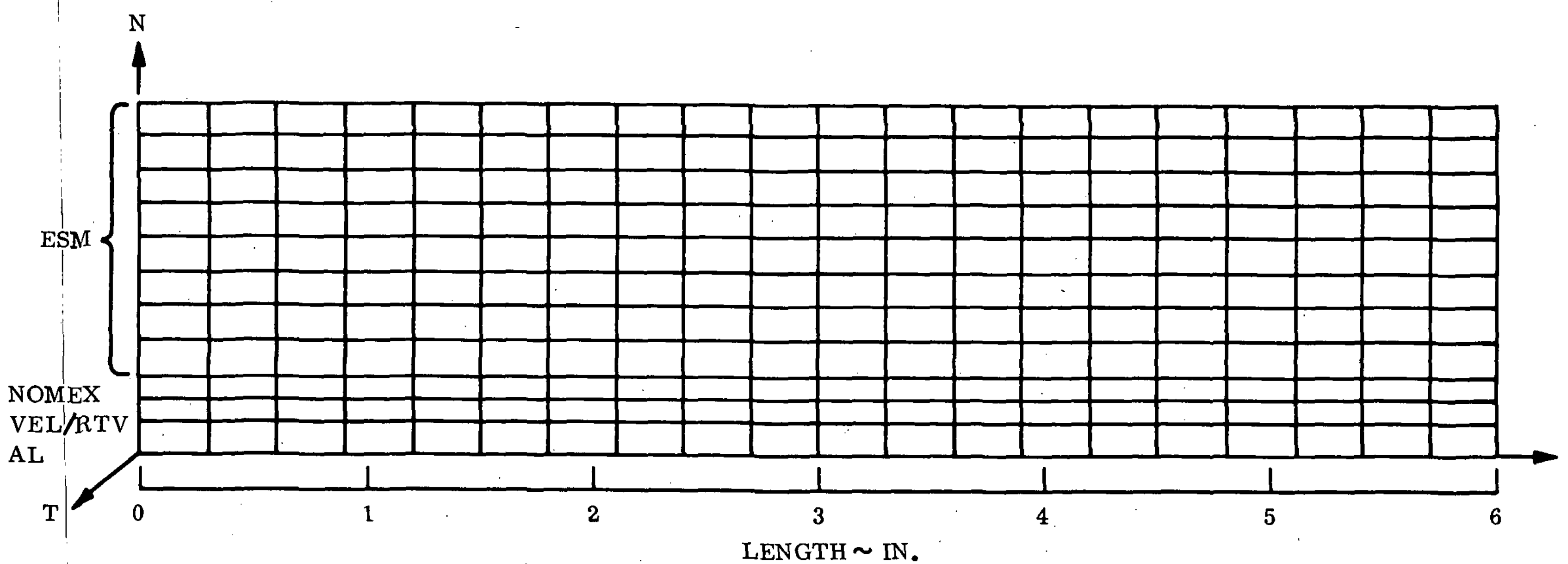

Figure 4-26. Finite Element Model

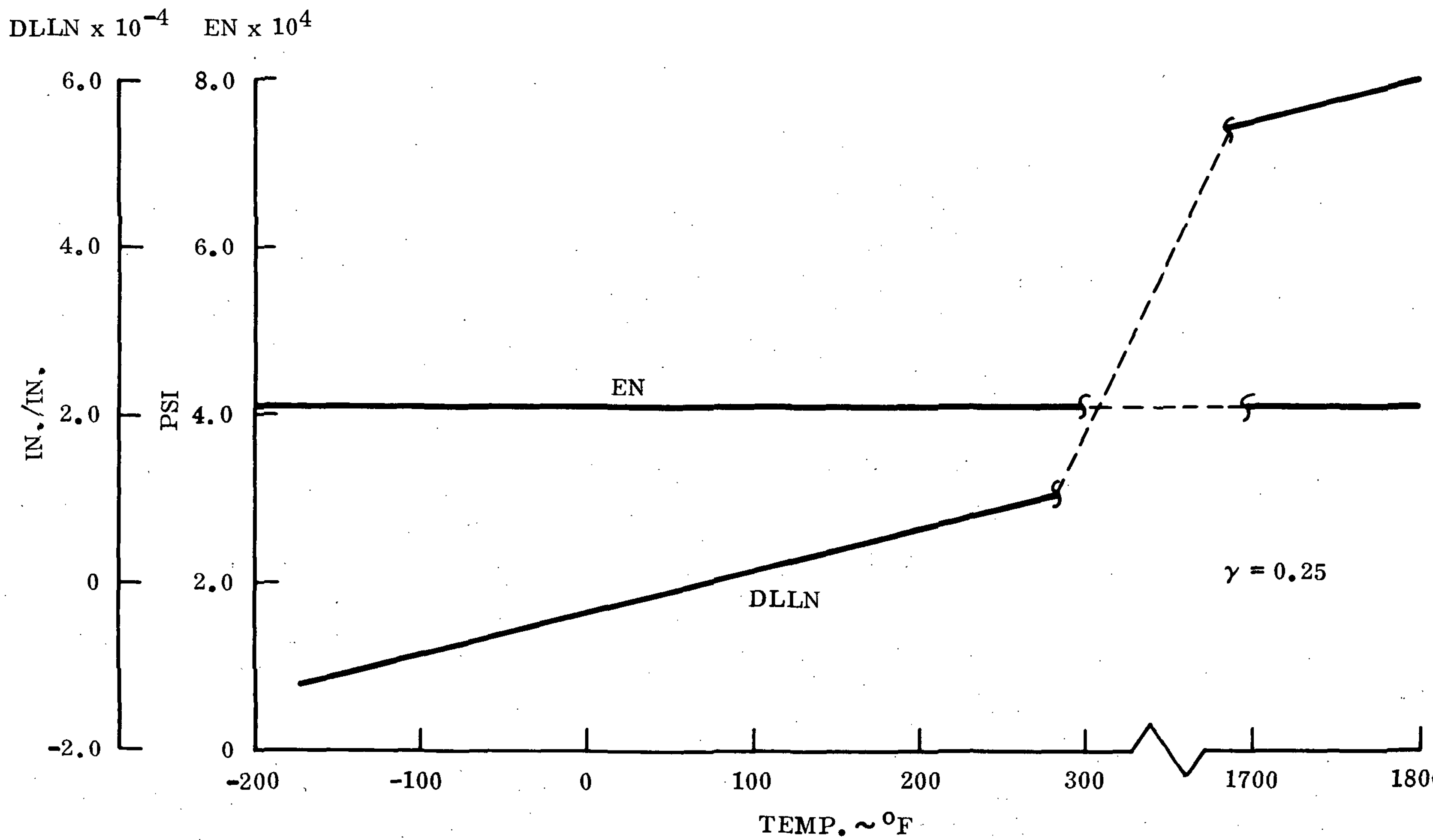

Figure 4-27. ESM 1004X with 9 Astroquartz Yarns/In^2

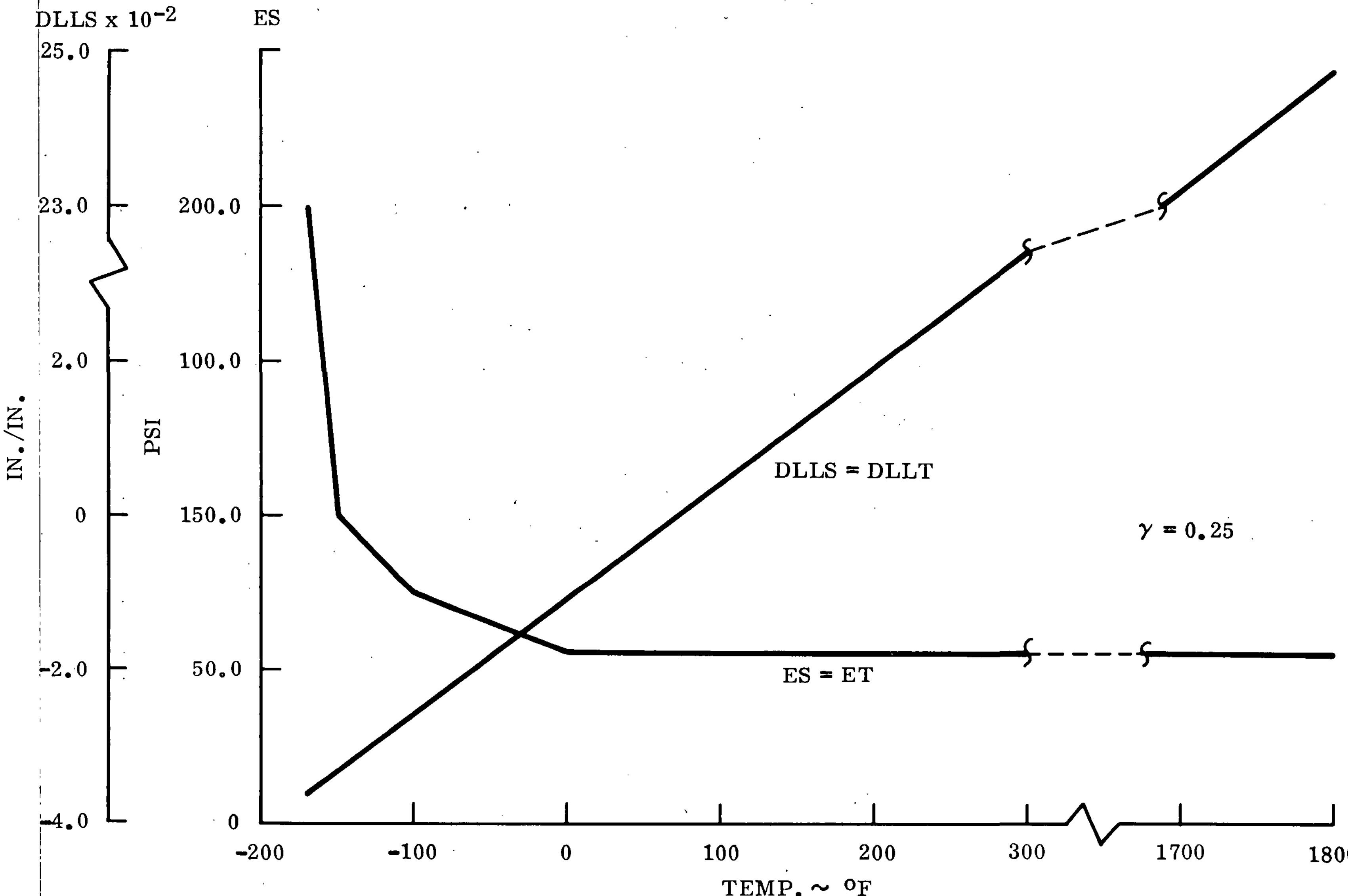

Figure 4-28. ESM 1004X

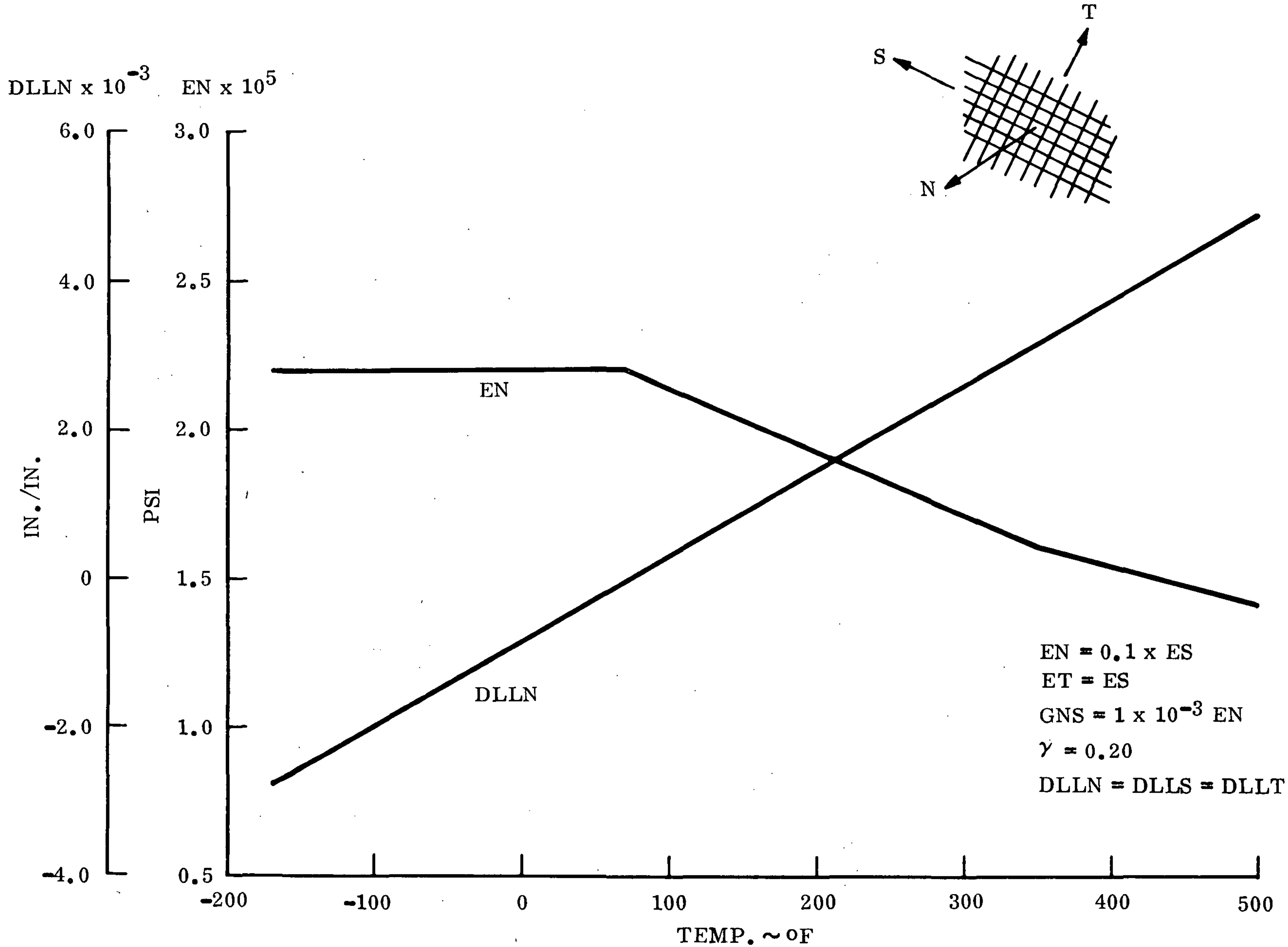

Figure 4-29. Nomex Weave

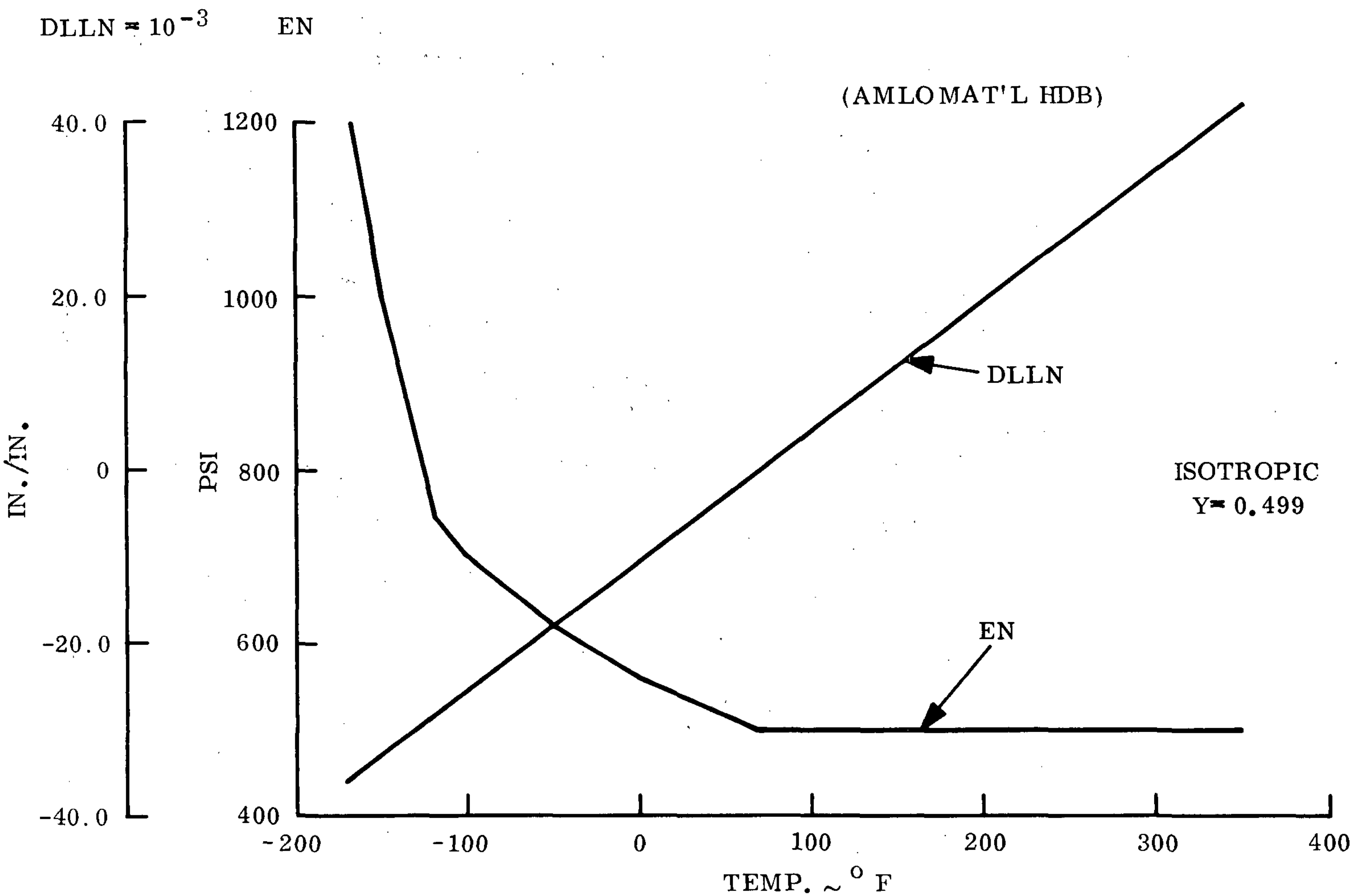

Figure 4-30. RTV 560

TABLE 4-9. ROOM TEMPERATURE PROPERTIES

ALUMINUM	
	$E = 10.4 \times 10^6$ psi
	$\gamma = 0.32$
	$\alpha = 12.8 \times 10^{-6}$ in/in/°F
VELCRO - NYLON LOOP AND HOOK	
	E_1 (Normal to Tape) = 10. *
	E_2 (Parallel to Tape) = 3.9×10^4 **
	γ_1 = .2 inplane of backing
	γ_2 = .01 across Loop and Pile
	$\alpha = 11.2 \times 10^{-6}$ in/in/°F
	G = 150. *
*	In-house Room Temperature Test
**	Effective E for .0065" tape sheets acting over the 0.1" Velcro thickness

TABLE 4-10. VELCRO TEST RESULTS

Room Temperature			
Tension Tests - 1 Square Inch			
Specimen	Test	Ultimate Stress	Modulus
1	1	2.15	8.
	2	2.95	7.8
	3	3.15	11.1
2	1	1.70	5.5
	2	2.32	7.7
	3	2.67	7.7
Shear Tests - 2 Square Inches			
Specimen	Test	Ultimate Stress	Modulus
1	1	5.6	111.
	2	5.1	143.
	3	5.0	129.

TABLE 4-11. CONDITIONS ANALYZED

CASE	1	2	3	4	5	6	7
Velcro	X	X	X			X	
RTV 560				X	X		X
6" Panel			X		X		
12" Panel	X	X		X			
20" Panel						X	X
1700°F Surface/ 70° Backface	X						
1700°F Surface/ -150° Backface		X	X	X	X		
0.1% Lineload						X	X

The inplane properties of the Velcro were derived assuming the backing faces carry all the inplane loads. Thus the inplane capability of the Velcro is considerably higher than 7 psi.

The loading conditions, configurations, and attachments analyzed are shown in Table 4-11, and the pertinent results of the analyses are summarized in Table 4-12. The thermal gradients used were predicted by the Thermodynamics Laboratory for the room temperature backface condition and estimated for the cold entry conditions as shown in Figure 4-31.

Examining Table 4-12, one finds that the through-the-thickness Velcro stresses were small for all thermal loading and would result in 3 psi for a 0.3% strain in the substructure due to lineload. However, the shear stress during lineload would be $\approx$ 33 psi at the panel edges. Consequently, the panel edges will require supplemental fastening; however, the remainder of the Velcro should remain attached.

For the bonded panels, the predicted stress levels are all low since RTV 560 has a stress capability of 100 psi at temperatures up to 400°F. Likewise, the ESM 1004X stress levels were all small.

The results of Table 4-12 do not include any installation stresses required to maintain a curved panel in a flat or reversed curvature position. Installation stresses would depend upon panel width and initial and final curvature, and would add tensile stresses to the attachment system. Present panels have exhibited no tendency to peel away from the attachment during either handling or thermal testing. Consequently, it is felt that the addition of edge fasteners would eliminate any tendency for the panel to peel away from its attachment during either installation or lineload.

The results, tabulated in Table 4-12, indicate very small dependency of stresses on the panel size, considering thermal loading. Consequently, panel size on a shuttle vehicle will be limited primarily by fabrication size rather than by a stress requirement. The exception to this may be consideration of charring cracks which develop in the char material and which are a function of panel size. No analysis of the char material was made in this study, since detailed char properties were not determined. Surface restraint induced by large panels could constrain panel size since char cracking should be limited to reasonable depths.

TABLE 4-12. RESULTS OF ANALYSIS

Case		12"/Velcro/ R.T. Entry	12"/Velcro/ Cold Entry	12"/RTV/ Cold Entry	6"/Velcro/ Cold Entry	6"/RTV/ Cold Entry	20"/Velcro/ .1% Line Load	20"/RTV/ .1% Line Load
Velcro	in-plane σ	3.3*	-5.0	-	-6.1	-	24.1	-
	T-T-T σ	.5	-0.5	-	.9	-	1.0	-
	Max. τ	3.0	5.4	-	5.4	-	10.9	-
RTV	in-plane σ	-	-	31.5	-	31.5	-	<<
	T-T-T σ	-	-	2.3	-	2.3	-	<<
	Max. τ	-	-	19.5	-	18.5	-	12.7
ESM 1004/Astro-quartz	in-plane σ	.1	2.1	2.1	2.1	2.1	<<	<<
	T-T-T ϵ	.43**	.4	.4	.4	.4	<<	<<
	Max. τ	7.4	7.2	7.6	7.1	7.5	.5	.6
Nomex	in-plane σ	74.6	17.0	-18.5	51.3	-13.9	530.	60

* All stresses in psi
** Strains - %

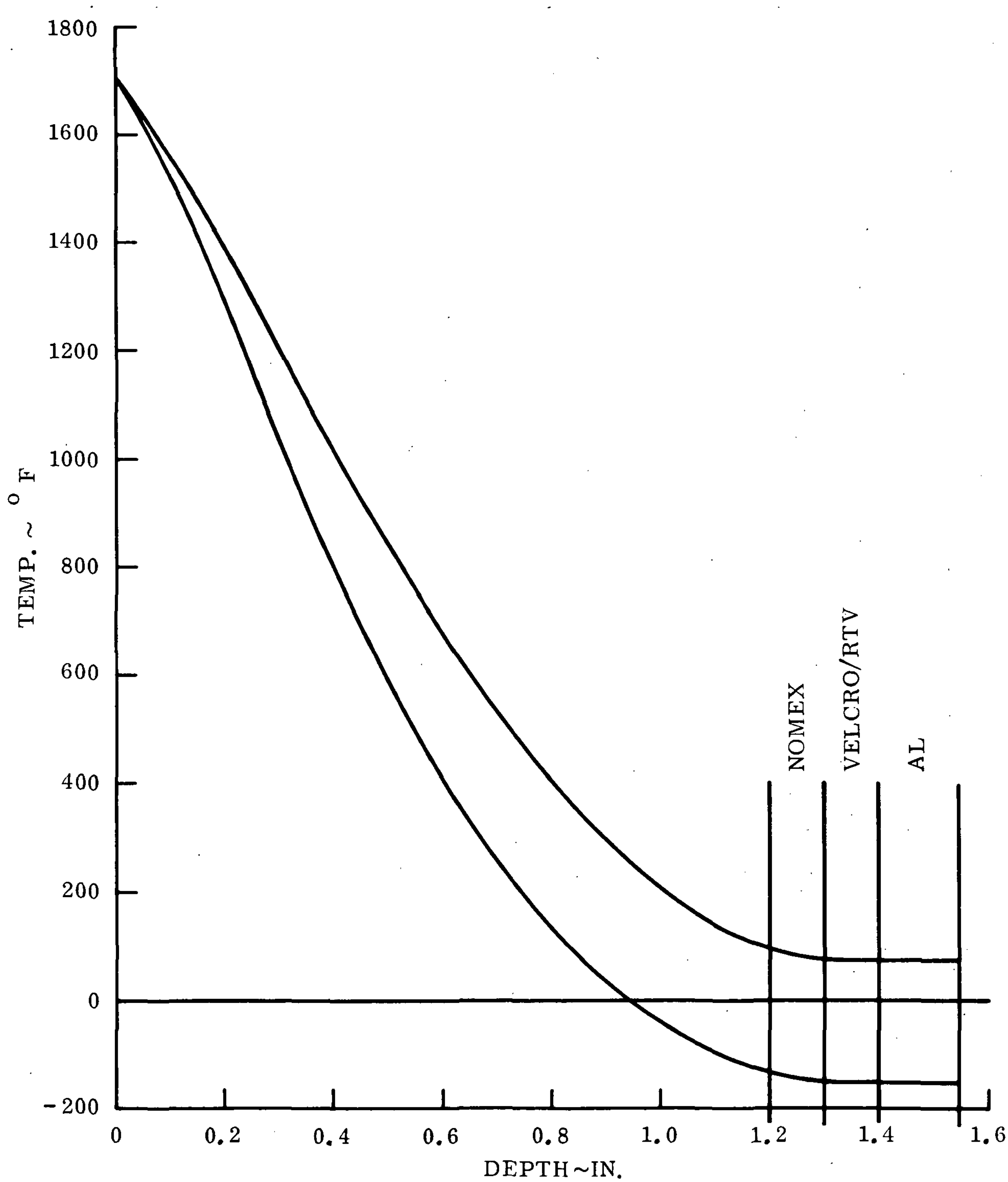

Figure 4-31. Thermal Gradients

A twelve inch panel of flexible ablator 2.4 inches thick has been modelled for area 1 heating gradients at 2047 seconds (REKAP run #54619). Velcro properties were assumed for the attachment, and the results shown in Table 4-13 indicate no severe stress levels existing in either the ablator or attachment.

TABLE 4-13. THERMAL STRESSES FOR AREA 1 PANEL

Thickness of Ablator - 2.4" Tile Width - 12"	
Velcro Attachment	
Through-Thickness Stress	1.1 psi
Shear Stress	1.3 psi
ESM 1004X	
In-Plane Stress	Negative
Shear Stress	3.3 psi

SECTION 5

COSTS

5. COSTS

5.1 FLEXIBLE ABLATOR FABRICATION

The following costs are estimates and are based on the assumption that a total of 100,000 ft^2 will be produced per year. The estimates are also based on current production methods. Two cases are presented: (1) foaming in the woven construction, and (2) bonding on a backing and tufting.

a. Foaming of Ablator in the Woven Carpet Construction

1. Cost of carpet (100 ft^2) = $1400.

2. Cost of ablative material to fill 100 ft^2 to a depth of 1" (+ coating) = $5000.

3. Labor costs (estimated) = $10,000.

Total costs/(100 ft^2) = $16,400.
Cost/square foot = ~ $164.

b. Bonding on Backing and Tufting

1. Cost of tufting (100 ft^2) = $450.

2. Cost of ablative material for 100 ft^2 to a thickness of 1" = $2000.

3. Labor costs (estimated) = $7500.

Total costs/100 ft^2 = $9950.
Cost/square foot = $100.

5.2 FLEXIBLE ABLATOR APPLICATION

These costs are based on a per-mission, per-vehicle basis. For the calculations, it was assumed that 8000 ft^2 would be applied per vehicle. Two cases are considered: (a) direct bonding, (b) BAS attachment concept.

a. Direct Bonding

1. Bonding

(a) Cost of RTV 560 for 100 ft^2 at a thickness of 10 mils + vacuum bagging + primer = $200.

(b) Labor costs (estimated) = $2500.

Total costs/100 ft^2 = $2700.
Cost/Square foot = $27.

2. Removal of Cured RTV 560 Bond Material from Aluminum Surface

(a) Material costs (minimal)

(b) Labor costs/100 ft^2 = $1000.

Cost/square foot = $10.

3. The cost of fabricating, applying and removing the flexible ablative covering (recommended concept) and cleaning the aluminum surface for re-application (per square foot) would be:

$100.00 - fabrication costs
27.00 - bonding costs
10.00 - removal & cleaning

Total = $137/square foot.

b. BAS Concept

1. Cost of barbs/100 ft^2 = $500.

2. Labor costs for installation of barbs/100 ft^2 = $300.

3. Labor costs for application of flexible ablative covering/100 ft^2 = $200.

Total cost/100 ft^2 = $1000. *
Cost/square foot = $10.

(*Note: $800. of the total cost/100 ft^2 is a non-recurring cost.)

SECTION 6

DELIVERABLES

6. DELIVERABLES

The following specimens were delivered to NASA MSC:

a. One 12" x 12" x 1-1/4" ESM 1004X foamed-in carpet with Fiberglas backing, 8 Astroquartz tufts/in^2 (Sample 15, Table 3-3) bonded to 1/8"-thick aluminum plate with RTV 560

b. Two 6" x 6" x 1-1/4" ESM 1004X foamed-in carpet with Fiberglas backing. 8 Astroquartz tufts/in^2 (Sample 16, Table 3-3), both bonded to 1/8"-thick aluminum plates with RTV 560.

All three samples were delivered on April 5, 1972, and each was instrumented with 4 thermocouples placed as shown in Figure 6-1.

c. Three 6" x 6" x 1-1/4" foamed in glass-backed carpet, bonded with RTV 560 to 62 mil aluminum

d. Three 6" x 6" x 1-1/4" foamed in Nomex-backed carpet, bonded with RTV 560 to 62 mil aluminum

e. One 12" x 12" x 1-1/4" flat panel bonded to Nomex backing in three sections with scarfed joints (Figure 6-2), attached to 62 mil aluminum with the molded arrowhead and pile Velcro concept.

f. One 12" x 12" x 1-1/4" panel, bonded to Fiberglas backing, in three sections with scarfed joints. Bonded to a 62 mil aluminum panel with 10 foot radius of curvature with RTV 560.

g. Three, 6" x 6" x 1-1/4" panels, foamed in Fiberglas backed carpet, unattached

h. One 6" x 6" aluminum panel with GE BAS attachments

The later series of samples was delivered to MSC on May 11, 1972.

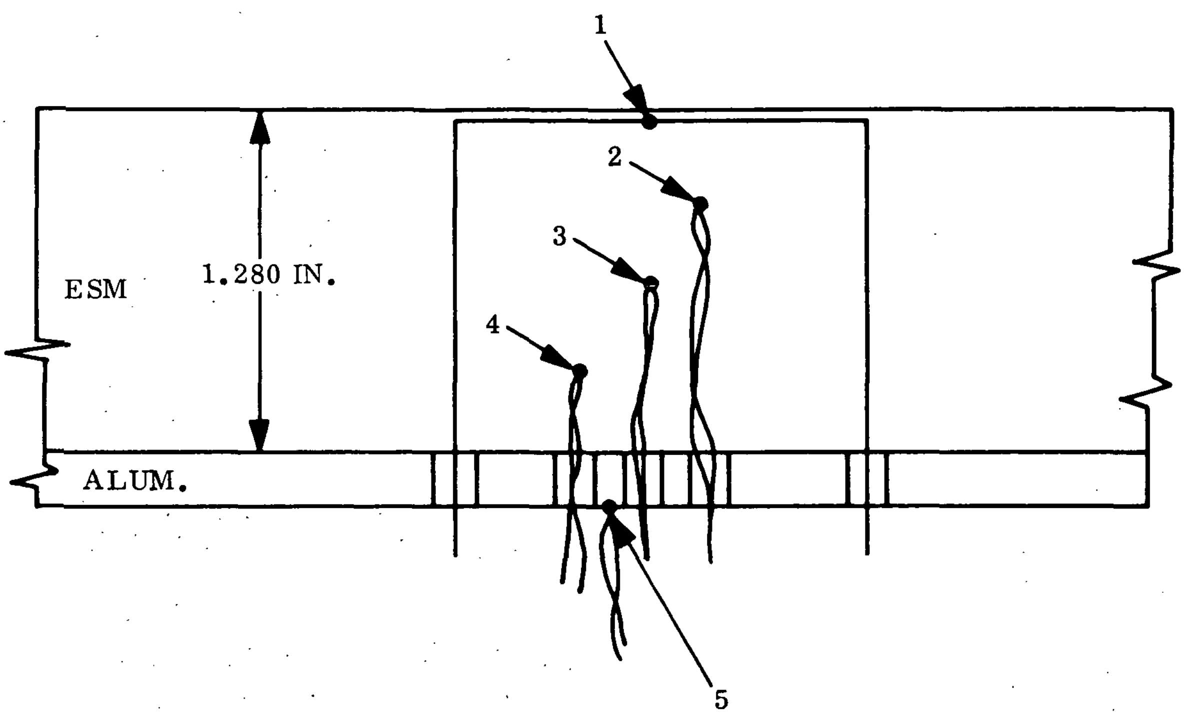

NO. 1 - PLAT. + 0.10% RHODIUM/100% PLAT. - JUST UNDER SURFACE

NO. 2 - C/A (K) 0.320 IN. FROM FRONT SURFACE

NO. 3 - C/A (K) 0.640 IN. FROM FRONT SURFACE

NO. 4 - C/A (K) 0.960 IN. FROM FRONT SURFACE

NO. 5 - C/A (K) ON BACKFACE OF ALUMINUM PLATE

NOT TO SCALE

Figure 6-1. Thermocouple Locations in Flexible Ablator Samples

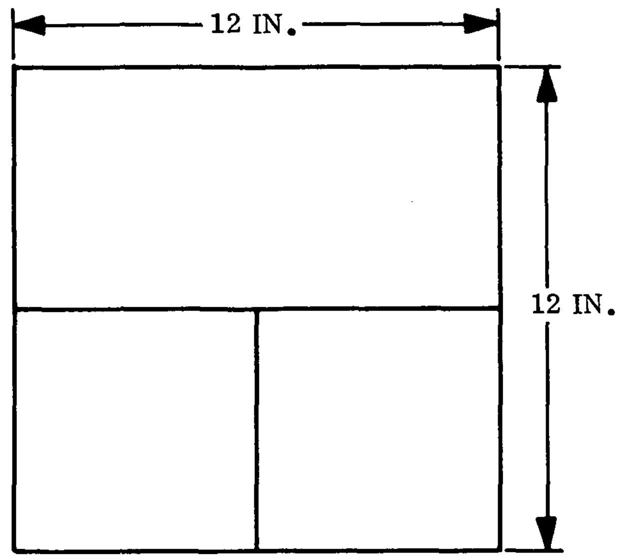

Figure 6-2. Joint Configuration

SECTION 7

CONCLUSIONS AND RECOMMENDATIONS FOR FUTURE STUDY

7. CONCLUSIONS AND RECOMMENDATIONS

7.1 CONCLUSIONS

a. The feasibility of the reinforced flexible ablator concept was demonstrated.

b. Ablation tests demonstrated the utility of the reinforcement concept and demonstrated the char reinforcement provided by the carpet pile fibers.

c. The flexible ablative material system shows a weight advantage over the RSI TPS for heat loads greater than 16,000-20,000 BTU/ft^2; i.e. for the hotter regions of the orbiter such as NASA-MSC point design Area 2P.

d. For increasing values of heat load (above 20,000 BTU/ft^2) typical of nose and wing leading edge heating, the increased thickness requirement for the flexible ablator is relatively small compared with the increased requirements for a material such as RSI.

e. Three models were tested in an extremely severe environment ($\dot{q} \sim 100$ BTU/ft^2 sec) and demonstrated excellent capability to withstand off-nominal entry conditions.

f. Three models tested at a nominal heat flux of 10 BTU/ft^2 sec and compared between in-depth and backface temperature data and analytical predictions using REKAP were very good, indicating that the thermal performance of the flexible ablator is producible using currently available design.

g. The excellent thermal performance exhibited by a modified ESM 1004X material suggests that further testing and characterization of this material should be pursued.

h. Thermal performance of various seam configurations tested in the plasma arc facility indicate that scarf joints are most efficient thermally.

i. Several attachment concepts were shown to be feasible for the flexible ablator, and three of these, viz, the Velcro, the GE BAS System, and the NASA MSC Spire system were shown to provide a convenient refurbishment method.

j. Structural analyses indicate no structural problems with the flexible ablator concept. The only restriction on panel size would derive from fabrication limitations.

7.2 RECOMMENDATIONS FOR FUTURE WORK

The exploratory work performed in this study has shown the overall feasibility and utility of the flexible ablator concept. It is suggested that additional work be done to prove the utility of the concept for two specific areas of the space shuttle orbiter: the top side and leading edges.

7.2.1 DEFINITION OF REQUIREMENTS

The definition of the requirements will include a review of the NASA MSC orbiter configuration and a review of the total mission environments as provided by NASA MSC. This will identify areas and magnitude of peak heating and time at temperature for those areas. This information will be used for definition of test conditions and sequence as well as definition of the range of TPS thickness for various areas of the vehicle.

7.2.2 TEST DEFINITION TO ESTABLISH RE-USE CAPABILITY

In conjunction with NASA MSC, a test plan will be formulated based on the requirements identified in Paragraph 1.1 to indicate the re-use capability of the flexible ablator concept. This will include a definition of the test facility, a definition of model pre- and post-test characteristics, instrumentation, and test conditions and sequence. Two categories of tests are contemplated:

a. Screening tests to determine the thermal (both high and low temperatures) and dimensional stability of the material.

b. Thermal Cycling Tests to determine the re-use capability of the material in a simulated mission environment.

7.2.3 MODEL DEFINITION AND FABRICATION

The test model configuration (dimensions and shape) will be recommended for NASA MSC approval prior to fabrication. It is estimated that a total of 50 models (each 12" x 12") will be fabricated to comply with the recommended concept. This consists of bonding a Fiberglas backing to preformed sheets of the low density ablator, ESM 1004X, and tufting the resulting composite with Astroquartz fiber to give 9 tufts/in^2. The model is then coated with 10 mils of RTV 560. However, for this application it could be preferable to coat with RTV 511, which is white and which will approximate an optical coating for control of α/ϵ.

7.2.4 PERFORM TEST PROGRAM

7.2.4.1 <u>Screening Tests</u>

The screening program will include, but will not necessarily be limited to, the following:

a. TGA at representative pressures and heating rates

b. Isothermal TGA at representative temperatures and pressures

c. Low temperature soak capability in the bonded configuration

d. Dimensional stability in vacuum-bonded and sealed

e. Effects of isothermal heating at a representative temperature and time on room temperature tensile properties and thermal conductivity of the TPS material

7.2.4.2 Thermal Cycling Tests

7.2.4.2.1 Preliminary - Bonded specimens will be exposed to 5 cycles at each of $600^{\circ}F$, $650^{\circ}F$, and $700^{\circ}F$ in a re-entry simulator in which the heating source is glo-bars. Tests will be conducted at representative pressures and for representative times.

The effects of these exposures will be determined on the compressive properties of the material. Using these results, the maximum practical re-use temperature will be established. Further cyclic tests will be run at this temperature. If this temperature is less than $700^{\circ}F$, additional cycles will be run at $700^{\circ}F$ to determine the re-use capability of the material at that temperature.

7.2.4.2.2 Multiple Exposure Tests - The cycle will include NDE before and after each exposure. The models will be bonded to representative structures and subjected to a cyclic exposure which will include the following:

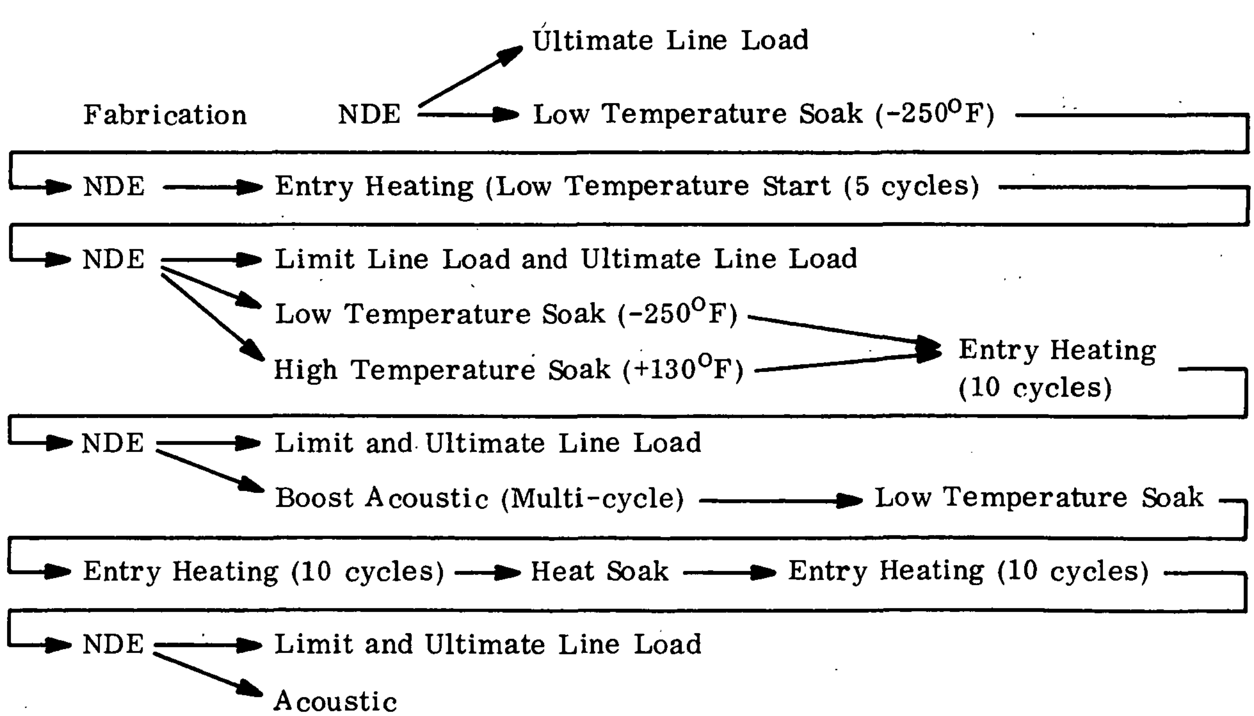

7.2.5 POST-TEST ANALYSES

Post-test evaluations will be made on the cyclic thermal response data to evaluate degradation of thermal conductivity as determined by back face temperature measurements made during the cyclic exposures.

Evaluations will also be made on the materials performance as indicated by weight changes, dimensional changes, and property changes as a result of the cyclic exposures.

7.2.6 REPORTING

In addition to monthly progress reports, a draft of a final report will be submitted for approval one month after completion of the study.

7.3 USE OF FLEXIBLE ABLATOR FOR LEADING EDGE APPLICATIONS

7.3.1 DEFINITION OF REQUIREMENTS

As for item 1.1 except as applies to the leading edge

7.3.2 REVIEW OF PRIOR EXPERIENCE WITH ABLATIVE LEADING EDGES

This will be a literature survey and will include both in-house and industry-wide experience with ablative leading edges. This will identify a density range which should perform in the specific environment.

7.3.3 MATERIAL AND CONCEPT DEFINITION

The preferred density for the ablative material will be bonded to a Fiberglas backing and tufted with Astroquartz. An alternate approach will be to form the ablative filler on the backing reinforcement to the leading edge configuration and tuft with Astroquartz.

A more thermally efficient approach would be a composite consisting of a more dense outer ablative portion over a low density re-usable insulative portion.

7.3.4 DEVELOPMENT OF TEST MATRIX (IN-HOUSE TESTS)

The in-house tests will be run in the 5 MW arc on flat 6" x 6" panels under representative heating rates and pressures. In addition to the normal one exposure tests, re-use capability will be assessed by exposing a tested model to the same ablation condition for one or more subsequent exposures.

7.3.5 DEFINITION OF TEST CONDITIONS FOR LEADING EDGE CONFIGURATION

Test conditions, test model geometry and test facility will be defined in conjunction with MSC.

7.3.6 APPLICATION OF FLEXIBLE ABLATION TECHNOLOGY TO LEADING EDGE APPLICATION

Since the leading edge may require a high density outer portion, the flexible ablator concept must be applied to these higher density materials. Also, since composites are feasible, modifications of the flexible ablator concept will be examined as a means of attaching the two different density portions to each other. Promising candidate systems will be incorporated into the test program.

7.3.7 MODEL FABRICATION, TEST AND ANALYSES

The technology (Paragraph 7.2.6) will be used for the fabrication of the test models which will be tested in a suitable facility, possibly the MSC plasma arc. Calibration data will be required for the selected model configuration and will include heat flux and pressure distributions. Surface, in-depth, and bond-line temperature response data will be used to evaluate the thermal performance of the TPS.

APPENDIX A

QUARTZ YARN DESCRIPTIONS

APPENDIX A

QUARTZ YARN DESCRIPTIONS

Quartz yarn is manufactured in a manner similar to glass, and all the descriptions for glass hold true for quartz. The material, as sold, is as follows:

> 300-1/0 — This is the basic material for all quartz yarn. It contains 120 filaments and has 30,000 yards per pound. Yarn with this description has no twist whatsoever.
>
> 300-2/0 — In developing quartz yarn, 2 strands of yarn are made together so that 300-2/0 is 2 strands of 300-1/0 produced simultaneously. This yarn has 240 filaments and has 15,000 yards per lb.

Current rovings are produced from 300-2/0 yarn, and for 20 end roving 20 strands of 300-2/0 are brought together without twist to form a roving.

In order to produce a yarn, twist must be added to the yarn. Most yarns are produced with a twist of 4 turns per inch in a "Z" direction in the base yarn. So, to produce a 2-ply yarn, 4 turns per inch are added to the 300-2/0 yarn and 2 strands of this are plied together. This results in a yarn designated as 300-2/2. In order to have the yarn balance so that it will not untwist twist is added while plying. Generally, 3.8 turns are added in the "S" direction in order to balance this yarn.

In order to produce a 300-2/4 yarn, 4 strands of the basic 300-2/0 are plied together.

To produce a 300-4/4 yarn, 2 strands of the 300-2/0 untwisted yarn are put together and the necessary twist is applied. Then 4 strands of the 300-4/0 are plied together to produce a 300-4/4 yarn. Again the twist is approximately the same.

Producing 300-8/8 is the same. Four strands of 300-2/0, untwisted, are twisted together to achieve a 300-8/0. Eight of these strands are plied together to give a 300-8/8.

Quartz sewing thread Q-24 — This is actually a 300-4/4 yarn, but it is made with a higher twist than normal in order to achieve the roundness of yarn suitable for sewing. Usually, to achieve the roundness, 8 turns are made in the "Z" direction and 6-1/2 turns in the "S" direction to balance the yarn.

APPENDIX B

WEAVING OPERATIONS

APPENDIX B

WEAVING OPERATIONS

All woven fabrics are made up of two sets of threads, the warp and the weft. The threads which extend throughout the length of the fabric are the warp threads, while those that go across are the weft threads. The technical names for these threads are "ends" and "picks" respectively. The weft threads are commonly referred to as "filling".

The Wilton Process

The Wilton weaving process is used for the fabrication of pile fabrics and consists of the ground yarn, chain yarn, stuffer yarn, filler yarn, and pile yarn. In effect, certain of the warp or filling yarns protrude out of the fabric base (ground cloth) to form surface pile of uncut loops. The ground fabric is woven separately and in such a way that closely and uniformly spaced loops of yarn are left on one side. Wires are inserted to form the loop and control the pile height. The loops may be cut to form cut pile.

The Jacquard Weaving Operation

In the Jacquard loom, each heddle (i.e., a needle through which the yarn is threaded) is attached to a wire or cord. These cords pass upwards to a device by means of which, at any time, any heddle can be raised on lowered, independently of the others. The device operates in a manner similar to that by which a player piano plays. Cards are punched with holes to correspond to the pattern which is to be woven. As these cards move, feelers which are sensitive to the holes, react and raise or lower the heddles to which they are attached.

APPENDIX C

DESCRIPTION OF REACTION KINETICS ABLATION PROGRAM (REKAP)

APPENDIX C

DESCRIPTION OF REACTION KINETICS ABLATION PROGRAM - (REKAP)

To describe the thermal behavior of a material in a re-entry environment (Reference 6), it is necessary to solve the transient heat conduction equation for each element of material through the char (if a char exists), the reaction zone, and the virgin material continuously and simultaneously throughout the re-entry heating period. In order to solve these second-order differential equations simultaneously, it is necessary to prescribe several boundary conditions. These boundary conditions are: (1) at the surface, the net heat transfer rate to a non-permeable surface is reduced by both surface re-radiation and the mass transfer effect of the injection of the decomposition gases into the boundary layer (blocking action); (2) at the backface of the virgin plastic or supporting substructure, the heat conducted out is zero.

In general, the heat conducted into a material element is equal to the sum of the heat stored in the element, the heat absorbed in the decomposition of the material element, the heat absorbed by the decomposition gases passing through the material element, and the heat absorbed by cracking or recombination of the decomposition gases. The general heat conduction equation, valid in both the porous char and virgin material is written in cartesian co-ordinates as:

$$\frac{\partial}{\partial x}\left[k\frac{\partial T}{\partial x}\right] = \rho C_p \frac{\partial T}{\partial t} + H_{GF}\frac{\partial \rho}{\partial t} - \left(Cp_G + \frac{\partial H_k}{\partial T}\right)\frac{\partial T}{\partial x}\int_{x = X'}^{x = \text{BACKFACE}} \frac{\partial \rho}{\partial t}\, dx \qquad (1)$$

$$\frac{\partial \rho}{\partial t} = \rho_v \left[\frac{\rho - \rho_c}{\rho_v}\right]^{n} \sum_{i=1}^{m} A_i\, e^{-\Delta E_i / RT} \qquad (2)$$

At the material surface - boundary layer interface, boundary condition (1) is the thermal energy balance written as:

$$\dot{q}_{net} = \dot{q}_c - \dot{q}_{RR} - \dot{q}_{Block} - \dot{q}_{Vaporization} \qquad (3)$$

where: $\dot{q}_c$ = hot wall convective heat flux = $H\,(h_r - h_w)$

$\dot{q}_{RR}$ = re-radiated heat flux = $\sigma\, F\epsilon\, Fa\, Tw^4$

$\dot{q}_{Block}$ = transpiration cooling due to injected gases

For laminar flow

$$\dot{q}_{Block} = \dot{q}_c \left[\left(\frac{\bar{M}_{BL}}{\bar{M}_{GAS}} \right)^{1/3} (.69)\, \frac{\Phi_o}{Pr^{1/3}} \right] \qquad (4)$$

For turbulent flow

$$\dot{q}_{Block} = \dot{q}_c \left[1 - e^{-.38 \left(\frac{Cp_{GAS}}{Cp_{BL}} \right) \Phi_o} \right] \qquad (5)$$

$$\Phi_o = \int_{Frontface}^{Backface} \dot{m}_G \, dx \left[\frac{h_r - h_w}{\dot{q}_c} \right] \qquad (6)$$

$\dot{q}_{VAP}$ = phase change energy associated with surface recession = $\rho_c\, L\dot{s}$

Surface recession rate is assumed to be a reaction rate controlled process that can be best described by an expression of the form suggested by Munson and Spindler (Reference 7)

$$\dot{S} = \beta_1\, Tw^{\beta_2}\, e^{-\beta_3 / T_w}$$

At the backface of the virgin plastic or supporting substructure, the second boundary condition on equation 4 is

$$k\left(\frac{\partial T}{\partial x}\right)_{BF} = 0$$

By solving the above equations simultaneously and continuously, through the heating period, the surface and subsurface temperatures and material degradation time histories are obtained. The Reaction Kinetics Ablation Program (REKAP) is the mechanized numerical solution to the above model.

The validity of the above approach for the prediction of the thermal response of a material undergoing thermal degradation has been proved by comparing calculated results with those obtained during ground and flight tests.

REFERENCES

1. Hiltz, A.A., D.E. Florence, and D.L. Lowe, "Selection, Development, and Characterization of a Thermal Protection System for a Mars Entry Vehicle", GE TIS 68SD211, February 1968. Also J Spacecraft 5 (11), 1278-1284 (1968).

2. Michalak, R.J. and T.E. Hess, "Final Report for Reusable Surface Insulation Thermal Protection System Development Program", Contract No. NAS 9-12084 (NASA/MSC), May, 1972.

3. Saydah, A.R., "Results of Hyperthermal Arc Calibration", GE-RESD PIR 9151-TEE-133, May 3, 1971.

4. Strong, H.M., F.P. Bundy, and H.P. Bovenkerk, "Flat Panel Vacuum Thermal Insulation," Journal of Applied Physics 31 (1), 39-50 (1960).

5. Kohr, J.W., "Evaluation of ESM 1004AP Prototype Heat Shield, Hyperthermal Arc Test Results", GE-TDM-9151-014, July 1968.

6. Segletes, J., "Thermal Degradation of a Thermosetting Plastic", GE-RSD-TIS 62SD202, January, 1962.

7. Munson, T. and R. Spindler, "Transient Thermal Behavior of Decomposing Materials, Part I; General Theory and Application to Convective Heating", paper presented at IAS 30th Annual Meeting, N.Y., January, 1962.

DISTRIBUTION LIST

NASA Manned Spacecraft Center R & T Space Station Procurement Section Houston, Texas 77058 Attn: R. E. Easley, Mail Code BC76	(1 Copy)
NASA Manned Spacecraft Center Technical Library Branch Houston, Texas 77058 Attn: Retha Shirkey, Mail Code JM6	(4 Copies)
NASA Manned Spacecraft Center Management Services Division Houston, Texas 77058 Attn: John T. Wheeler, Mail Code JM7	(1 Copy)
NASA Manned Spacecraft Center Houston, Texas Attn: Marvin F. Matthews Bldg. 45	(1 Copy)
NASA Manned Spacecraft Center Structures and Mechanics Division Houston, Texas 77058 Attn: D.M. Curry /ES 32	(29 Copies)
NASA Ames Research Center Moffett Field, California 94035 Attn: Mr. H. Goldstein/MS 234-1	(1 Copy)
NASA Ames Research Center Moffett Field, California 94035 Attn: Mr. H. Larson /MS 234-1	(1 Copy)

NASA Langley Research Center (1 Copy)
Langley Station
Hampton, Virginia 23365
Attn: Mr. L.F. Vosteen /MS-206

NASA Langley Research Center (1 Copy)
Langley Station
Hampton, Virginia 23365
Attn: Mr. Bill Brooks/MS-188A

NASA Langley Research Center (1 Copy)
Langley Station
Hampton, Virginia 23365
Attn: Mr. Stephen Tompkins/MS-206

NASA George C. Marshall Space Flight Center (1 Copy)
Marshall Space Flight Center, Alabama 35812
Attn: Mr. F. Huneidi, S&E-ASTN-PT

NASA George C. Marshall Space Flight Center (1 Copy)
Marshall Space Flight Center, Alabama 35812
Attn: Mr. W.A. Riehl, S&E-ASTP-M

Aerotherm Corporation (1 Copy)
485 Clyde Avenue
Mountain View, California 94040
Attn: Dr. Lewis J. Alpinieri

Aerotherm Corporation (1 Copy)
485 Clyde Avenue
Mountain View, California 94040
Attn: Mr. E.P. Bartlett

AVCO Government Products Group (1 Copy)
AVCO Systems Division
201 Lowell Street
Wilmington, Massachusetts 01887
Attn: Mr. John W. Graham

Bell Aerosystems Company (1 Copy)
Post Office Box 1
Buffalo, New York 14240
Attn: Mr. Frank Anthony

National Aeronautics And Space Admin. (1 Copy)
Headquarters
Washington, D.C. 20546
Attn: Geo. Deutsch, Code RR-1

National Aeronautics And Space Admin. (1 Copy)
Headquarters
Washington, D.C. 20546
Attn: Mr. N. Peil, Code MH

Grumman Aerospace Corporation (1 Copy)
Plant 25 Space Shuttle
Bethpage, Long Island
New York 11714
Attn: Mr. Fred Raynes

Lockheed Missile and Space Company (1 Copy)
Post Office Box 504
Sunnyvale, California 94088
Attn: Mr. J. F. Milton
Alternate Space Shuttle
Concept Study
Department 66-02

General Dynamics Corporation (1 Copy)
Convair Aerospace Division
Post Office Box 1128
San Diego, California 92112
Attn: Dr. K.D. Whitehead

North American Rockwell Corporation (1 Copy)
12214 Lakewood Blvd.
Downey, California 90241
Attn: C. Statham
ACO7, Dept. 190

McDonnell-Douglas Corporation (1 Copy)
Thermodynamics, Advanced Technology
P. O. Box 516
St. Louis, Missouri 63166
Attn: Paul Bauer
B106-L1-PB2

Grumman Aerospace Corporation (1 Copy)
Bethpage, Long Island
New York, 11714
Attn: Willie Wolter
Dept. 411, Plant 25

Lockheed Missile And Space Company (1 Copy)
Post Office Box 504
Sunnyvale, California 94088
Attn: Mr. R.P. Banas, Dept. 62-63

General Dynamics Corporation (1 Copy)
Convair Aero-space Division
Post Office Box 1128
San Diego, California 92112
Attn: Mr. K.R. Carnahan

General Electric Company (43 Copies)
Re-entry and Environmental Systems Division
Post Office Box 8555
Philadelphia, Pennsylvania 19101
Attn: Arnold A. Hiltz, Room U7026 VFSC